Methodologies for the Design and Control of Central Cooling Plants

by

James Edward Braun

A thesis submitted in partial fulfillment of the
requirements for the degree of

DOCTOR OF PHILOSOPHY
(Mechanical Engineering)

at the

UNIVERSITY OF WISCONSIN - MADISON

1988

Methodologies for the Design and Control of Central Cooling Plants

James Edward Braun

Under the supervision of Professors
Sanford A. Klein, John W. Mitchell, and William.A. Beckman

This work presents general methodologies useful to engineers and plant managers for designing, retrofitting, and controlling the equipment in large central chilled water systems. The methodologies are in the form of: 1) mathematical models for the individual equipment, 2) optimal control algorithms, and 3) general guidelines for design and control.

Mathematical models of varying complexity are developed for the purpose of: 1) component design and retrofit analyses, 2) system simulation and control optimization studies, and 3) on-line optimal control. The models developed in this study represent improvements over those that appear in the literature. Where possible, measurements are used to validate the models.

Two methodologies are presented for determining optimal control of systems without thermal storage. A component-based algorithm is developed for non-linear optimization applied to system simulations. Results of a program implementation of this optimization algorithm are used to develop a "simple" near-optimal control methodology. This near-optimal methodology relies on an empirical model for the total power consumption of the system that lends itself to rapid determination of optimal

control variables and may be fit to measurements using linear regression techniques.

For systems with stratified thermal storage in parallel with the chillers and load, two methodologies are also presented for optimal control. A methodology is developed for determining the optimal control of stratified thermal storage systems using Dynamic Programming. For systems with time-of-day utility rates, a simple strategy for near-optimal control is also identified.

The methodologies developed for evaluating the optimal control of chilled water systems are utilized to study the effects of alternative control strategies and system configurations. In addition, control guidelines useful to plant engineers for improved control practices are identified.

Sanford A. Klein 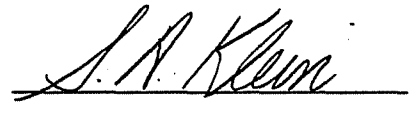

Acknowledgements

I must admit that I never had a burning desire to undertake this task. I wouldn't have done it anywhere but at the Solar Energy Laboratory. Jack, Bill, Sandy, and John, you've created a tremendous working environment that stimulates independence, creative thought, and comraderie. Thanks for all the support , ideas, and friendship.

I can't honestly say that these have been the best years of my life. However, there have been some very special people who've made difficult times alot better. Special thanks to Sandy for always being supportive and understanding. You're always moving forward and doing positive things, even though you're seldom satisfied. Chris, Joe, Jill, David, Jim, Al, and Ruth: Thanks for listening to me when I needed it most. Most importantly, thanks Liz for being you. You've added meaning and balance to my life.

The financial support from ASHRAE is gratefully acknowledged. The TC 4.6 Research Subcommittee provided the right amount of independence and supervision for this project.

Table of Contents

List of Figures

List of Tables

Nomenclature

Chapter 2

A	-	area
A_x	-	exit flow area from compressor impeller
C_{pw}	-	specific heat of water
h	-	specific enthalpy of refrigerant or heat transfer coefficient
LMTD	-	log-mean temperature difference
$\dot{m}$	-	mass flow rate
P	-	refrigerant pressure
P_{ch}	-	power consumption of compressor drive motor
$\dot{Q}$	-	rate of heat transfer
r	-	ratio of outside (finned) tube area to inside area or impeller radius
R	-	heat transfer resistance of tube, including fouling factor
T	-	temperature
UA	-	overall heat transfer conductance
u_x	-	velocity of tip of impeller
v	-	refrigerant specific volume
V	-	refrigerant velocity
w	-	compressor work input per unit mass of refrigerant
w_{pol}	-	polytropic work per unit mass of refrigerant, defined as the compressor work required for a reversible polytropic process occurring between the actual inlet and outlet states

β - blade angle of compressor impeller

ϕ_x - dimensionless flow coefficient, defined as the ratio of the fluid velocity normal to the impeller to the impeller tip speed

μ_x - work coefficient, defined as the ratio of the tangential component of the fluid velocity to the impeller tip speed

μ_{pol} - work coefficient for a polytropic process

η_{pol} - polytropic efficiency, defined as the ratio of the polytropic work to the actual compressor work required

η_m - overall efficiency associated with the motor and gearbox

η_{ref} - peak compressor polytropic efficiency

ω - angular velocity of impeller

Additional Subscripts

c - condenser conditions

chw - chilled water conditions

cw - condenser water conditions

chwr - chiller water return from the load

chws - chilled water supply to the load

cwr - leaving water temperature from the condenser

cws - supply water to the condenser

e - evaporator conditions

i - inside

n - normal component

o - outside

r - radial component

R - refrigerant

t - tangential component

x - conditions at tip of compressor impeller

1 - refrigerant state at exit of evaporator

2 - refrigerant state at exit of compressor

3 - refrigerant state at exit of condenser

4 - refrigerant state at inlet to evaporator

Chapters 3 and 4

A - surface area

A_V - surface area of water droplets per volume of cooling tower

C_{pa} - constant pressure specific heat of dry air

C_{pm} - constant pressure specific heat of moist air

C_{pv} - constant pressure specific heat of water vapor

C_{pw} - constant pressure specific heat of liquid water

C_s - derivative of saturation air enthalpy with respect to temperature

C^* - ratio of air to water capacitance rate for dry analysis

h_a - enthalpy of moist air per mass of dry air

h_C - convection heat transfer coefficient

h_D - mass transfer coefficient

h_f - enthalpy of liquid water

h_g - enthalpy of water vapor

h_s - enthalpy of saturated air

$\dot{m}$ - mass flow rate

$\dot{m}_a$ - mass flow rate of dry air

m^* - ratio of air to water effective capacitance rate for wet analysis

Le - Lewis number

Ntu - overall number of transfer units

P - power consumption

$\dot{Q}$ - overall heat transfer rate

T_a - air temperature

T_{dp} - ambient air dewpoint temperature

T_{ref} - reference temperature for zero enthalpy of liquid water

T_s - surface temperature

T_w - water temperature

T_{wb} - ambient air wet bulb temperature

UA - overall heat transfer conductance

V - volume

ΔP - pressure drop or rise

ΔP_o - static pressure drop

ε_a - air-side heat transfer effectiveness

γ - pump speed relative to maximum design speed

ω_a - air humidity ratio

ω_s - humidity of saturated air

Additional Subscripts

a	-	air stream conditions
ahu	-	air handler
cw	-	condenser water loop
chw	-	chilled water loop
des	-	design conditions
dry	-	dry surface
e	-	effective
i	-	inlet or inside conditions
max	-	maximum
o	-	outlet or outside conditions
p	-	pump conditions
s	-	surface conditions
T	-	total
w	-	water stream conditions
wet	-	wet surface

Chapter 5

J	-	instantaneous operating cost
f	-	vector of uncontrolled variables
g	-	vector of equality constraints
h	-	vector of inequality constraints
M	-	vector of discrete control variables

$\mathbf{u}$ - vector of continuous control variables

$\mathbf{x}$ - vector of component input stream variables

$\mathbf{y}$ - vector of component output stream variables

Chapter 7

J - integrated operating cost

L - instantaneous or stage operating cost

P - system power consumption

R - cost of electricity

t - time

T - storage temperature

T_{wb} - ambient wet bulb temperature

$\dot{Q}_{ch}$ - rate of cooling provided by the chillers

$\dot{Q}_L$ - rate of cooling provided by the cooling coils to meet the load

$\dot{Q}_s$ - rate of energy transfer from storage to meet the load (positive) or to storage as supplied by the chillers (negative)

v - velocity in the x direction

x - position measured from the storage inlet

X_t - output of a pure time-series model at time t

Y_t - output of a combined deterministic and time-series model at time t

$\mathbf{f}$ - vector of uncontrolled variables

$\mathbf{u}$ - vector of continuous control variables

$\mathbf{x}$ - vector of state variables

v - velocity relative to tank height measured in the x direction

x - position of front between storage temperature zones measured from the bottom of storage relative

Δt - timestep associated with stage

Chapter 1
Introduction

1.1 Background

The heating and cooling requirements of many building complexes in this country are provided with centrally located facilities. The University of Wisconsin at Madison has two such central plants that provide the bulk of the heating and cooling requirements for the university. Total annual fuel costs for both plants are on the order of ten million dollars. Even a small relative savings in the energy requirements of a plant such as this can translate into significant reductions in operating costs. In large buildings, a significant portion of the total energy requirements are associated with air conditioning. The potential for reductions in operating costs associated with improved design and control practices for central cooling systems provides the impetus for this project.

A centralized cooling plant consists of one or more chillers, cooling towers, pumps, and air handlers controlled so as to satisfy the cooling requirements of one or more buildings. Figure 1.1 shows a simplified schematic of a typical centralized chilled water system. Return air from the zones is mixed with an outside ventilation air stream and is cooled and dehumidified through cooling coils. In a variable air volume system, the air handler air flows are typically adjusted depending upon the supply air temperatures to maintain fixed zone temperatures. The supply air temperatures are controlled by modulating the water flows through each cooling coil with control valves. Cool and relatively dry air is supplied to the zones where both the temperature and humidity rise due to sensible and latent energy gains from people, lights, equipment,

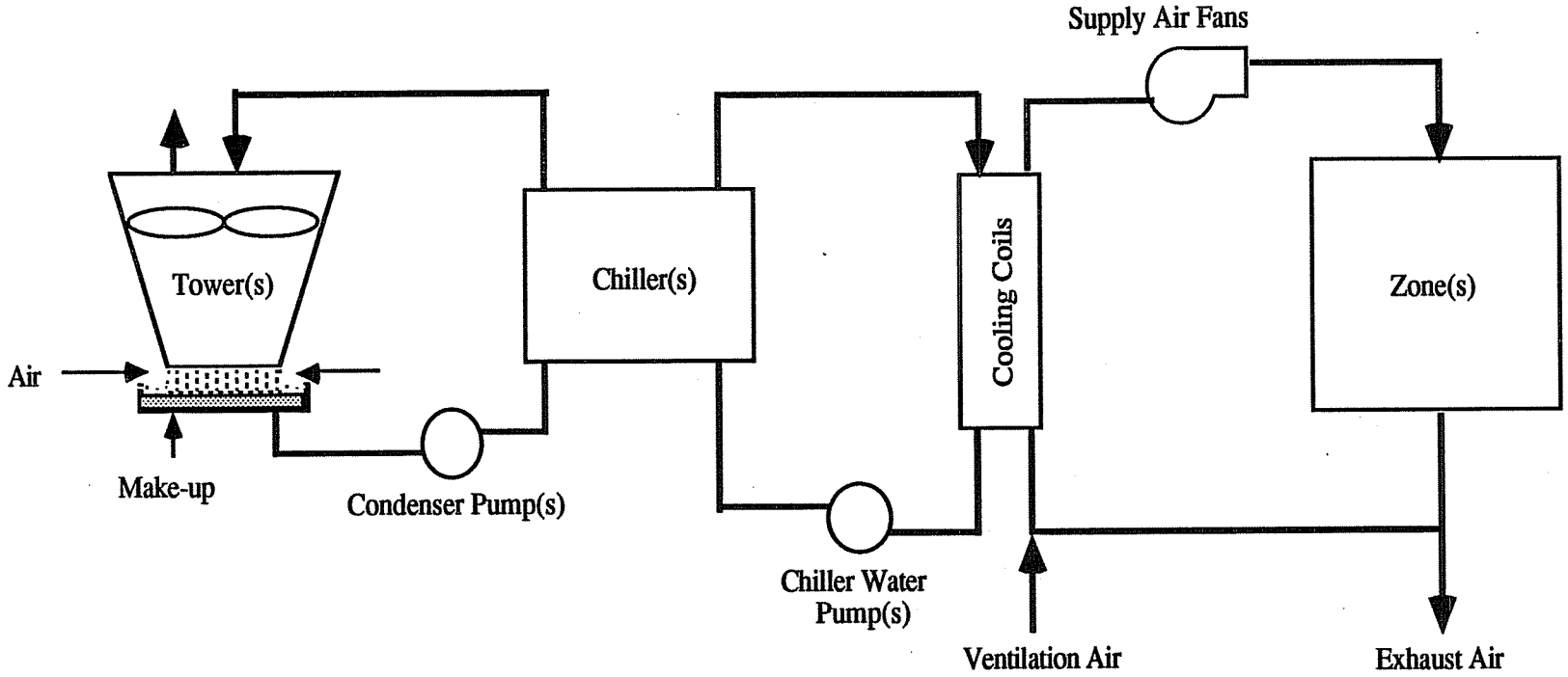

Figure 1.1 Schematic of a Typical Chilled Water System

solar radiation through windows, infiltration, and conduction through the envelope. The heat extracted from the air streams across the cooling coils warms the water returning to the chiller. The chilled water supply temperature is maintained by control of the chiller refrigerant flow through modulation of the compressor and expansion device. Cooling towers with multiple cells sharing common sumps are typically used to reject heat from the condenser of a chiller to the environment.

Design retrofits to existing systems may provide significant savings in operating costs. Many systems were designed using old technology, with little concern for energy costs. For instance, most large cooling systems utilize pumps and cooling tower fans that operate at fixed speeds. Modulation of flow rates in response to changing load conditions is limited to the on/off cycling of individual equipment operated in parallel or series. A more efficient method of operation is to continuously vary flow rates using variable-speed equipment. Recently, the cost and reliability of variable-speed electric motors has improved to the point where their use is cost effective in many applications. Treichler [1985] concluded that variable-speed pumping is economically attractive for both chilled water distribution and condenser water systems.

Centrifugal chillers are the largest consumers of energy in a central cooling system. Significant operational savings can be realized with certain chiller retrofits. Many applications utilize chillers that are operated at fixed speeds. Control of the chilled water setpoint temperature is maintained by varying the position of pre-rotation inlet vanes to the centrifugal compressor. An alternative method, which gives significantly higher efficiencies at part-load conditions, utilizes variable-speed control of the compressor.

Another possibility for improving the overall chiller performance is through a change in refrigerant. The refrigerant that gives the best performance depends upon the

load requirement. As an existing plant improves its energy management practices and applies conservation methods to reduce the building load, the load requirement of the chiller is reduced. As a result, the optimal refrigerant choice may change from that of the original design.

The addition of chilled water storage, if properly controlled, can significantly reduce operating costs (ASHRAE Bulletin [1985]). For systems with electrically driven chillers, storage can be utilized to take advantage of time-of-day charges and limit demand charges by shifting the load requirements. In the absence of special rate structures, storage may also reduce costs by shifting the load to times when environmental conditions result in improved chiller performance.

In addition to design retrofits, plant operating costs can be reduced through better control practices. A central cooling plant has many operating variables that may be controlled in a manner that minimizes the operational costs. At any given time, it is possible to meet the cooling needs with any number of different modes of operation and setpoints. Optimal supervisory control of the equipment involves determination of the control that minimizes the total operating cost. The optimal control depends upon time, through changing cooling requirements and ambient conditions. Currently, the operators of central cooling plants determine control practices that yield "reasonable" operating costs by experience gained through trial and error operation over a long period of time. Little research has been performed in developing general methodologies that would be suitable for optimal control of large centralized cooling systems. The major independent control variables in a plant without chilled water storage are the chilled water and supply air setpoint temperatures, number of chillers, pumps, and cooling tower cells in operation, and cooling tower cell air flow and condenser pump water flow rates. These variables may interact strongly and with proper control it is possible to significantly reduce operating costs.

Much of the literature related to cooling systems pertains to sizing of the equipment. The ASHRAE Handbook of Fundamentals [1981] gives background necessary for individual equipment sizing. In order to properly evaluate the economics associated with design retrofits or improved control practices, it is necessary to perform annual simulations of the complete system using long-term average weather data and load conditions. However, with inexpensive energy costs, there has been little incentive for the use of detailed simulations in defining designs and control strategies that minimize operating costs. More often than not, systems have been designed based upon minimizing the first cost, while ensuring that the capacity of the system was sufficient to meet the worst possible conditions. This has often resulted in systems being oversized and operating inefficiently.

A transient system simulation program, TRNSYS [1984] was developed over 10 years ago by the University of Wisconsin Solar Energy Laboratory for analyzing the performance of solar energy systems. TRNSYS is a modular program in which models of system components (e.g. pipes, heat exchangers, storage) are written as FORTRAN subroutines. The user can formulate or modify existing models and add them to a library of components. The models are connected together to form a complex system simulation model, analogous to the way pipes and wires connect the physical pieces of equipment. The modular approach is advantageous in that it provides a format in which a number of individuals can work independently and it minimizes the programming required to investigate alternative component models and plant configurations. This feature makes TRNSYS a good choice as a tool for studying the design and control characteristics of cooling plants as compared with other existing simulation programs (DOE-2 [1980], BLAST [1981], TRACE). However, since TRNSYS has been used primarily for solar energy systems, its standard component library does not include models for all of the equipment found in central cooling

systems. It also does not have the ability to determine the optimal control associated with simulation of a system.

Simulations involving cooling systems have primarily been used for equipment selection and building design. Most of the control studies which have been performed have been concerned with the local-loop control of an individual component or subsystem needed to maintain a prescribed set point, rather than the global determination of optimum set points that minimize operating costs. Global optimum plant control has been studied by Marcev [1980], Sud [1984], Lau [1985], Hackner [1984,1985], Johnson [1985], and Nugent[1988].

Lau studied the effect of control strategies on the overall energy costs of a large facility located in Charlotte, North Carolina through the use of annual simulations. The operating costs associated with the existing control strategy were compared with those resulting from "near-optimal" control of the condenser flow rates, the tower fan flows, and the number of chillers operating, along with the use of storage. The reduction in the utility bill was about 5.2 % of the total. The 50,000 gallon storage capacity was small relative to the 6000 ton plant capacity. In addition, no time-of-day or peak demand electric rates were in effect.

Hackner investigated optimal control strategies for a cooling system without storage at a large office building in Atlanta, Georgia. Optimal control of the chiller plant resulted in a reduction in the utility bill of about 8.7% when compared with the existing control strategy. If the plant had been operated with fixed setpoints, similar to conventional practice, the optimal control would have resulted in a cost reduction of about 19%. Similar conclusions were reached by Arnold, Sud, and Johnson. These studies demonstrated the potential savings through the use of optimal control in a plant without storage.

The goal of these control studies was to quantify the cost savings associated with optimal control rather than to produce general algorithms suitable for on-line optimal plant control. Optimal control set points were identified in Hackner's study for the specific plant through the use of performance maps. These maps were generated by many simulations of the plant over the range of expected operating conditions. The use of established performance maps for on-line plant control is advocated by Johnson. This procedure lacks generality and is not useful when storage is utilized.

Very little work has been performed in developing general methodologies that would be suitable for on-line optimal control of large cooling systems. Nizet [1984] applied a state-space model to a building zone in order to minimize the energy consumption with respect to a single control variable, the supply air flow rate to the zone. This optimization was carried out over a single day with the known weather data utilized for forecasts. The conjugate gradient method was applied to an integral objective function that accounted for the cost of energy associated with the boiler, chiller, and the supply air fans. Constant efficiencies were assumed for the boiler and chiller. Thermal comfort constraints associated with upper and lower temperature setpoints for the zone were considered through the introduction of penalty terms in the cost function. Since component efficiencies were constant, the opportunity for savings associated with optimal control of this hypothetical system resulted from operation closer to the limits of comfort. Depending upon the comfort constraints, optimal control of the supply air flow rate resulted in energy savings of between 12 and 30 % when compared with the existing control. The authors concluded that there were difficulties associated with the use of penalty functions for handling constraints. The proper choice of the penalty coefficients is difficult and sometimes leads to a badly conditioned problem. They also concluded that it was not practical to apply this methodology to more complicated systems in an on-line application.

Gunewardana [1979] applied dynamic programming techniques for minimizing the costs associated with a cooling system for power plants. The cooling system consisted of a cooling tower and spray pond that could be operated in series or parallel through eight possible modes in order to reject heat from the condenser of the power plant. The overall cost to be minimized included the cost of operating the power plant and the cost associated with pumping water through the cooling system. The dynamics of both the cooling sump and spray pond were considered. A sampling interval of 15 minutes and an optimization period of 2 hours were found to be adequate for this problem. Forecasts of the ambient conditions and load were made by assuming that their rates of change were constant. Depending upon the weather conditions, substantial cost savings could be realized.

1.2 Research Objectives and Approach

The goal of this work is to develop general methodologies useful to engineers and plant managers for designing, retrofitting, and controlling the equipment in large central chilled water systems. The methodologies would be in the form of:

1) mathematical models for the individual equipment
2) optimal control algorithms
3) general guidelines for design and control

The methodologies developed are of a general nature so as to be applicable to a wide variety of systems.

1.2.1 Model Development

Appropriate model development and selection depends strongly upon the desired goals. There are three distinct uses for models in this study that result in three different levels of mathematical representation.

1) Component Design and Analysis: Detailed mechanistic models are necessary in order to evaluate design retrofits of individual equipment. They are also useful in identifying the important variables that affect a components' overall performance and provide a basis for the development of simpler models. When little or no performance data are available, mechanistic models are a means of generating a complete performance map for a particular component.

2) System Simulation: It is possible to correlate the performance of individual components with simple mathematical relationships. In this manner, the time required to perform a simulation of a complete system for studying the effects of different control strategies and system configurations on overall performance is significantly reduced.

3) On-Line Optimal Control: In order to practically apply on-line optimal control to cooling systems, it is advantageous to have a simple model of the overall power consumption of the plant in terms of a minimum of inputs and with which optimal control setpoints can be readily determined. If the characteristics of the system or measuring equipment is changing with time, it may necessary to update parameters of the model using recursive identification techniques. This is most easily carried out for models that are linear with respect to the

empirical coefficients. For systems with thermal storage, it is necessary to forecast cooling requirements and ambient conditions in order to perform optimal control.

In this study, models are developed for all three of the above purposes. The models developed in this study represent improvements over those that appear in the literature. Where possible, measurements from the cooling system at the Dallas/Fort Worth (DF/W) airport and from the literature are used to validate the models.

1.2.2 Methodologies for Optimal Control

Methodologies for determining the minimum of a given cost function are well established. For systems without significant thermal storage, the dynamics of the cooling equipment can be neglected (Hackner [1985]) and the plant optimization involves minimizing the total instantaneous energy consumption of the chillers, cooling tower fans, pumps, and cooling coil fans in terms of the current load and ambient conditions. In this study, two methodologies are presented for determining optimal control. First of all, a component-based algorithm is developed for non-linear optimization applied to system simulation. In this study, this methodology is used primarily as a simulation tool for analyzing the design and control characteristics of chilled water systems under optimal control. Theoretically, the algorithm could be used for on-line optimization of the simulation of an operating system using "simple" component models. The simulation would proceed in parallel with the actual system with the possibility of updating parameters of the component models using on-line measurements. However, in this study, results of the optimization program are used to develop a "simple" near-optimal control methodology. An overall empirical cost function for the total power consumption of the cooling plant is inferred from the cost

functions associated with the components utilized in chilled water systems. This cost function lends itself to rapid determination of optimal control variables and may be fit to measurements using linear regression techniques.

Optimal control of a system with thermal storage involves minimizing the integral of the instantaneous operating costs, while satisfying required constraints. In this study, a methodology is developed based upon dynamic programming for determining the optimal control of systems with stratified thermal storage. Optimization results are then used to develop a "simple" near-optimal control strategy when time-of-day electric utility rates are present.

For systems with storage, it is necessary to forecast cooling requirements and ambient conditions in order to perform optimal control. A combined deterministic and time series model is developed for forecasting cooling loads and is evaluated using data from the D/FW airport.

1.2.3 Applications

In order to make any general conclusions concerning design and control of central cooling plants, it is necessary to simulate the performance of a variety of system configurations under optimal control. The methodologies developed for evaluating the optimal control of chilled water systems are utilized in studying the effects of alternative control strategies and system configurations. In addition, control guidelines useful to plant engineers for improved control practices are identified.

1.3 Description of the D/FW Airport System

The central cooling plant at the Dallas/Fort Worth (D/FW) airport is used as the primary test facility for this study. This particular system is of general interest because

of the large data acquisition system and the unique retrofits that the plant personnel have undertaken.

The D/FW central facility provides heating and cooling for approximately 3 million square feet of floor area for airport terminals, hotels, and office space. This system has three centrifugal chillers originally rated at 8700 tons each. There are two sets of cooling towers, each having four cells originally with two-speed 125 hp fans. Each bank of tower cells shares a common sump and has two 500 hp condenser water pumps in parallel that draw off the towers sumps. One set of cells has an additional 250 hp pump that is utilized at low load conditions. The chilled water pumping is provided with two 500 hp pumps and one 250 hp pump. An additional unique feature of the D/FW system is that there are several hours of thermal storage available within the chilled water distribution system that is used to increase the overall plant cooling capacity and improve part-load operation.

The data acquisition system records a wide range of conditions including temperatures, pressures, flow rates, and power consumptions on magnetic tape each minute. This information is utilized by the plant operators for the purpose of billing the individual energy users and for energy management of the system as a whole. For this study, this data is invaluable in developing and validating computer simulation models of the equipment that are used in evaluating both improved control strategies and retrofits for the plant.

Foremost among the retrofits implemented in the D/FW plant to reduce energy consumption was the conversion of the drive for the primary centrifugal chiller. Each of the three 8700 ton chillers as initially installed was driven with a steam turbine. As a result of poor turbine efficiencies at low speeds, these chillers were primarily operated at fixed compressor speeds. The capacity modulation was provided by control of inlet pre-rotation and outlet diffuser vanes. Through good energy management practices, the

energy consumption at the D/FW airport has been reduced to the point where a single chiller provides the necessary cooling requirements. To further reduce energy consumption at part-load operation, the primary chiller was retrofitted with a 5000 hp variable-speed electric motor. At the same time, the refrigerant was changed from R-22 to R-500 and the chiller capacity was derated to 5500 tons. This cooling capacity in conjunction with the use of thermal storage is sufficient to satisfy the system demand most of the time. Additional retrofits at the D/FW system include conversion of chilled water distribution pumps and cooling tower fans with variable-speed motors. All of these retrofits improve the part-load performance of the cooling plant.

1.4 Organization

The main body of the thesis is presented in Chapters 2 - 7. Both detailed and simplified models for the individual system equipment are developed and compared in Chapters 2, 3, and 4. Results of these models are also compared with measurements. Both the component-based and system-based optimization algorithms are developed in Chapter 5. Results of applications of these methodologies to systems without storage are given in Chapter 6. Included in these results are control simplifications that are useful as guidelines for plant operators and that simplify the methodology for near-optimal control. Typical results for the savings associated with optimal control and comparisons between different system configurations under optimal control are also presented in Chapter 6. In Chapter 7, dynamic programming is applied to fully-stratified thermal storage systems in order to identify control simplifications for near-optimal control. In addition, a model for forecasting cooling loads is developed based upon time-series methods. Computer programs developed in this study are listed in a separate document (Braun [1988]).

Chapter 2

Models for Centrifugal Chillers

In this chapter, mathematical models are developed for centrifugal chillers. A mechanistic model is presented for chillers operated with variable-speed control. Results of this model are used to identify a simpler empirical model more suitable for system simulation and optimal control studies. The empirical model correlates data for both variable and fixed-speed chillers.

The models described in this chapter are compared with performance data for the 5500 ton centrifugal chiller at the Dallas/Fort Worth (D/FW) airport under both variable-speed and fixed-speed control. They are also used to study the performance characteristics of the D/FW chiller.

2.1 A Mechanistic Model for Variable-Speed Chillers

A common method for modeling the performance of chillers for use in the simulation of central cooling plants is to fit empirical relationships to manufacturers' data. Stoecker [1971] and Bullock [1984] give examples of functional forms that are adequate for this purpose. One limitation of this approach is that the model can only be trusted within the range of conditions for which it was fit. Often the available data are too limited to provide a complete performance map. In addition, empirical models are not useful for investigating design retrofits associated with the chiller, such as changes in refrigerant type or conversion from fixed-speed with vane control to variable-speed capacity modulation. Such models are also limited in studying the importance of certain control variables, such as chilled and condenser water flow rates. Although manufacturers' have developed mechanistic models of centrifugal chillers, their

descriptions are not available in the open literature.

In this section, a mechanistic model of a centrifugal chiller with variable-speed control is described. The model utilizes mass, momentum, and energy balances on the compressor, evaporator, condenser, and expansion device. Given a chilled water set temperature and entering chilled and condenser water temperatures and flow rates, the model determines both the required compressor speed and power consumption. In addition, it may be used to estimate, for any given set of conditions, the chiller capacity at a specific speed or power consumption or the compressor speed at which compressor surge develops.

When little or no performance data are available, the mechanistic model described in this section provides a tool for generating a complete chiller performance map. A simpler empirical model appropriate for system simulation is then fit to the generated data.

2.1.1 Model Formulation

Figure 2.1 shows a schematic and associated pressure-enthalpy diagram of a centrifugal chiller with single-stage compression. The refrigerant entering the compressor at state 1 is assumed to be a saturated vapor. Both the enthalpy and pressure rise as the refrigerant passes through the compressor to a superheated state 2. In the condenser, the refrigerant is cooled and condensed at a relatively constant pressure and is assumed to exit at state 3 as a saturated liquid. It is then expanded at constant enthalpy to the evaporator pressure (state 4). In the development that follows, the chilled water supply and return temperatures, T_{chws} and T_{chwr}, refer to supply and return to the load (i.e. from and to the evaporator), while the condenser water supply and return, T_{cws} and T_{cwr}, are to and from the condenser. Each of the components are modeled as follows.

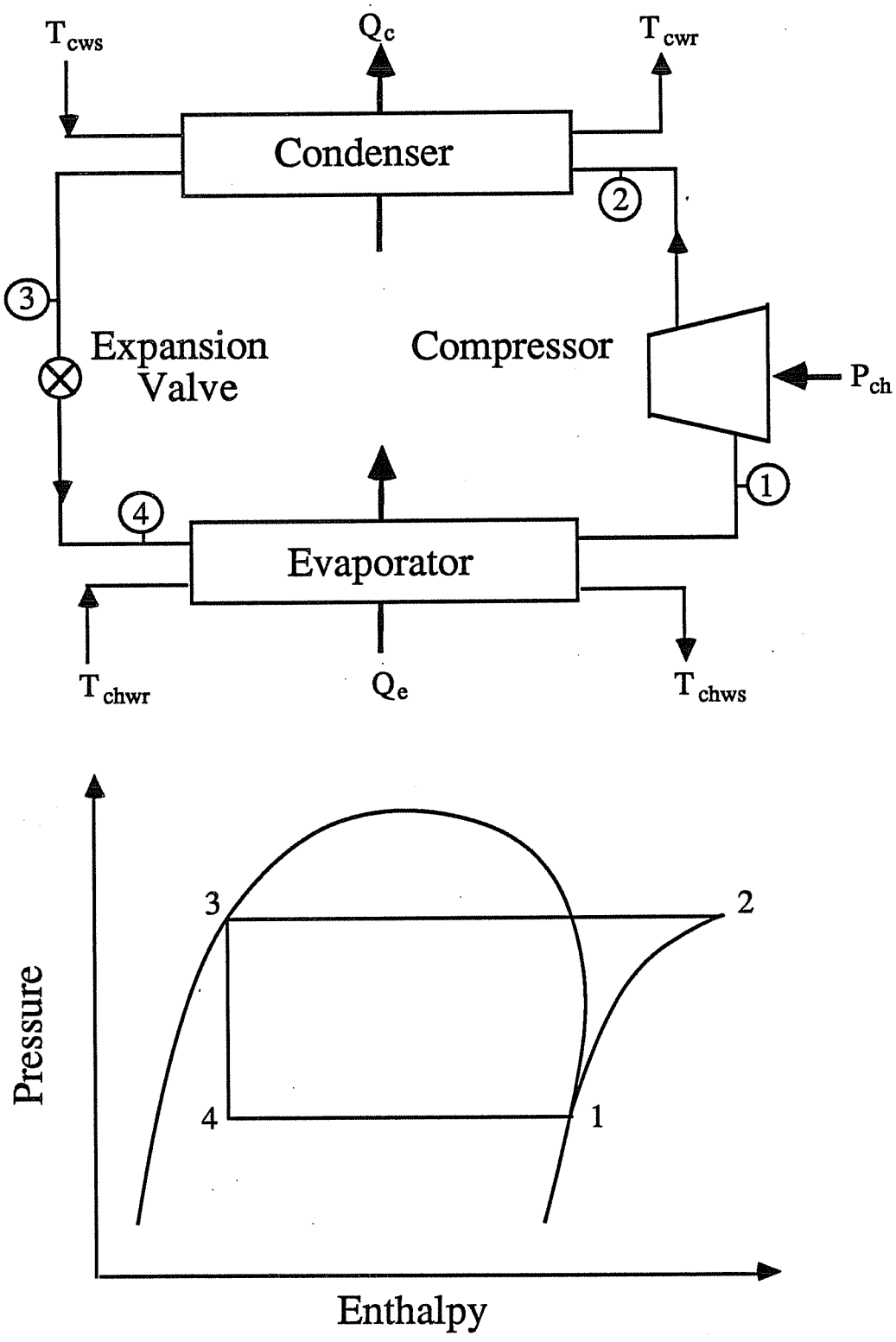

Figure 2.1. Schematic and Pressure-Enthalpy Diagram for a Single-Stage Chiller

Evaporator

The evaporator is assumed to be a flooded shell and tube type design. Refrigerant boils at the outside of horizontal tubes and rises out the top. Heat transfer in the evaporator is modeled using an overall conductance and log-mean temperature difference. Three expressions for evaporator heat flow that result from this model and from energy balances on the two fluid streams are

$$\dot{Q}_e = UA_e LMTD_e \tag{2.1.1}$$

$$= \dot{m}_R (h_1 - h_4) \tag{2.1.2}$$

$$= \dot{m}_{chw} C_{pw} (T_{chwr} - T_{chws}) \tag{2.1.3}$$

where,

$\dot{Q}_e$ = rate of heat transfer to evaporator

UA_e = overall evaporator conductance

$LMTD_e$ = evaporator log-mean temperature difference

$\dot{m}_R$ = refrigerant mass flow rate

h_1 = specific enthalpy of refrigerant exiting evaporator

h_4 = specific enthalpy of refrigerant entering evaporator

$\dot{m}_{chw}$ = chilled water flow rate

C_{pw} = specific heat of water

The log-mean temperature difference and overall conductance are determined as

$$LMTD_e = \frac{T_{chwr} - T_{chws}}{\ln\left[\frac{T_{chwr} - T_e}{T_{chws} - T_e}\right]} \tag{2.1.4}$$

$$UA_e = \frac{A_{e,i}}{\frac{1}{h_{e,i}} + \frac{1}{r_e h_{e,o}} + R_e} \tag{2.1.5}$$

where,

T_e = refrigerant evaporation temperature

$A_{e,i}$ = total inside surface area of evaporator tubes

$h_{e,i}$ = heat transfer coefficient for water flow through evaporator tubes

$h_{e,o}$ = boiling refrigerant heat transfer coefficient

r_e = ratio of effective outside evaporator tube area (product of overall fin efficiency and total surface area) to inside area

R_e = the resistance to heat transfer associated with the tube material, including the fouling factor.

Nucleate boiling is assumed to take place from the evaporator tubes to the pool of refrigerant. Bubbles nucleate and grow from spots on the surface in a thin layer of superheated liquid formed adjacent to the tubes. There is much data available for boiling heat transfer coefficients, but there is no universally accepted correlation. Generally, the heat transfer coefficient for a particular application may be correlated in the form

$$h_{e,o} = a\,(T_{e,s} - T_e)^b \tag{2.1.6}$$

where a and b are empirical constants that depend upon the properties of the refrigerant and the nucleate characteristics of the surface and $T_{e,s}$ is the average tube outside surface temperature. Myers (1952) gives typical results for the heat transfer coefficient of Refrigerant 12 with finned tubes that are used in this study. An expression for the tube surface temperature obtained by considering the heat transfer resistance between the water and the outside tube surface is

$$T_{e,s} = \overline{T}_{chw} + \frac{\dot{Q}_e}{A_{e,i}}\left[\frac{1}{h_{e,i}} + R_e\right] \tag{2.1.7}$$

where $\overline{T}_{chw}$ is the average of the entering and leaving chilled water temperatures.

The chilled water flow through the evaporator tubes is assumed to be turbulent such that the heat transfer coefficient is given as (ASHRAE [1985])

$$h_{e,i} = 0.023\left[\frac{k_w}{d_e}\right] Re_e^{0.8}\, Pr^{0.4} \tag{2.1.8}$$

where k_w is the thermal conductivity of water, d_e is the inside tube diameter, Re_e is the Reynolds number associated with water flow in an individual evaporator tube, and Pr is the Prantl number for water.

Condenser

The condenser is also considered to be a horizontal shell and tube design. Refrigerant condenses on the outside of the tubes and drains out the bottom.

Analogous to the evaporator, the three equations for heat transfer are

$$\dot{Q}_c = UA_c LMTD_c \tag{2.1.9}$$

$$= \dot{m}_R (h_2 - h_3) \tag{2.1.10}$$

$$= \dot{m}_{cw} C_{pw} (T_{cwr} - T_{cws}) \tag{2.1.11}$$

where,

h_2 = specific enthalpy of refrigerant entering condenser

h_3 = specific enthalpy of refrigerant exiting condenser

$\dot{m}_{cw}$ = condenser water flow rate

and

$$LMTD_c = \frac{T_{cwr} - T_{cws}}{\ln\left[\frac{T_c - T_{cwr}}{T_c - T_{cws}}\right]} \tag{2.1.12}$$

$$UA_c = \frac{A_{c,i}}{\frac{1}{h_{c,i}} + \frac{1}{r_c h_{c,o}} + R_c} \tag{2.1.13}$$

T_c = refrigerant condensing temperature

$A_{c,i}$ = total inside surface area of condenser tubes

$h_{c,i}$ = heat transfer coefficient for water flow through condenser tubes

$h_{c,o}$ = condensing refrigerant heat transfer coefficient

r_c = ratio of effective outside condenser tube area (product of overall fin efficiency and total surface area) to inside area

R_c = the resistance to heat transfer associated with the tube material, including the fouling factor.

It is not strictly correct to use the refrigerant condensing temperature, T_c, in determining the log-mean temperature difference for the entire condenser. Refrigerant entering the condenser is superheated and is cooled sensibly to the saturation temperature at a relatively constant pressure prior to condensation. During this process, the heat transfer coefficient is lower and the temperature difference higher than during condensation. These tradeoffs justify the use of a single condenser temperature and a single condensing heat transfer coefficient in the model.

Theoretical expressions for determining the heat transfer coefficients for laminar film condensation of pure vapors on plates and tubes were first developed by Nusselt. The average heat transfer coefficient associated with a vapor condensing on N horizontal tubes is estimated from

$$h_{c,o} = 0.725\left[\frac{k_f^3(\rho_f-\rho_v)^2 g h_{fg}}{N d_c \mu_f (T_c - T_{c,s})}\right]^{0.25} \qquad (2.1.14)$$

where,

k_f = conductivity of the liquid refrigerant

h_{fg} = heat of vaporization of the refrigerant

g = gravitational acceleration

ρ_f = density of saturated liquid refrigerant

ρ_v = density of saturated vapor refrigerant

d_c = condenser tube diameter

μ_f = viscosity of saturated liquid refrigerant

$T_{c,s}$ = average tube outside surface temperature

The vapor density is usually small compared to the liquid density and may be neglected. Analogous to the evaporator analysis, the tube surface temperature is

$$T_{c,s} = \overline{T}_{cw} + \frac{\dot{Q}_c}{A_{c,i}}\left[\frac{1}{h_{c,i}} + R_c\right] \tag{2.1.15}$$

where $\overline{T}_{cw}$ is the average condenser water temperature.

The correlation for turbulent flow in tubes, equation (2.1.8), is applicable to a condenser tube and is used for evaluating the water side heat transfer coefficient for the condenser, $h_{c,i}$.

Compressor

One approach to modeling the performance of the compressor is to use performance curves from the manufacturer. Davis (1974) presents a method of correlating data that reduces the family of compressor head characteristics to a single curve of dimensionless head versus a dimensionless flow. A limitation associated with this approach is that complete performance data is not always readily available or it is presented in such a way as to be specific to the refrigerant employed.

The model developed in this study relies on relationships that are commonly used in the design of centrifugal compressors. It employs fundamental mass, momentum, and energy balances and empirical correlations that are representative of well-designed centrifugal compressors.

Ferguson [1963] provides a good background for much of the presentation to follow concerning the compressor. Figure 2.2 shows a cross-section of the impeller of a centrifugal compressor showing a single blade with pertinent dimensions and velocities.

The impeller rotates with an angular velocity ω having a tip speed equal to u_x. The refrigerant vapor exits the impeller with a relative velocity $V_{x,r}$ and an absolute velocity V_x. The components of velocity tangential and normal to the impeller wheel are denoted as $V_{x,t}$ and $V_{x,n}$.

Neglecting the angular momentum of the incoming refrigerant, a momentum balance on the impeller gives an expression for the required work input per unit mass of refrigerant.

$$w = \omega V_{x,t} r = u_x V_{x,t} = \mu_x u_x^2 \tag{2.1.16}$$

where the work coefficient, μ_x, is defined as the ratio of the tangential component of the fluid velocity to the impeller tip speed.

$$\mu_x = \frac{V_{x,t}}{u_x} \tag{2.1.17}$$

If the velocity of the fluid relative to the impeller, $V_{x,r}$, exits tangential to the blade (i.e. no slippage), then the theoretical work coefficient determined from the vector diagram of Figure 2.2 is

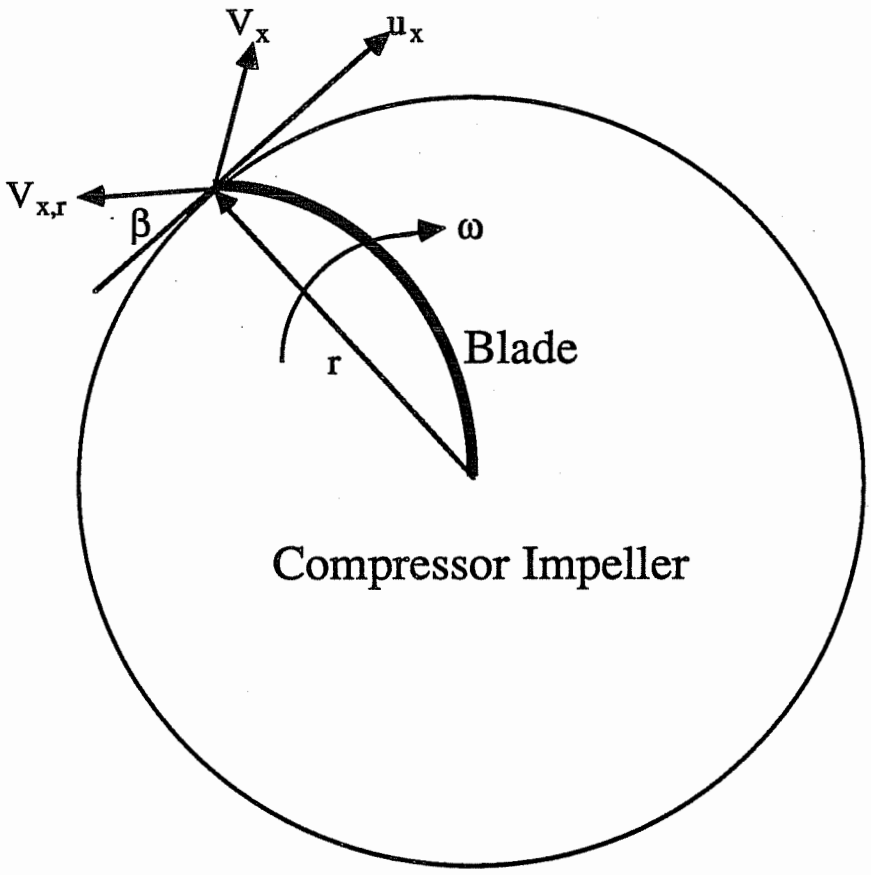

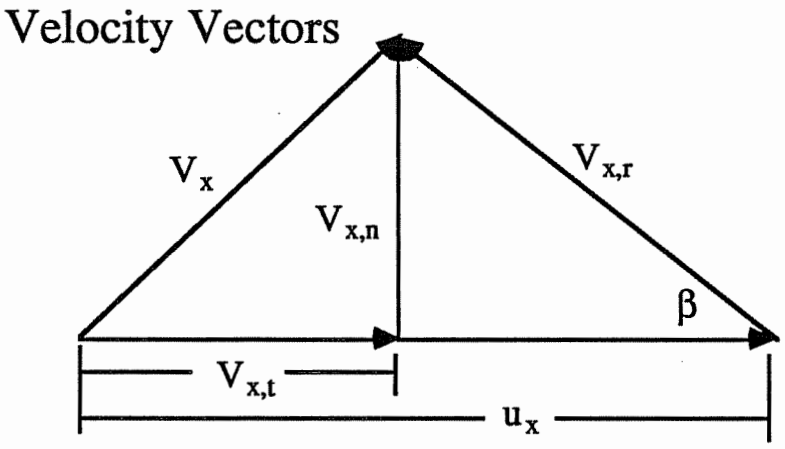

Figure 2.2. Velocity Components for Refrigerant Exiting a Compressor Impeller

$$\mu_{x,th} = \frac{u_x - V_{x,n}\cot(\beta)}{u_x}$$

$$= 1 - \phi_x \cot(\beta) \qquad (2.1.18)$$

The dimensionless flow coefficient, ϕ_x, is the ratio of the fluid velocity normal to the impeller to the impeller tip speed.

$$\phi_x = \frac{V_{x,n}}{u_x} = \frac{\dot{m}_R v_x}{A_x u_x} \qquad (2.1.19)$$

where A_x is the exit flow area of the impeller and v_x is the exiting vapor specific volume.

In reality, slippage and non-uniform velocity profiles at the impeller exit limit the accuracy of this formulation. Wiesner [1959, 1960] has correlated the real performance of centrifugal compressors with vaneless diffusers. His results are presented as curves of polytropic efficiency, η_{pol}, and polytropic work coefficient, μ_{pol}, versus the dimensionless flow coefficient, ϕ_x, where,

$$\eta_{pol} = \frac{w_{pol}}{w} \qquad (2.1.20)$$

$$\mu_{pol} = \frac{w_{pol}}{u_x^2} \qquad (2.1.21)$$

The polytropic work, w_{pol}, is the quantity of work required for a reversible polytropic process occurring between the actual inlet and outlet states. A polytropic

process satisfies

$$Pv^n = \text{constant} \tag{2.1.22}$$

The polytropic coefficient, n, is determined by the actual initial and end states.

$$n = \frac{v_2}{v_1} \ln\left[\frac{P_2}{P_1}\right] \tag{2.1.23}$$

Since there is an increase of entropy in the actual irreversible compressor, there must be a reversible heat input to the reversible compressor for the end states to be the same. The polytropic work is given by

$$w_{pol} = \int_{P_1}^{P_2} v dP = P_1 v_1 \frac{n}{n-1} \left\{ \left[\frac{P_2}{P_1}\right]^{\frac{n-1}{n}} - 1 \right\} \tag{2.1.24}$$

The stage work coefficient, μ_x, is determined from the polytropic coefficient and efficiency as

$$\mu_x = \frac{\mu_{pol}}{\eta_{pol}} \tag{2.1.25}$$

Wiesner's results for μ_{pol} are a series of straight lines that can be represented by

$$\mu_{pol} = 0.69\,(1 - \phi_x \cot(\beta)) = 0.69\,\mu_{x,th} \tag{2.1.26}$$

The polytropic efficiency results of Wiesner are presented as curves of relative efficiency versus the dimensionless flow coefficient, ϕ_x, for different rotational Mach Numbers, M_o, where

$$M_o = \frac{u_x}{a_o} \tag{2.1.27}$$

and a_o is the sonic velocity in the refrigerant at the impeller inlet conditions. The following equation provides a good fit to the graphical data of Wiesner.

$$\frac{\eta_{pol}}{\eta_{ref}} = \left[1 + a\,(1.1 - M_0)\right]\left[1 - \exp(\phi_x\,(b\phi_x^2 + c\phi_x + d))\right] \tag{2.1.28}$$

The reference polytropic efficiency, η_{ref}, is the peak value associated with a reference rotational Mach Number of 1.1. It is typically in the range of 0.80 to 0.85. The empirical constants (a, b, c, d) that provide a good match to Wiesner's data are 0.109, 58.5, -6.0, and -18.8, respectively. Wiesner also presents a correction factor for polytropic efficiencies due to differences in Reynolds numbers associated with the use of different refrigerants. This effect is relatively small and is negligible for the refrigerants considered in this study (R-500, R-22, and R-12).

In order to evaluate the flow coefficient using equation (2.1.19), it is necessary to determine the specific volume of the refrigerant at the exit of the impeller. Most of the entropy rise associated with the compression process occurs within the diffuser. For this reason, the entropy at the impeller exit is assumed to be equal to the entropy at the inlet.

$$s_x = s_1 \tag{2.1.29}$$

The additional property necessary to define the state at the impeller outlet is determined from an energy balance on the diffuser. Assuming that the kinetic energy exiting the diffuser is small compared to that at the diffuser inlet, the incoming enthalpy is

$$h_x = h_2 - \frac{V_x^2}{2} \tag{2.1.30}$$

From an energy balance on the impeller and equation (2.1.16)

$$h_2 = h_1 + \mu_x u_x^2 \tag{2.1.31}$$

So,

$$h_x = h_1 + \mu_x u_x^2 - \frac{V_x^2}{2} \tag{2.1.32}$$

The absolute refrigerant velocity at the impeller exit, V_x, is determined from the normal and tangential components (Figure 2.2), such that

$$V_x^2 = V_{x,n}^2 + V_{x,t}^2 = u_x^2(\phi_x^2 + \mu_x^2) \tag{2.1.33}$$

Thus the exit impeller enthalpy is

$$h_x = h_1 + u_x^2\left[\mu_x - \frac{\mu_x^2}{2} - \frac{\phi_x^2}{2}\right] \qquad (2.1.34)$$

The thermal expansion device is assumed to modulate the refrigerant flow such that a saturated vapor state is maintained at the compressor inlet. The entering and exiting enthalpy of the expansion device are assumed to be equal.

$$h_4 = h_3 \qquad (2.1.35)$$

Finally, the power input to the motor driving the compressor is calculated as

$$P_{ch} = \frac{\dot{m}_R (h_2 - h_1)}{\eta_m} \qquad (2.1.36)$$

where η_m is the overall efficiency associated with the motor and gearbox if present.

The model, as defined through equations (2.1.1) - (2.1.36), requires properties of the refrigerant at various states. A computer program developed from the equations given by Downing (1981) was used to evaluate thermodynamic properties of the refrigerants at any state. Additionally, curve-fits were developed for viscosity and conductivity at saturated liquid conditions for refrigerants considered in this study. The sonic velocity associated with the vapor refrigerant exhibits very little variation over a wide range of temperatures. It was assumed to be constant evaluated at 50 degrees Fahrenheit. Appendix A gives the viscosity and conductivity curve-fits and

sonic velocity data. A listing of the refrigerant properties program is given by Braun [1988].

2.1.2 Solution of the Equations

For a given chiller design, there are five independent input variables that define the chiller performance through the equations presented in the previous section. It is possible to solve these equations in different ways depending upon the desired inputs and outputs. Most commonly, the independent variables controlling the compressor performance would be the entering chilled and condenser water temperatures and flow rates and the chilled water setpoint. In this case, the primary outputs would be the compressor power requirement and speed. Alternatively, it is possible to specify the compressor speed as an input, in which case the leaving chilled water temperature and power requirement are outputs. Other possibilities include specifying the leaving in place of entering condenser water temperature or the power consumption. In any case, the solution of the equations is not as complicated as it might first appear.

For a single-stage compressor with a specified chilled water setpoint and entering or leaving condenser water temperature, the equations are solved in two separate steps.

1) Given the chilled water entering flow rate and temperature and the setpoint, determine the evaporator refrigerant temperature, T_e, by iteratively solving equations (2.1.1) and (2.1.3)-(2.1.8). This can be accomplished with Newton's method applied to the function.

$$F(T_e) = UA_e LMTD_e - \dot{m}_{chw} C_{pw} (T_{chwr} - T_{chws}) \qquad (2.1.37)$$

2) The solution of the remaining set of equations can be reduced to finding the

zeros of three functions with three unknowns using Newton's method. The three iteration variables are T_c, u_x, and ϕ_x, while the three functions are

$$F_1 = UA_c LMTD_c - \dot{m}_{cw} C_{pw} (T_{cwr} - T_{cws}) \tag{2.1.38}$$

$$F_2 = \phi_x - \frac{\dot{m}_R v_x}{A_x u_x} \tag{2.1.39}$$

$$F_3 = (h_2 - h_1) - \frac{w_{pol}}{\eta_{pol}} \tag{2.1.40}$$

For given values of the iteration values, each of the terms in the above equations are uniquely defined with equations (2.1.2) , (2.1.9) - (2.1.35) and property data.

The analysis is complicated a bit further if two-stage compression is considered. In this case, the energy and momentum balances are applied to both compression stages. In the absence of an economizer, the outlet from the first stage is the inlet the second.

Most multi-stage centrifugal chillers utilize an economizer. For a two-stage compressor, refrigerant exiting the condenser is expanded to the intermediate pressure between compression stages and enters a flash tank. Saturated refrigerant vapor is removed from the flash tank, mixed with the outlet stream from the first stage and fed to the second-stage compressor. Liquid refrigerant from the flash tank is expanded to the evaporator pressure. In order to include an economizer in the analysis, mass and energy balances are applied to the economizer to determine the additional states and refrigerant flow rates.

In the solution of equations for two-stage compression, two additional iteration variables are the intermediate pressure and the flow coefficient for the second stage.

Equations (2.1.39) and (2.1.40) apply to the first stage and an analogous two additional equations are used for the second stage.

The maximum cooling capacity of a chiller is limited by several factors. For instance, it may be controlled by the maximum allowable power input to the motor or the maximum rotational speed. Alternatively, there may be a lower limit on the refrigerant temperature in order to avoid localized ice formation within the evaporator or an upper limit on the condenser pressure. In any of these situations, the model can be adapted to determine the maximum capacity and associated power input and compressor speed. The D/FW chiller capacity is primarily limited by the power input to the motor. In this case, the equations are solved such that power is an input and cooling capacity is output. Equations (2.1.37) - (2.1.40) are solved concurrently, rather than separately in this situation. Listings of computer programs for evaluating the chiller power consumption, operating speed, and cooling capacity for single and two-stage compression (with or without an economizer) appear in a separate document (Braun [1988]).

2.1.3 Parameter Estimation and Comparison with Measurements

The D/FW chiller has two-stage compression with an economizer. Many of the parameters characterizing this design were available from the manufacturer and are presented in Table 2.1. Additional parameters necessary for evaluating the chiller performance were determined by regression using measurements from the D/FW airport. The data used in the regression was randomly selected from two different time periods to give a range of conditions.

The ratios of the outside finned tube area to the inside area for both the evaporator and condenser were unknown. Sufficient data were available to estimate these ratios

from a regression analysis. The saturation temperatures were estimated from compressor suction and discharge pressure measurements using refrigerant property data for R-500. Good agreement between the model and the saturation temperatures is obtained for values of r_e and r_c of 3.1 and 3.2.

Table 2.1
Known D/FW Chiller Parameters

Description	Value	Units
Effective evaporator internal tube surface area	11,300	sq. ft.
Number of evaporator tubes	3560	
Number evaporator tube passes	3	
Evaporator tube length	22	feet
Tube inside diameter (evaporator and condenser)	0.75	inches
Effective condenser internal tube	14,800	sq. ft.
Number of condenser tubes	3349	
Number of condenser tube passes	1	
Condenser tube length	30	feet
Diameter of compressor impellers	2.33	feet

The efficiency of the electric motor driving the compressor is approximately 95%. Additionally, there is significant energy loss in the gearbox between the motor and the compressor. At maximum loading of 5000 hp, the energy loss is approximately 200 hp. This gives an overall efficiency of about 91%.

There are three additional unknown parameters concerning the compressor that are necessary in order to analyze the chiller performance: 1) the impeller blade angle, β, 2) the impeller exit flow area, A_x, 3) the reference polytropic efficiency, η_{ref}. Estimates of these parameters were obtained from the D/FW plant personnel and the

literature as follows.

From a photograph of a centrifugal compressor impeller available from the D/FW plant personnel, the blade angle appears to be approximately 30 degrees. The impeller width at the exit is between 2 and 3 inches. This gives an impeller exit area of between 1.2 and 1.8 square feet. Wiesner's [1960] curves of polytropic efficiency derived from measurements of several centrifugal compressors operating with R-500, R-22, or R-12 give a relative polytropic efficiency of about 0.82.

In order to fine-tune these estimates, a regression analysis was applied to the centrifugal compressor. Measurements included the motor electrical consumption and the compressor suction and discharge pressures. Table 2.2 gives the parameter values determined from the regression analysis that yield the best agreement with the data. They are surprisingly close to the original estimates.

Figures 2.3 - 2.6 show comparisons between measurements and the overall model predictions of refrigerant temperatures in the evaporator and condenser and the compressor power and speed. Overall, the agreement is very good. The best predictions are of the power consumption and the evaporator temperature. The estimates of the condenser temperature and compressor rpm are not quite as good. There appears to be a slight bias in the comparisons. The model tends to underestimate power consumption and speed at low values. One possibility is that the motor and gearbox efficiencies are lower at lower speeds and loadings. The model assumes a fixed overall efficiency for these components at all conditions. Another possibility is that the compressor polytropic efficiency may fall-off more significantly at low loads than the Wiesner data exhibits.

Table 2.2
Compressor Parameters Determined from Regression

Parameter	Value	Units
β	27.2	degrees
A_x	1.53	square feet
η_{ref}	0.814	

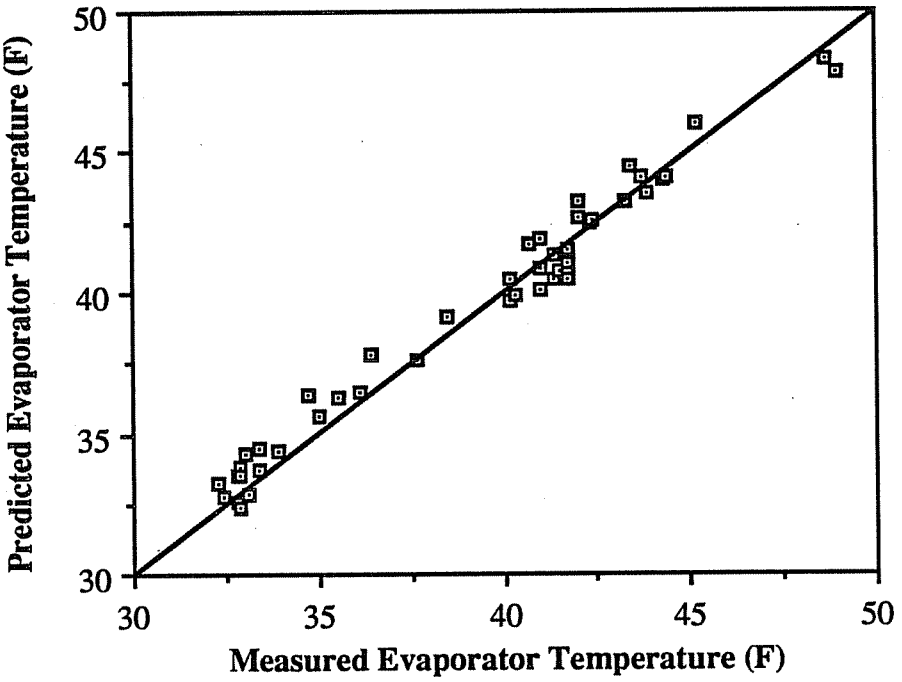

Figure 2.3. Comparison of Modeled Evaporating Temperatures with D/FW Data

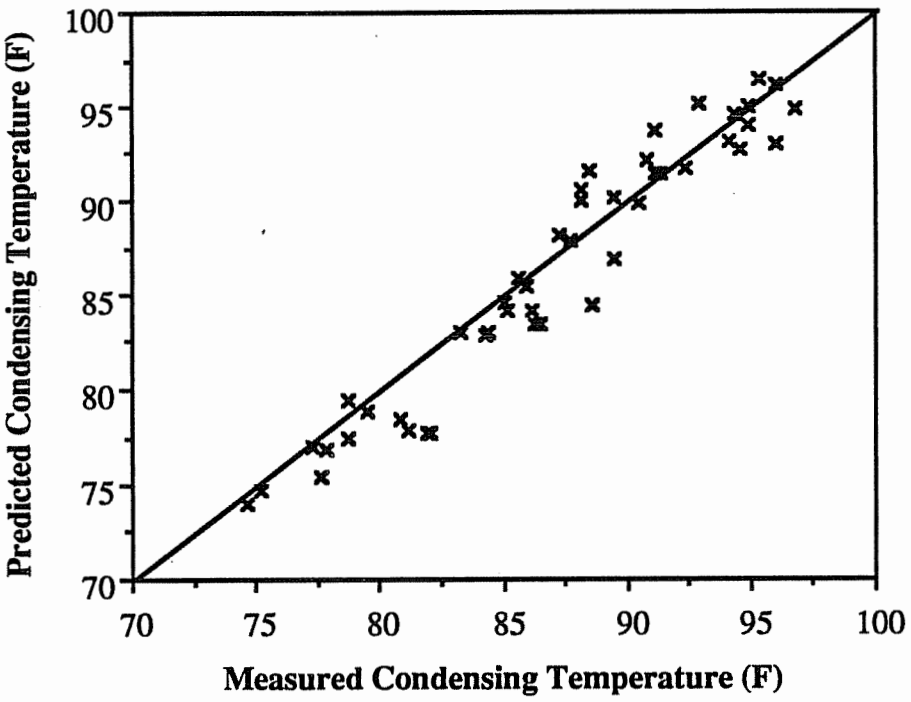

Figure 2.4. Comparison of Modeled Condensing Temperatures with D/FW Data

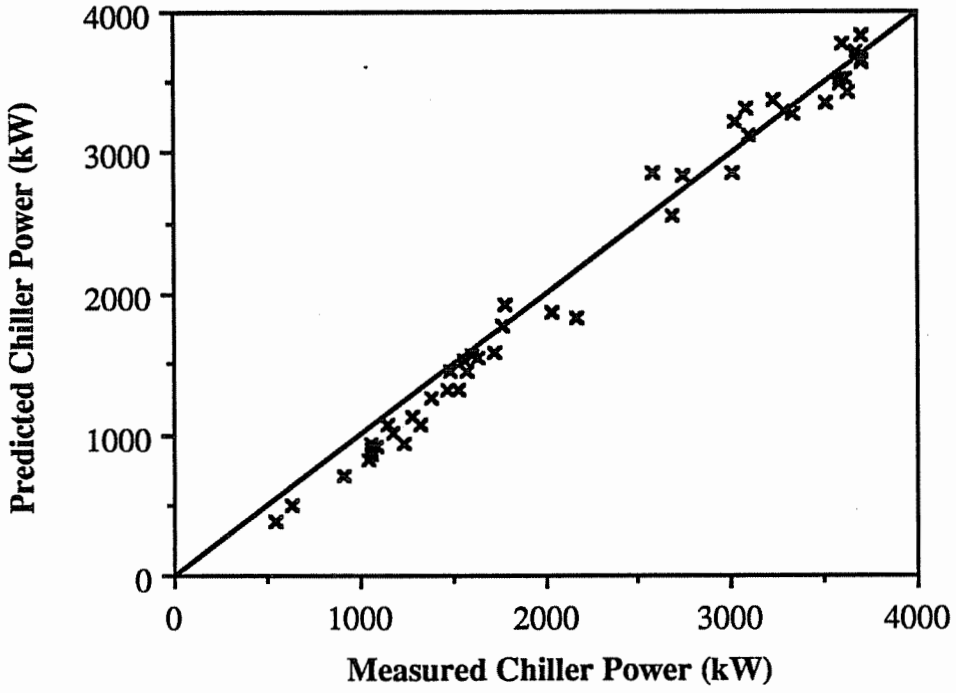

Figure 2.5. Comparison of Modeled Chiller Power with D/FW Data

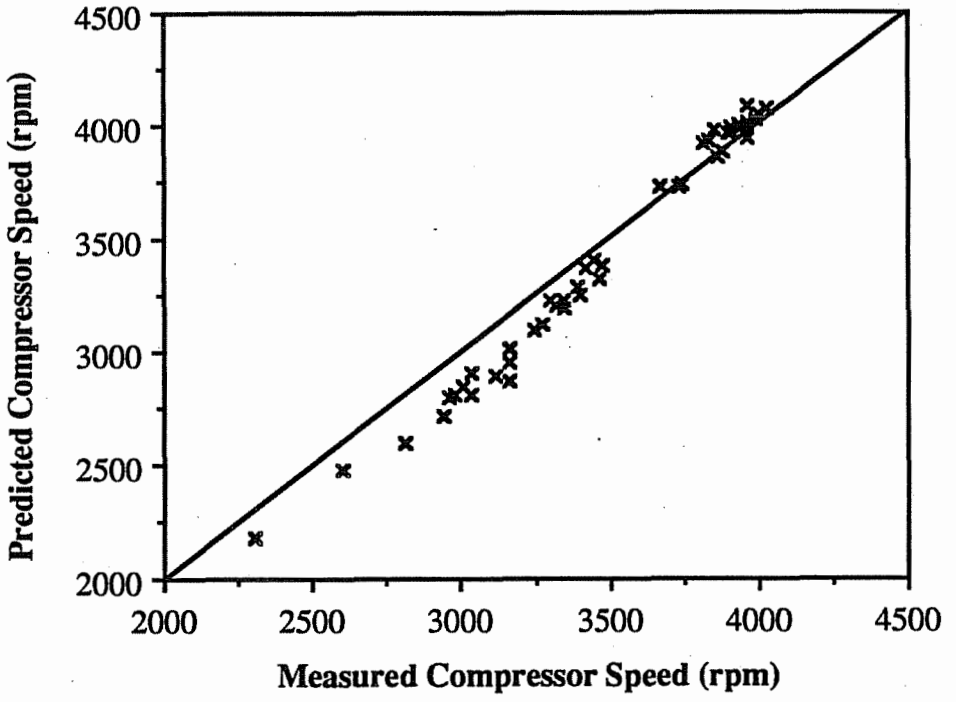

Figure 2.6. Comparison of Modeled Compressor Speeds with D/FW Data

The D/FW measurements were originally recorded on magnetic tape at one minute intervals. For the comparisons of Figures 2.3 - 2.6, the data were selected randomly. Part of the variability in these results may be a result of unsteady conditions. As another test of the accuracy of the model, controlled tests were performed on the chiller and compared with model predictions for a range of conditions. The conditions for all measurements were stabilized for at least 15 minutes. Both the chilled and condenser water flow rates were held relatively constant for all tests. The results of the comparisons as summarized in Table 2.3 show that the model agrees well with the data. Once again, the estimates of power consumption are better than for compressor speed. The root-mean-square of the differences is 84 kW for power and 140 rpm for compressor speed. The relative error of the power consumption estimates is larger at low loads. This may be due in part to the much larger uncertainty in the load evaluation

at this condition. Errors in measurements of chilled water temperature differences used to determine the chiller load, have a much more significant effect when the differences are small.

Table 2.3
Comparisons of Chiller Model with Controlled Tests

Load(tons)	T_{chws}(F)	T_{cwr}(F)	Power (kW)		Speed (rpm)	
			Data	Model	Data	Model
1375	40	57	364	302	2350	2177
2475	41	64	650	755	2600	2695
2800	40	69	1010	1082	3100	2992
2750	40	79	1411	1421	3400	3258
2710	40	64	805	867	1400	1563
1355	50	57	126	134	1400	1562
5420	40	69	2416	2248	3600	3572
5460	40	76	2736	2774	3700	3755
5420	40	86	3580	3519	3900	3971
2690	50	62	415	461	2700	2498
2750	50	69	610	689	2700	2497
2730	50	82	1299	1154	3200	2955
4065	50	64	940	864	2650	2624
4065	50	75	1316	1391	3000	3004

2.1.4 Surge Predictions

The operating temperature and pressure of the refrigerant in the evaporator are uniquely determined by the chilled water load, the water flow rate, and the chilled water setpoint. Similarly, the condensing pressure depends upon the total heat rejection and the condenser water stream conditions. A surge condition occurs when the compressor is unable to develop a discharge pressure sufficient to satisfy the condenser heat rejection requirements. This results in an unstable mode of operation in which the total

flow in the compressor oscillates.

A mathematical characteristic of the surge condition is that it first develops at a point of zero slope of the compressor discharge pressure versus flow relationship. This also corresponds to a point of zero slope of the compressor speed versus chiller loading characteristic. Figure 2.7 shows results of the model for required compressor

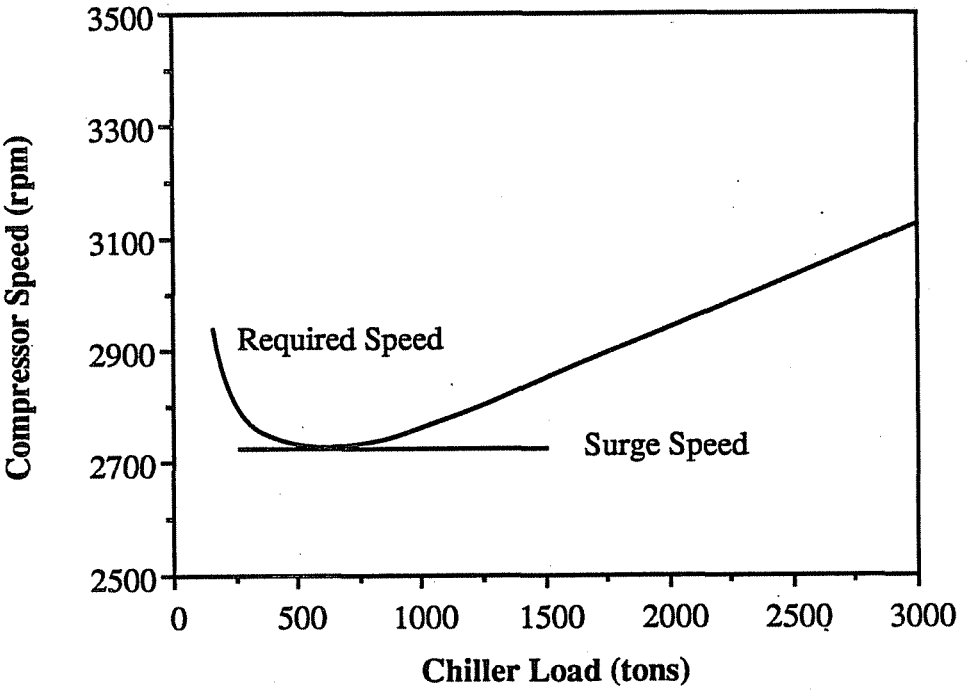

Figure 2.7. Modeled Compressor Speed Versus Load Requirement

speed versus loading. The modeled surge point occurs at the minimum speed. To the left of this point the model predicts that the compressor speed increases with decreasing load. The minimum modeled compressor speed is 2700 rpm at a load of about 500 tons. It is difficult to predict the load associated with the development of surge. As evident in Figure 2.7, the chiller cooling capacity is more sensitive to compressor speed

near the surge point. The determination of the onset of surge requires a subjective decision and cannot be measured directly. In this work, the approach used in modeling surge is to first determine the minimum possible compressor speed for any given set of conditions. The point at which surge develops is then assumed to occur at 50 rpm's greater than this minimum. At this point, Figure 2.7 indicates that there is essentially a linear relationship between speed and chiller capacity.

The chiller model is easily adapted to determine the compressor speed at which surge first occurs for a given set of chilled and condenser water conditions. An optimization routine, such as golden section search, is used to calculate the minimum compressor speed as a function of chiller loading. A program listing for determining the surge point is given by Braun [1988].

Figure 2.8 shows a comparison of compressor speeds at which surge develops for the model and D/FW data as a function of the temperature difference between the leaving condenser and evaporator water flow streams. The agreement is surprisingly good.

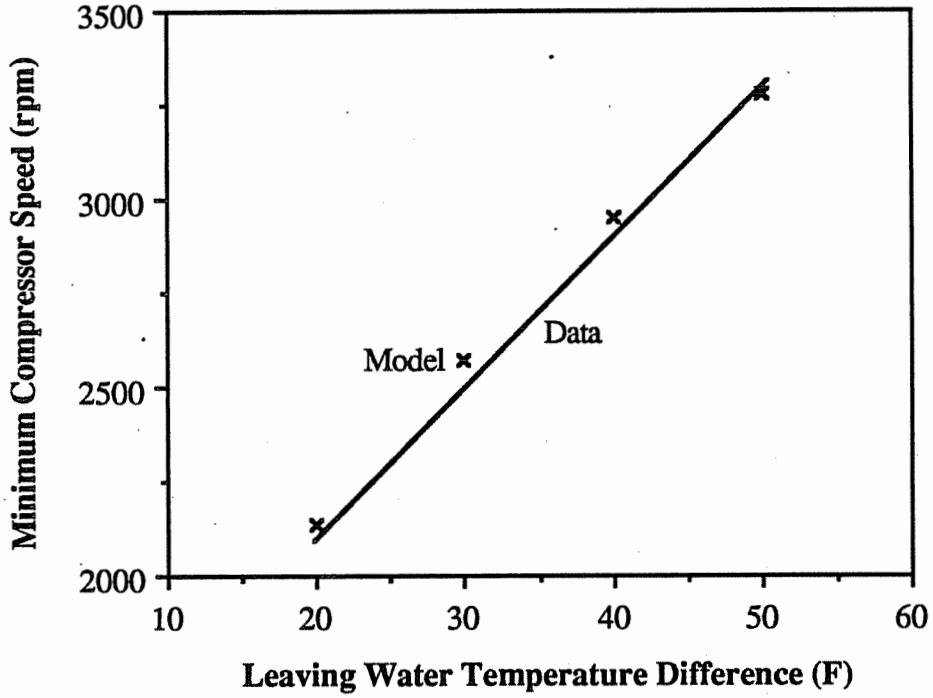

Figure 2.8. Comparison of Modeled Surge Speed with D/FW Data

2.2 A Model for Correlating Performance Data

The mechanistic model described in the previous section is useful for investigating the performance of variable-speed chillers in detail. However, it requires too much computation to be used in system simulation or optimization studies. In this section, a simpler empirical model for correlating the performance of variable or fixed-speed chillers is presented.

There are five independent input variables that uniquely define the performance of a chiller. One possible set of independent variables is 1) chilled water load, 2) chilled water supply temperature, 3) chilled water flow rate, 4) leaving condenser water temperature, 5) condenser water flow rate. Alternatively, entering chilled water and condenser water temperatures could be utilized in place of leaving conditions.

By correlating chiller performance in terms of leaving rather than entering

temperatures, the dependence on either the chilled water or condenser water flow rate is not significant. Figure 2.9 shows the effect of chilled and condenser water flow rates on the coefficient of performance (COP) of the D/FW variable-speed chiller determined with the mechanistic model described in Section 2.1. In the normal operating range of

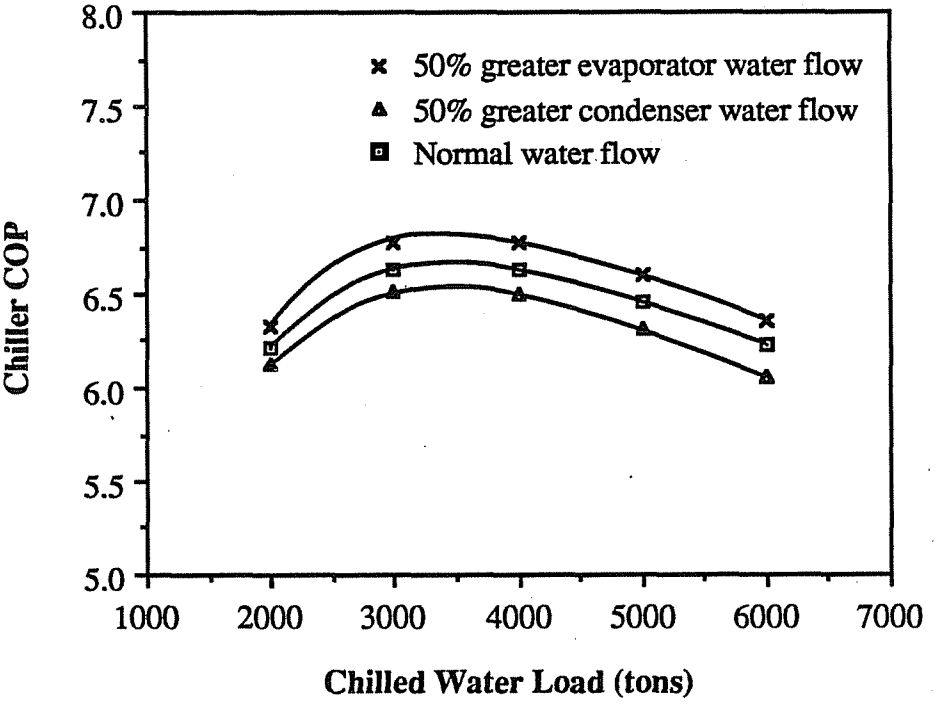

Figure 2.9. Effect of Water Flow Rates on Chiller Performance for Fixed Leaving Water Temperatures

this chiller, the effect of variations in either flow rate on the overall chiller performance is relatively small (< 2%) when the results are presented in terms of leaving water temperatures. It is interesting to note that reducing the evaporator flow shows an improvement in the performance. This results from the characterization of the performance in terms of the load and leaving chilled water temperature. For a given load and chilled water setpoint, a lower flow gives a higher chilled water return temperature. Assuming that this dominates over the reduced heat transfer coefficient

effect, the evaporation temperature rises and the performance improves. In practice, the chilled water return temperature is constrained by comfort considerations at the distribution points to the load.

The number of independent variables effecting the chiller performance is reduced to three, when utilizing leaving evaporator and condenser water temperatures and neglecting the effect of variations in flow rate. Correlating chiller performance may be further simplified by utilizing the difference between the leaving condenser and evaporator water temperatures as an independent variable rather than the individual temperatures. Figure 2.10 shows a comparison between modeled chiller COP as a function load for a leaving water temperature difference of 40 F for different chilled water supply and leaving condensing water temperatures. The performance is

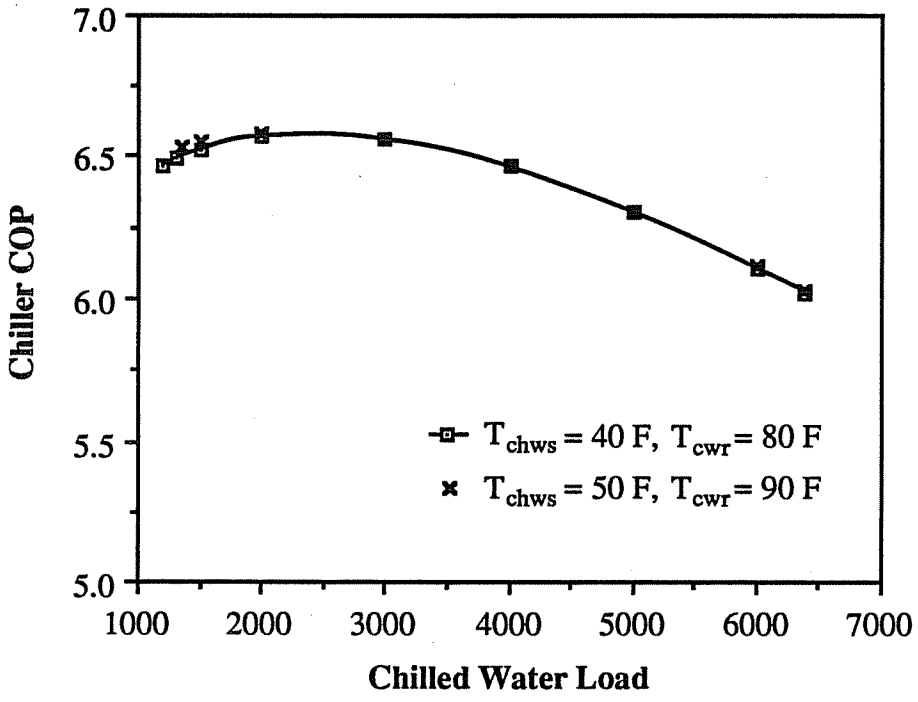

Figure 2.10. Dependence of Chiller Performance on Leaving Water Temperatures for Fixed Temperature Differences

nearly independent of the individual leaving evaporator and condenser water temperatures, depending primarily upon their difference. Similar results were obtained for a range of other conditions.

Results of the mechanistic chiller model indicate that chiller power consumption is primarily a function of only two variables, the load and the temperature difference between the leaving condenser and chilled water flows. The following functional form correlates the chiller power in terms of these variables.

$$\frac{P_{ch}}{P_{des}} = a_0 + a_1X + a_2X^2 + a_3Y + a_4Y^2 + a_5XY \qquad (2.2.1)$$

where X is the ratio of the chiller load to a design load, Y is the leaving water temperature difference divided by a design value, P_{ch} is the chiller power consumption, and P_{des} is the power consumption associated with the design conditions. The empirical coefficients of the above equation (a_0, a_1, a_2, a_3, a_4, and a_5) are determined with linear least-squares curve-fitting applied to measured or modeled performance data.

It is also necessary to model the limits of chiller operation associated with maximum chiller capacity and compressor surge. The following relationships were found to work well for estimating the maximum and minimum capacities.

$$X_{max} = b_0 + b_1Y \qquad (2.2.2)$$

$$X_{min} = c_0 + c_1Y + c_2Y^2 \qquad (2.2.3)$$

where X_{max} and X_{min} are the maximum and minimum possible chilled water loads associated with the capacity and surge limits divided by the design load. Again, the empirical coefficients of the above equations are determined with linear regression applied to measurements or model generated data.

In order to estimate chiller power consumption using the above relationships, it is necessary to know the leaving water temperatures. The chiller is controlled to give a specified leaving chilled water temperature. The leaving condenser water temperature, on the other hand, is not known. It depends upon the entering conditions, load, and power consumption. An implicit relationship for the dimensionless leaving water temperature difference results from the use of an overall energy balance on the chiller.

$$\dot{Q}_e + \eta_m P_{des}(a_0 + a_1 X + a_2 X^2 + a_3 Y + a_4 Y^2 + a_5 XY) = \dot{m}_{cw} C_{pw}\left[Y(T_{cwr} - T_{chws})_{des} - (T_{cws} - T_{chws})\right] \quad (2.2.4)$$

Equation (2.2.4) is quadratic in Y and may solved explicitly. If the design conditions are appropriately chosen, then Y will typically vary between about 0.2 and 1. This may be used as a criteria for selecting between the two solutions of equation (2.2.4).

If the specified chiller load falls outside of the limits imposed by equations (2.2.2) and (2.2.3), then it is necessary to adjust the setpoint such that operation occurs at the limit. In this case, the load is given by equations (2.1.3) and (2.2.2) or (2.2.3) and Y is determined with (2.2.4). These equations are solved to find the load, chilled water setpoint, and value of Y that give performance at the operation limit. Equation (2.2.1) is then used to evaluate the chiller power consumption.

The empirical relationships for estimating chiller power consumption and the capacity and surge limits were tested over a wide range of operating conditions using data derived from the mechanistic model of a variable-speed chiller. In all cases, these

models provided an excellent fit to the generated data.

The model for power consumption was also fit to measurements from the D/FW airport system for both variable and fixed-speed control. Tests were performed for both types of control at nearly identical conditions. Table 2.4 summarizes the results of these tests. The test conditions are given in sets of two. The first of each set is for the variable-speed measurements, the second for fixed-speed control. The chilled and condenser water flow rates were held constant for these tests. The compressor speed for the fixed-speed, vane control tests was also held constant at 4000 rpm and the inlet pre-rotation and outlet diffuser vanes were operated using the automatic control implemented by the manufacturer.

Table 2.4
Measurements of the D/FW Chiller Performance
for Variable and Fixed-Speed Control

Test	Load(tons)	T_{chws}(F)	T_{cwr}(F)	Power Consumption (kW)	
				Variable-Speed	Fixed-Speed
1	1375, 1355	40, 40	57, 58	364	860
2	2475, 2625	41, 40	64, 62	650	1410
3	2800, 2710	40, 40	69, 69	1010	1800
4	2750, 2670	40, 40	79, 80	1411	1930
5	2710, 2710	40, 40	64, 64	805	1410
6	1355, 1625	50, 49	57, 57	126	1036
7	5420, 5420	40, 40	69, 70	2416	2780
8	5460, 5420	40, 40	76, 76	2736	2736
9	5420, 5420	40, 40	86, 86	3580	3627
10	2690, 2710	50, 50	62, 62	415	1560
11	2750, 2750	50, 50	69, 69	610	1326
12	2730, 2730	50, 50	82, 82	1299	1830
13	4065, 4065	50, 50	64, 64	940	2446
14	4065, 4065	50, 50	75, 75	1316	2480

Figure 2.11 shows a comparison between measured and correlated chiller power consumption. Separate curve-fits were performed for the D/FW chiller operated with both variable and fixed-speed control. The design conditions for equation (2.2.1) were taken to be those associated with the maximum measured power consumption. The root-mean-square of the error in the modeled power is 64 kW for the variable-speed and 152 kW for the fixed-speed control. The larger errors for fixed-speed

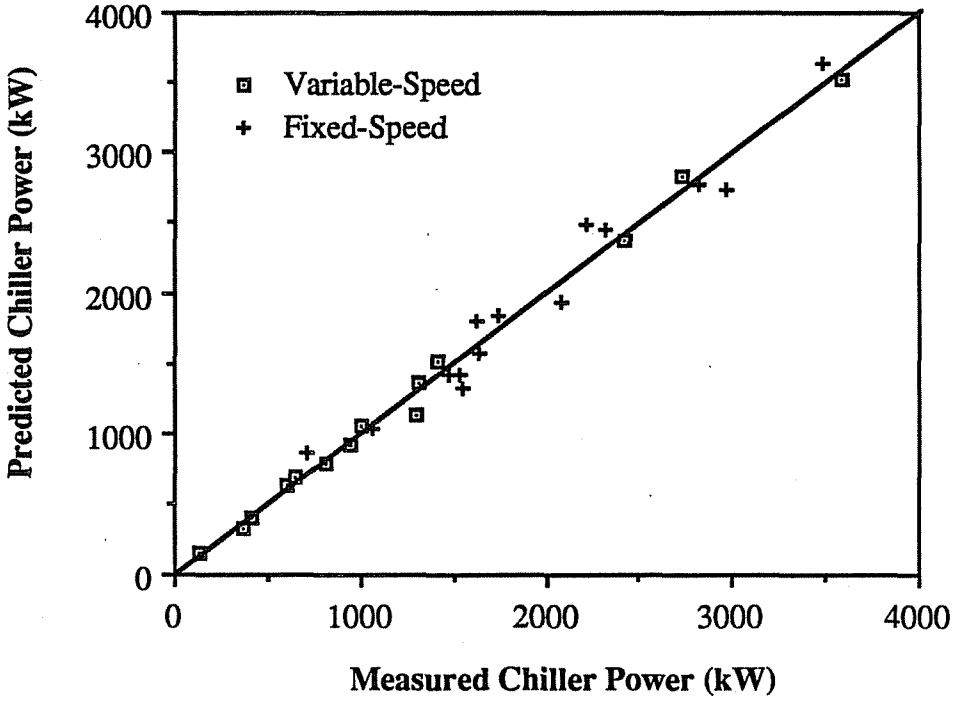

Figure 2.11. Comparison of Measured and Correlated Chiller Power

operation may be due to a more unstable control characteristic. In examining the test results in Table 2.4, there is more inconsistency in the results of the fixed-speed tests. For instance, in comparing tests 7 and 8 (or 13 and 14), the only condition that changed appreciably was the leaving condenser water temperature. However, the power

consumption associated with vane control did not increase as would be expected. In this mode of operation, both the inlet and outlet vanes are adjusted in some automatic fashion to meet the desired conditions. Therefore, it is possible to realize the same conditions with different power consumptions. The inconsistencies in the fixed-speed measurements and resulting errors in the empirical fit to the data may be due to inconsistent control of the inlet and outlet compressor vanes.

2.3 Performance Characteristics of the D/FW Chiller

The performance of the D/FW chiller operated with both variable and fixed-speed control may be compared directly through the test results of Table 2.4. At all part-load conditions, the performance associated with the variable-speed control is superior. However, the power requirements come together at loads approaching the capacity of the chiller. This is expected, since at this condition the vanes are wide open and the speed under variable-speed control approaches that of the fixed-speed operation.

In order to see the differences between variable and fixed-speed operation more clearly, their performance was correlated using the form of equation (2.2.1). Figures 2.12 and 2.13 show chiller performance for both controls in terms of COP as a function of load for different condenser to evaporator leaving water temperature differences. For the variable-speed control, the COP reaches a maximum at part-load conditions. This peak occurs as a result of tradeoffs between increasing heat transfer efficiencies due to decreased water to refrigerant temperature differences in the evaporator and condenser and the decreased polytropic efficiencies of the compressor that occur at low refrigerant flow rates. The peak COP moves to lower loads at lower temperature differences.

It is typical for centrifugal chillers with either variable or fixed-speed control to exhibit a peak in performance at part-load conditions of between 40% to 70% of the

chiller design capacity. However, the fixed-speed performance data shown in Figure 2.13 does not exhibit such a peak. The best performance occurs at the capacity of the chiller. The capacity of the D/FW chiller was derated when retrofit with a different refrigerant, so that the evaporator and condenser are oversized at the current capacity relative to the original design capacity. As a result, the performance is more sensitive to penalties associated with part-load operation of the compressor than to heat exchange improvements. Part of the improvement with variable-speed chiller control may result from the unique characteristics of the D/FW chiller.

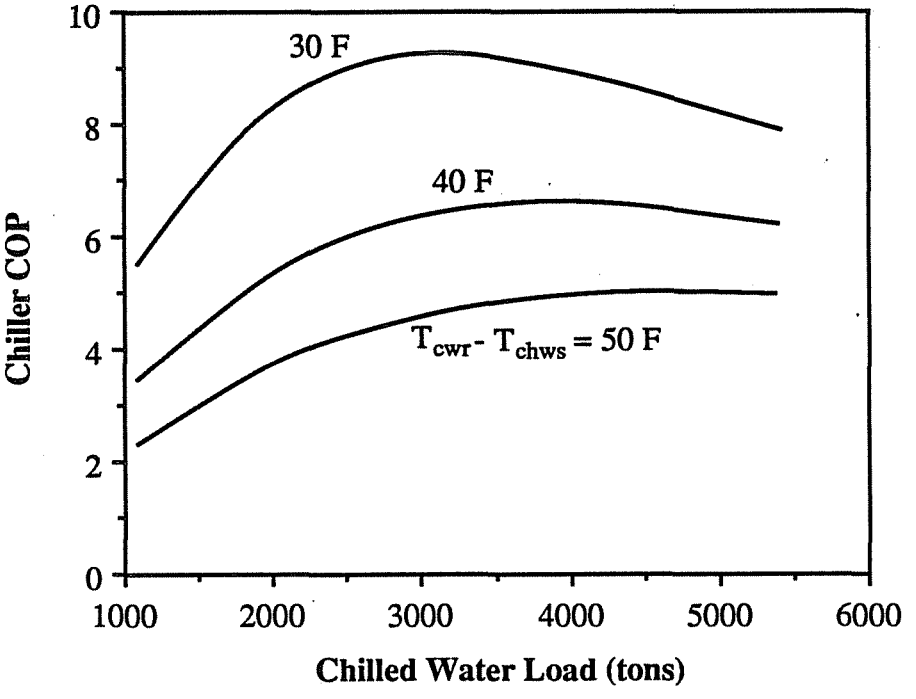

Figure 2.12. D/FW Chiller COP for Variable-Speed Control

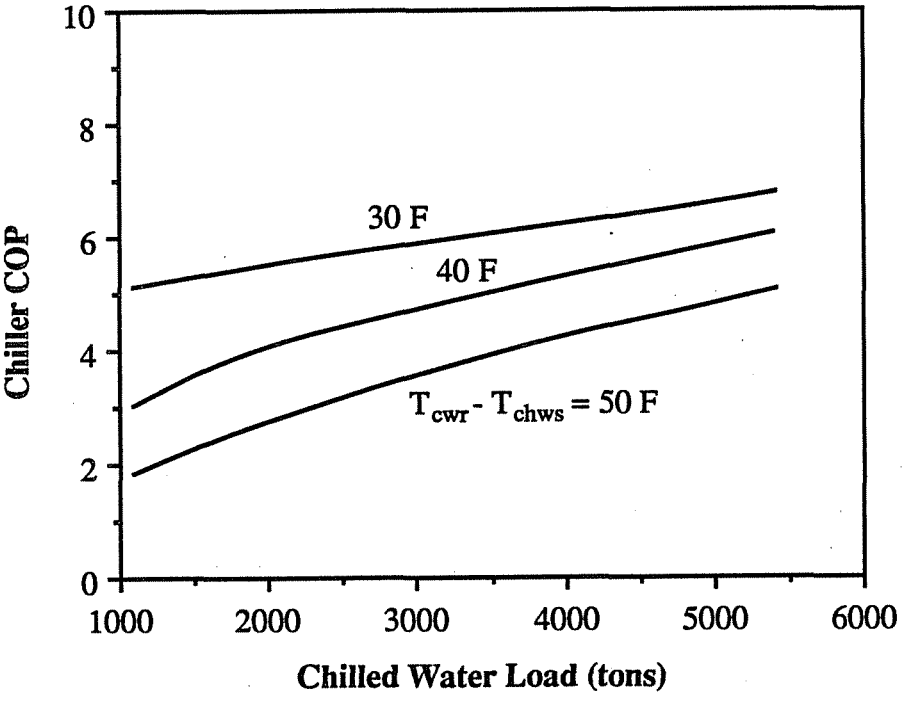

Figure 2.13. D/FW Chiller COP for Vane Control

Figure 2.14 shows a direct comparison of the results of Figures 2.12 and 2.13. The ratio of power under variable-speed control to that with vane control is plotted as a function of load and leaving water temperature differences. At typical summer conditions of 5500 tons and temperature differences of between 40 and 50 F, the performance ratio is near unity. As the load decreases, the COP of the variable-speed control increases, while that associated with fixed-speed operation is reduced. At part-load conditions of about 3000 tons and temperature differences between 30 and 40 F, the variable-speed control uses about 30% less power.

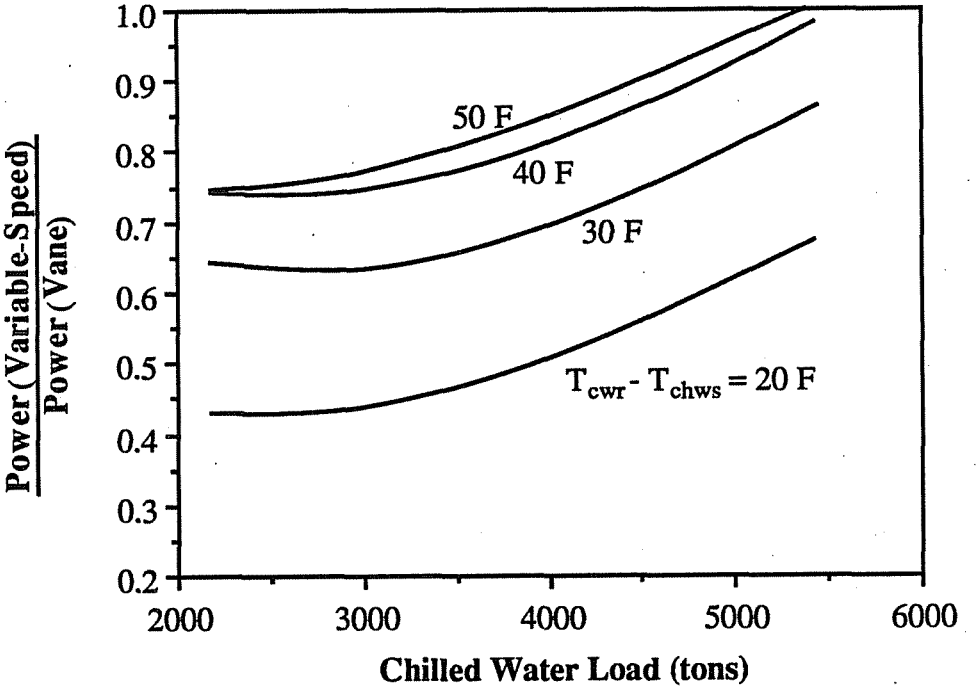

Figure 2.14. Comparison of Chiller Power Consumptions under Vane and Variable-Speed Control

The mechanistic chiller model is useful for studying the effect of different refrigerants on the overall chiller performance. Figure 2.15 shows COP as a function of load for R-500, R-22, and R-12 at a leaving water temperature difference of 30 F. The D/FW chiller as installed was charged with R-22. Upon retrofit with a variable-speed drive, the refrigerant was changed to R-500. Since the maximum chiller load is generally less than about 5500 tons, Figure 2.15 indicates that this was a relatively good choice. Overall, R-22 does well at very high loads, both R-12 and R-500 are good at loads near 5500 tons, and R-12 is a clear choice at lower loads. It appears that R-12 may be a better overall choice than R-500 for the D/FW system.

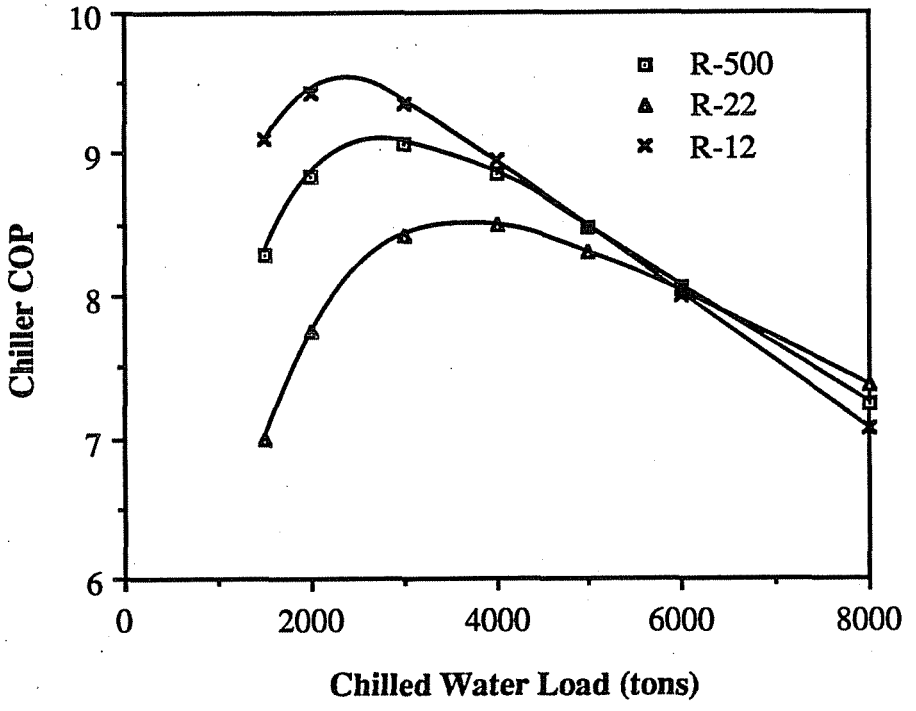

Figure 2.15. Effect of Refrigerant Type on Chiller Performance

2.4 Summary

A detailed mechanistic model for variable-speed centrifugal chillers was developed. The model requires only design parameters and the operating conditions in order to estimate the power requirement. The model is also capable of estimating the compressor speed at which surge develops or the maximum chiller cooling capacity at a given power input or speed. Results of the model compare favorably with measurements from the D/FW airport for both power requirement and the speed associated with the onset of surge.

Using results of the mechanistic model, a simpler empirical model for correlating performance data was also identified. Chiller power consumption is correlated as a quadratic function of only two variables, the load and temperature difference between the leaving condenser and chilled water flows. This model fits data for both variable-

speed and fixed-speed with vane control chillers. Models for correlating the limits of chiller operation associated with surge and capacity were also presented.

Results of the models were used to study the performance of the D/FW chiller. Data for both variable-speed with wide-open vanes and fixed-speed with vane control were correlated using the empirical model and compared over a wide range of conditions. At design conditions, the power consumption associated with the two controls is essentially equal. At 60% of the design load, the variable-speed operation requires 50% to 80% of the power requirements for fixed-speed, vane control. The magnitude of the improvement depends upon the temperature difference between the leaving condenser and chilled water streams. The use of different refrigerants was also investigated. The peak performance associated with using R-500 shows on the order of 5 - 10% improvement over the original charge of R-22.

Chapter 3
Condenser-Side Component Models

In this chapter, models are presented for cooling towers and condenser water pumping requirements. These are the primary components associated with rejecting heat from chiller condensers to the environment.

3.1 Effectiveness Models for Cooling Towers

This section presents a simple, yet mechanistic method for modeling the performance of cooling towers. Through the introduction of an air saturation specific heat, effectiveness relationships are developed. The advantages of this approach are its simplicity, accuracy, and consistency with the methods for analyzing sensible heat exchangers. The accuracy of the effectiveness model is as good or better than that associated with standard methods presented in the literature and has significantly less computational requirements.

The first practical theory of cooling tower operation was developed by Merkel [1925]. Merkel's method has been the basis of most cooling tower analyses (Nottage [1941], Lichtenstein[1943], Mickley [1949], Carey [1950], Webb [1984]) and is outlined in the ASHRAE Equipment Guide [1983].

In the Merkel analysis, the water loss due to evaporation is neglected and a Lewis number of unity is assumed. The determination of outlet states requires an iterative numerical integration of two differential equations. A more rigorous analysis of a cooling tower that did not utilize the assumptions of Merkel was performed by Sutherland [1983]. He found that counterflow cooling towers can be undersized between 5% and 15% through the use of the Merkel method if "true" mass transfer

coefficients are used. In practice, however, the errors are not nearly as large, because the mass transfer coefficients utilized in the Merkel method are generally determined by matching results of the model to measurements from small-scale tests. Another approach for modeling cooling towers was presented by Whillier [1976]. Whillier developed a simple method for correlating performance data. However, this method is not useful for design purposes.

In this section, an effectiveness model is developed for cooling towers by utilizing the assumption of a linearized air saturation enthalpy. On its own, the linearization is not a unique contribution. It was utilized for cooling coils by Threlkeld [1970] and suggested for, but not evaluated for cooling towers by Nizet [1985]. Berman [1961] described a log-mean enthalpy method for analyzing cooling towers that implicitly assumes a linear saturation curve. Maclaine-Cross [1985] also developed a model for wet surface heat exchangers that incorporated the assumption of a linearized saturation humidity ratio. Recently, an effectiveness model for cooling towers was also presented by Jaber and Webb [1987]. The contributions of the work described in this chapter are primarily: 1) development of the basic equations leading to effectiveness relationships for cooling towers analogous to those for sensible heat exchangers, 2) development of a simple method for estimating the water loss in cooling towers, and 3) validation of the methodologies over wide ranges of conditions. Results of the methods are compared with both numerical solutions to the detailed heat and mass transfer modeling equations and with measurements. In Chapter 4, a similar analysis is applied to modeling the performance of cooling coils.

3.1.1 Detailed Analysis

The assumptions and basic equations employed here closely follow those of Sutherland [1983]. A schematic of a counterflow cooling tower showing pertinent states and dimensions is given in Figure 3.1.

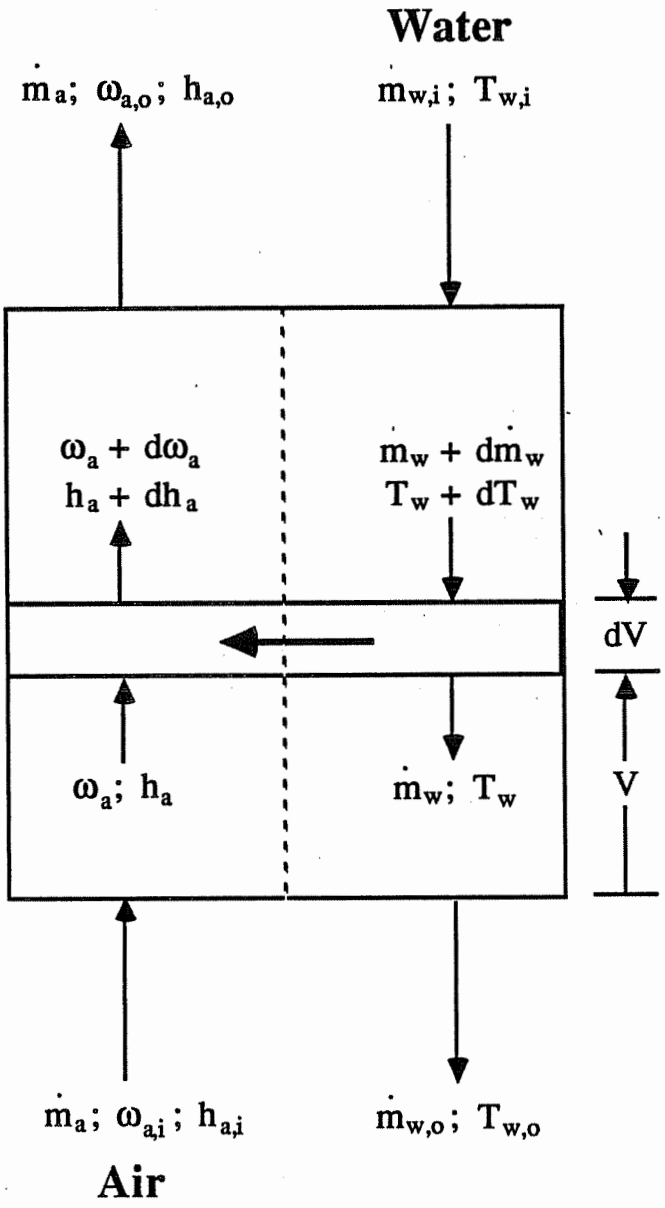

Figure 3.1. Schematic of a Counterflow Cooling Tower

For negligible heat transfer from the tower walls, a steady-state energy balance on the incremental volume, dV, gives the following relation between the water and air enthalpies.

$$\dot{m}_a dh_a = d(\dot{m}_w h_{f,w})$$

$$= \dot{m}_w dh_{f,w} + h_{f,w} d\dot{m}_w \qquad (3.1.1)$$

where,

$\dot{m}_a$ = mass flow rate of dry air

h_a = enthalpy of moist air per mass of dry air

$\dot{m}_w$ = mass flow rate of water

$h_{f,w}$ = enthalpy of liquid water

Relationships for the incremental water loss, $d\dot{m}_w$, and the water flow rate at any point within the tower, $\dot{m}_w$, are determined from steady-state mass balances on the water.

$$d\dot{m}_w = \dot{m}_a d\omega_a \qquad (3.1.2)$$

$$\dot{m}_w = \dot{m}_{w,i} - \dot{m}_a(\omega_{a,o} - \omega_a) \qquad (3.1.3)$$

where,

ω_a = local air humidity ratio

$\dot{m}_{w,i}$ = inlet water flow rate

$\omega_{a,o}$ = outlet air humidity ratio

From equations (3.1.1), (3.1.2), and (3.1.3) and assuming a constant water

specific heat, the change in water temperature across the incremental control volume (water inlet minus outlet) is

$$dT_w = \frac{dh_a - C_{pw}(T_w - T_{ref})d\omega_a}{\left[\frac{\dot{m}_{w,i}}{\dot{m}_a} - (\omega_{a,o} - \omega_a)\right]C_{pw}} \tag{3.1.4}$$

where T_w is the local water temperature, T_{ref} is the reference temperature for zero enthalpy of liquid water, and C_{pw} is the constant pressure specific heat of liquid water.

The incremental increase in enthalpy of the air stream is equal to the rate of energy transfer from the water droplets due to both heat and mass transfer or

$$\dot{m}_a dh_a = h_C A_V dV(T_w - T_a) + h_{g,w}\dot{m}_a d\omega_a \tag{3.1.5}$$

where,

h_C = convection heat transfer coefficient

A_V = surface area of water droplets per unit volume of cooling tower

$h_{g,w}$ = enthalpy of water vapor at the local water temperature.

Assuming that the mass fraction of water vapor in the mixture of air and vapor is approximately equal to the humidity ratio, the rate of mass transfer of water vapor to the air stream may be expressed as

$$\dot{m}_a d\omega_a = h_D A_V dV(\omega_{s,w} - \omega_a) \tag{3.1.6}$$

where

h_D = mass transfer coefficient

$\omega_{s,w}$ = saturated air humidity ratio at the local water temperature.

Substituting equation (3.1.6) into (3.1.5) and making use of the Lewis number definition ($Le = h_C/(h_D C_{pm})$) and the definitions for the enthalpy of water vapor, the result may be written as

$$\dot{m}_a h_a = h_D A_V dV\left[Le C_{pm}(T_w - T_a) + (\omega_{s,w} - \omega_a)h_{g,w}\right]$$

$$= Le h_D A_V dV\left[(h_{s,w} - h_a) + (\omega_{s,w} - \omega_a)(1/Le - 1)h_{g,w}\right] \qquad (3.1.7)$$

where,

C_{pm} = constant pressure specific heat of moist air = $C_{pa} + \omega_a C_{pv}$

C_{pa} = constant pressure specific heat of dry air

C_{pv} = constant pressure specific heat of water vapor

h_{go} = enthalpy of water vapor at 0 degree reference level

The overall number of transfer units for mass transfer is defined as

$$Ntu = \frac{h_D A_V V_T}{\dot{m}_a} \qquad (3.1.8)$$

where V_T is the total tower volume. Utilizing the Ntu definition, equations (3.1.6) and (3.1.7) may be reduced to

$$\frac{d\omega_a}{dV} = -\frac{Ntu}{V_T}(\omega_a - \omega_{s,w}) \tag{3.1.9}$$

$$\frac{dh_a}{dV} = -\frac{Le\ Ntu}{V_T}\left[(h_a - h_{s,w}) + (\omega_a - \omega_{s,w})(1/Le - 1)h_{g,w}\right] \tag{3.1.10}$$

For given Ntu, Le, and inlet conditions, equations (3.1.9), (3.1.10), and (3.1.4) may be solved numerically for the exit conditions of both the air and water stream. The solution is iterative with respect to two variables, $\omega_{a,o}$ and $T_{w,o}$. At each iteration, equations (3.1.9), (3.1.10), and (3.1.4) are integrated numerically over the entire tower volume from air inlet to outlet.

3.1.2 Merkel Analysis

In order to simplify the analysis, Merkel [1925] made two assumptions. Most significantly, he neglected the effect of the water loss due to evaporation on the right-hand side of equation (3.1.1). In equation (3.1.1), this eliminates the last term and implies that the water flow rate at each point in the tower in the first term on the right-hand side is equal to the inlet flow. The second assumption is a Lewis number of unity. With these approximations, the equations for the cooling tower may be reduced to

$$\frac{dh_a}{dV} = -\frac{Ntu}{V_T}(h_a - h_{s,w}) \tag{3.1.11}$$

$$\frac{dT_w}{dV} = \frac{\dot{m}_a(dh_a/dV)}{\dot{m}_w C_{pw}} \tag{3.1.12}$$

The primary computational savings associated with the Merkel assumptions is that the solution of equations (3.1.11) and (3.1.12) is iterative with respect to a single variable, $T_{w,o}$, instead of two variables. However, the solution of equations (3.1.11) and (3.1.12) gives only the exit temperature of the water stream and exit enthalpy of the air stream. In order to obtain the exit humidity ratio, it is still necessary to numerically integrate equation (3.1.9) after the solution of equations (3.1.11) and (3.1.12) has been obtained.

3.1.3 Effectiveness Model

Equation (3.1.12) may be rewritten in terms of only air enthalpies by introducing the derivative of the saturated air enthalpy with respect to temperature evaluated at the water temperature.

$$\frac{dh_{s,w}}{dV} = \frac{\dot{m}_a C_s(dh_a/dV)}{\dot{m}_w C_{pw}} \tag{3.1.13}$$

where,

$$C_s = \left[\frac{dh_s}{dT}\right]_{T = T_w} \tag{3.1.14}$$

C_s has the units of specific heat and will be termed the saturation specific heat. If the saturation enthalpy were linear with respect to temperature, (i.e constant C_s), then

equations (3.1.11) and (3.1.13) could be solved analytically for the exit conditions. These equations are analogous to the differential equations that result for a sensible heat exchanger with C_s, h_a, and $h_{s,w}$ replaced by C_{pm}, T_a, and T_w. Figure 3.2 shows the variation of saturation enthalpy with temperature, along with a straight line connecting two typical water inlet and outlet states. It is apparent that the saturation enthalpy is not linear with respect to temperature. However, by choosing an appropriate average slope between inlet and outlet water conditions, as depicted in Figure 3.2, an effectiveness relationship may be derived in terms of C_s.

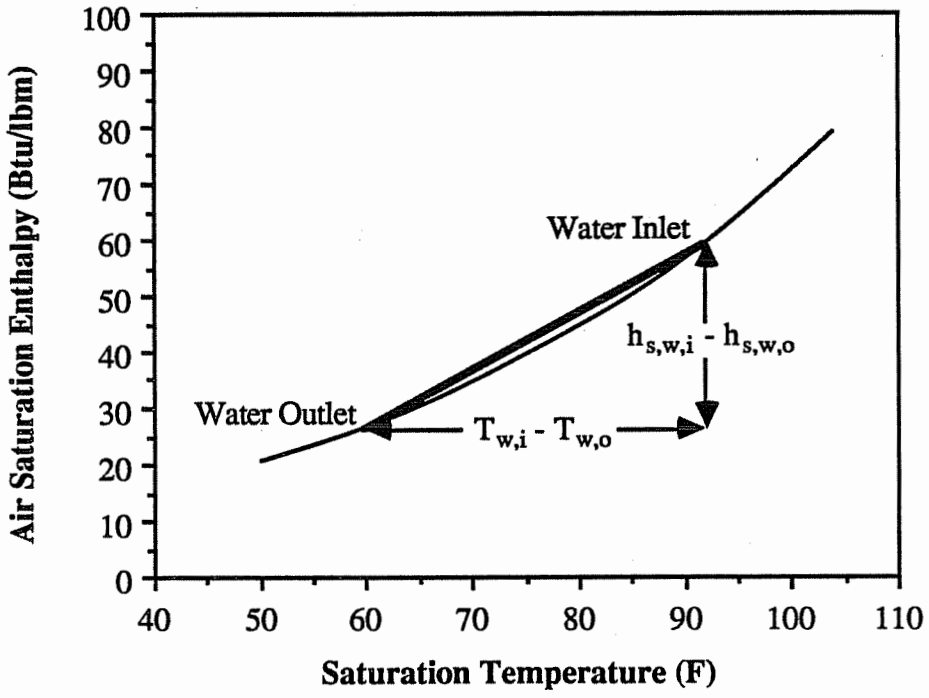

Figure 3.2. Saturation Air Enthalpy versus Temperature

Effectiveness is usually defined as the ratio of the actual to maximum possible heat transfer. However, when C_s is taken as the slope of the straight line between the water inlet and outlet conditions, then an air-side effectiveness rather than an overall

effectiveness relationship should be used. The air-side effectiveness is defined as the ratio of the actual heat transfer to the maximum possible air-side heat transfer that would occur if the exiting air stream were saturated at the temperature of the incoming water (i.e. $h_{a,o} = h_{s,w,i}$). The actual heat transfer is then given in terms of this effectiveness as

$$\dot{Q} = \varepsilon_a \dot{m}_a (h_{s,w,i} - h_{a,i}) \tag{3.1.15}$$

where, analogous to a dry counterflow heat exchanger, the effectiveness is evaluated as

$$\varepsilon_a = \frac{1 - \exp(-Ntu(1 - m^*))}{1 - m^* \exp(-Ntu(1 - m^*))} \tag{3.1.16}$$

where,

$$m^* = \frac{\dot{m}_a}{\dot{m}_{w,i}(C_{pw}/C_s)} \tag{3.1.17}$$

The exit air enthalpy and water temperature are determined from overall energy balances on the flow streams.

$$h_{a,o} = h_{a,i} + \varepsilon_a (h_{s,w,i} - h_{a,i}) \tag{3.1.18}$$

$$T_{w,o} = \frac{\dot{m}_{w,i}(T_{w,i} - T_{ref})C_{p,w} - \dot{m}_a(h_{a,o} - h_{a,i})}{\dot{m}_{w,o}C_{pw}} \tag{3.1.19}$$

Equation (3.1.19) is written in terms of the mass flow rates of water entering and leaving the cooling tower. The simplest strategy is to completely neglect the water loss as is done with the Merkel method. In this case, equations (3.1.15) - (3.1.19), along with psychrometric data, are sufficient for determining the overall heat transfer and exit conditions. The enthalpies associated with the inlet air and saturated air at the water inlet temperature are evaluated with a psychrometric chart or using empirical correlations as given in the ASHRAE Handbook of Fundamentals [1985]. The average saturation specific heat, C_s, is estimated as the average slope between the inlet and outlet water conditions.

$$C_s = \frac{h_{s,w,i} - h_{s,w,o}}{T_{w,i} - T_{w,o}} \tag{3.1.20}$$

Since C_s depends upon $T_{w,o}$, the solution of equations (3.1.15) - (3.1.20) is iterative. However, C_s is only weakly dependent upon the exit temperature, so that any reasonable initial guess of $T_{w,o}$ (such as the entering air wet bulb temperature) usually results in convergence in only 2 iterations.

3.1.4 Estimating the Water Loss

Due to water loss, the water flow rate exiting the cooling tower is on the order of 1% to 4% less than the entering flow rate. Neglecting this loss may result in up to a 2 degree Celcius error in the exit water temperature. This error can effect the calculated performance of other system equipment such as a chiller. The computation of the exit water temperature given by equation (3.1.19) is improved if the water loss is considered. It is also necessary to know the water loss in order to perform mass and

energy balances on the cooling tower sump. From an overall mass balance, the exit water flow rate is

$$\dot{m}_{w,o} = \dot{m}_{w,i} - \dot{m}_a(\omega_{a,o} - \omega_{a,i}) \tag{3.1.21}$$

The exit air humidity ratio could be determined by numerically integrating equation (3.1.9) over the tower volume. An alternative approach, which allows an analytic solution, is to assume that equation (3.1.9) is approximately satisfied over the entire tower volume with the local $\omega_{s,w}$ replaced with a constant appropriately averaged value. Assuming a Lewis number of unity, integration of equation (3.1.9) gives

$$\omega_{a,o} = \omega_{s,w,e} + (\omega_{a,i} - \omega_{s,w,e})\exp(-Ntu) \tag{3.1.22}$$

By integrating equation (3.1.11) for constant $h_{s,w}$, an effective saturation enthalpy is determined as

$$h_{s,w,e} = h_{a,i} + \frac{(h_{a,o} - h_{a,i})}{1 - \exp(-Ntu)} \tag{3.1.23}$$

The effective saturation humidity ratio, $\omega_{s,w,e}$, associated with $h_{s,w,e}$ is found from psychrometric data.

3.1.5 Model Comparisons

Figures 3.3 - 3.5 show comparisons between cooling tower results obtained with: 1) a detailed analysis defined by the numerical solution of equations (3.1.4), (3.1.9), and (3.1.10) with a Lewis number of unity; 2) the Merkel analysis; 3) the effectiveness model.

In Figure 3.3, cooling tower air heat transfer effectiveness is plotted versus Ntu for different ratios of water to air flow rate for entering conditions typical of those associated with heat rejection from the condenser of a chiller. Neglecting the water loss in the Merkel approach causes a slight underprediction in the cooling tower effectiveness resulting from a reduced mass transfer. Errors associated with the effectiveness method are primarily a result of the assumption of a linear saturation enthalpy relationship. Overall, both the Merkel and effectiveness models agree closely with the detailed analysis for these conditions.

Figure 3.4 shows cooling tower water temperature effectiveness results for the same conditions as for Figure 3.3. The water temperature effectiveness is defined as the ratio of the temperature difference between the inlet and outlet water to the maximum possible temperature difference if the leaving water were at the entering air wet bulb temperature. As a result of the water loss, this temperature effectiveness does not correspond to a heat transfer effectiveness. In Figure 3.4, the Merkel model somewhat overestimates the water temperature effectiveness due to the assumption of no water loss. The effectiveness model gives results that are closer to the more exact analysis.

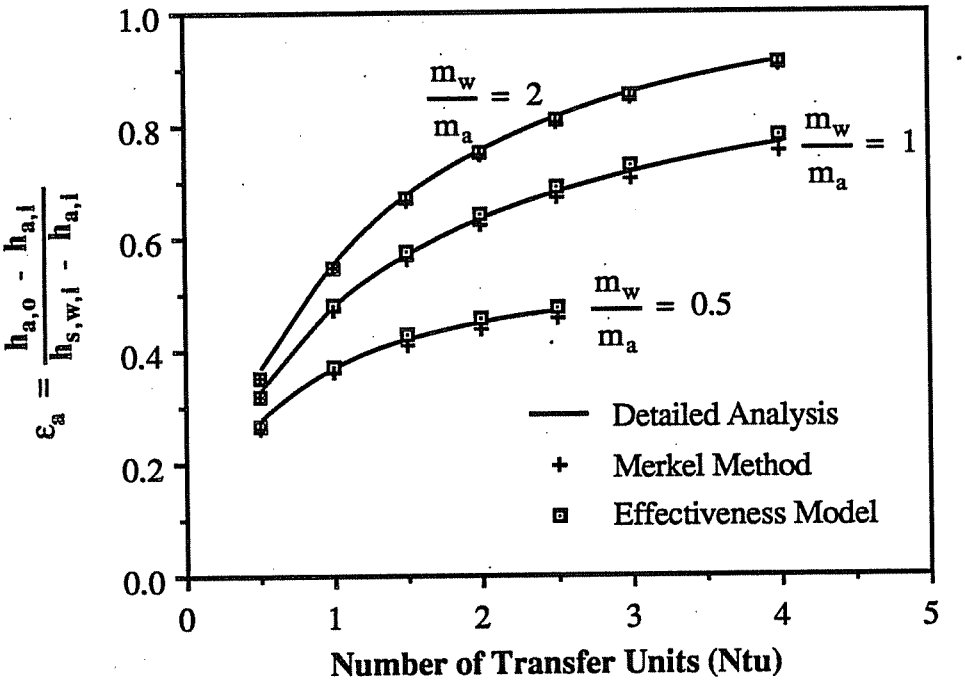

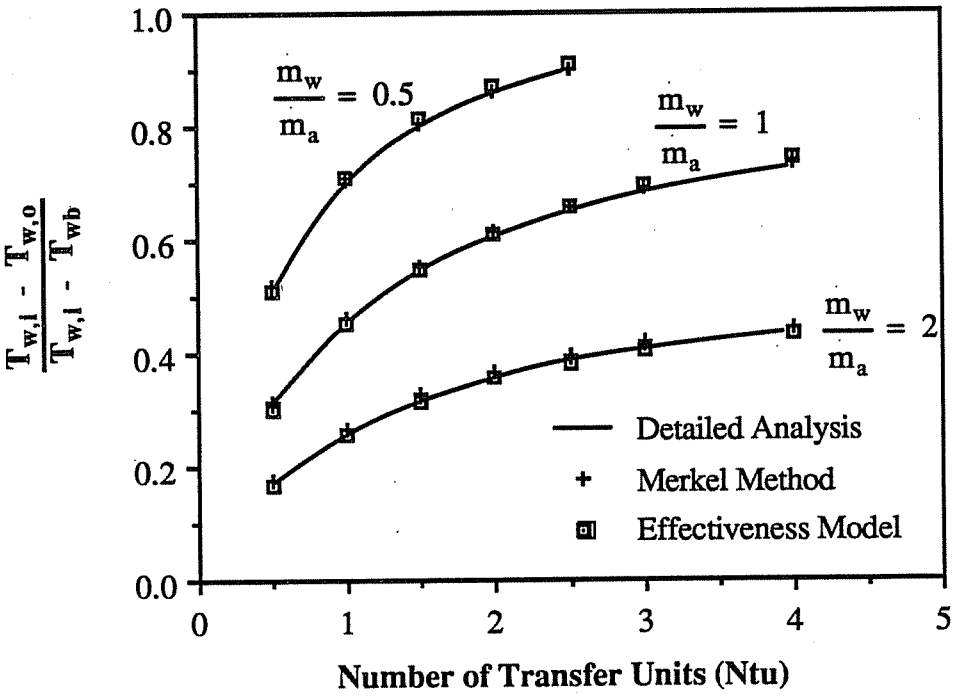

Figures 3.3 & 3.4. Air Heat Transfer and Water Temperature Effectiveness Comparisons (Dry Bulb, Wet Bulb, and Water Inlet Temperatures of 70 F, 60 F, 90 F)

Figure 3.5 gives comparisons between tower water loss evaluated with a detailed analysis and the loss determined using the simplified approach presented in Section 3.1.4 (The Merkel method neglects the water loss). Water loss as a percentage of the inlet water flow rate is plotted versus Ntu for different ratios of water to air flow rates. No significant differences are evident in these comparisons.

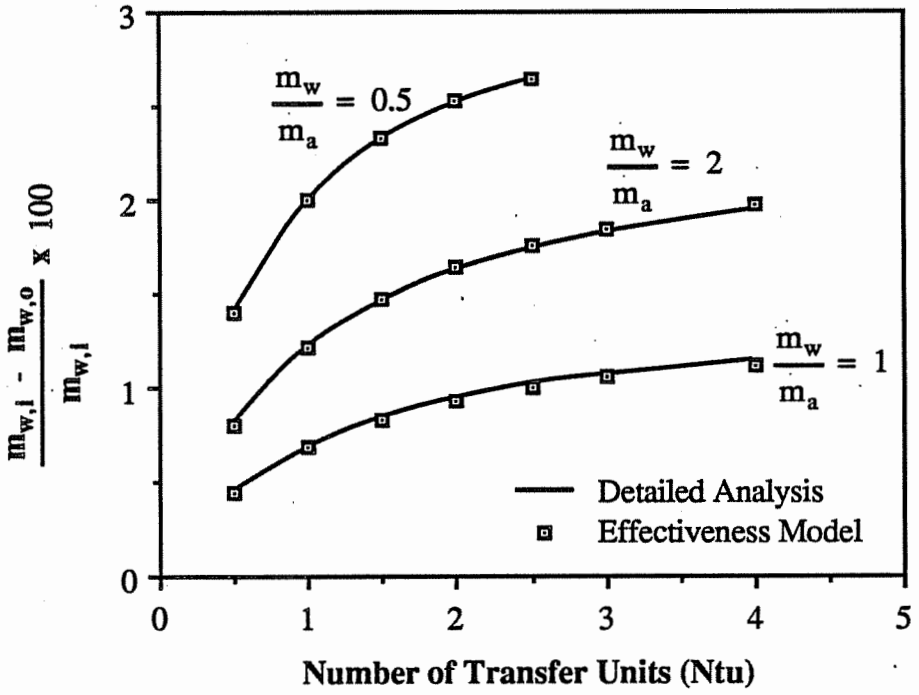

Figure 3.5. Comparisons of Relative Water Loss (Dry Bulb, Wet Bulb, and Water Inlet Temperatures of 70 F, 60 F, and 90 F)

3.1.6 Correlating Performance Data

General correlations for heat and mass transfer in cooling towers in terms of the physical tower characteristics do not exist. It is usually necessary to correlate data for specific tower designs. Mass transfer data are typically correlated with the following form (ASHRAE [1983]).

$$\frac{h_D A_V V_T}{\dot{m}_w} = c\left[\frac{\dot{m}_w}{\dot{m}_a}\right]^n \tag{3.1.24}$$

where c and n are empirical constants specific to a particular tower design. Multiplying both sides of the above equation by $\dot{m}_w/\dot{m}_a$ and utilizing the definition for Ntu gives

$$Ntu = c\left[\frac{\dot{m}_w}{\dot{m}_a}\right]^{1+n} \tag{3.1.25}$$

According to the above equation, data should correlate as a straight line on a log-log plot of Ntu versus the flow rate ratio. The slope and intercept of this line are (1+n) and log(c), respectively. Linear regression may be utilized to determine the "best" fit straight line through the data. For given entering conditions and heat transfer rate, the tower Ntu is estimated from equation (3.1.16) with the air-side effectiveness computed using equation (3.1.15).

Simpson and Sherwood [1946] give data for a number of different tower designs. The coefficients of equation (3.1.25) were fit to the measurements of Simpson and Sherwood for four different tower designs over a range of performance conditions. Table 3.1 gives the coefficients of the mass transfer correlation determined from the regressions for each tower. The data include measurements of outlet states for both the water and air flow streams. A comparison between results of model estimates for leaving water temperature and measurements are shown in Figure 3.6. The model matches these data quite closely over a wide range of conditions. Water loss was computed from the measurements using a mass balance and compared with model

predictions as shown in Figure 3.7. The model tends to underpredict the water loss as compared with the data. This bias may be associated with the assumption of Lewis number of unity or may be due to errors in the measurements of the air outlet state. Energy balances on the data close only to within 10 percent.

Table 3.1
Mass Transfer Correlation Coefficients for Data of Simpson and Sherwood [1946]

Tower	c	n
R-1	1.684	-0.391
R-2	1.405	-0.727
M-1	0.984	-0.852
M-2	1.130	-0.617

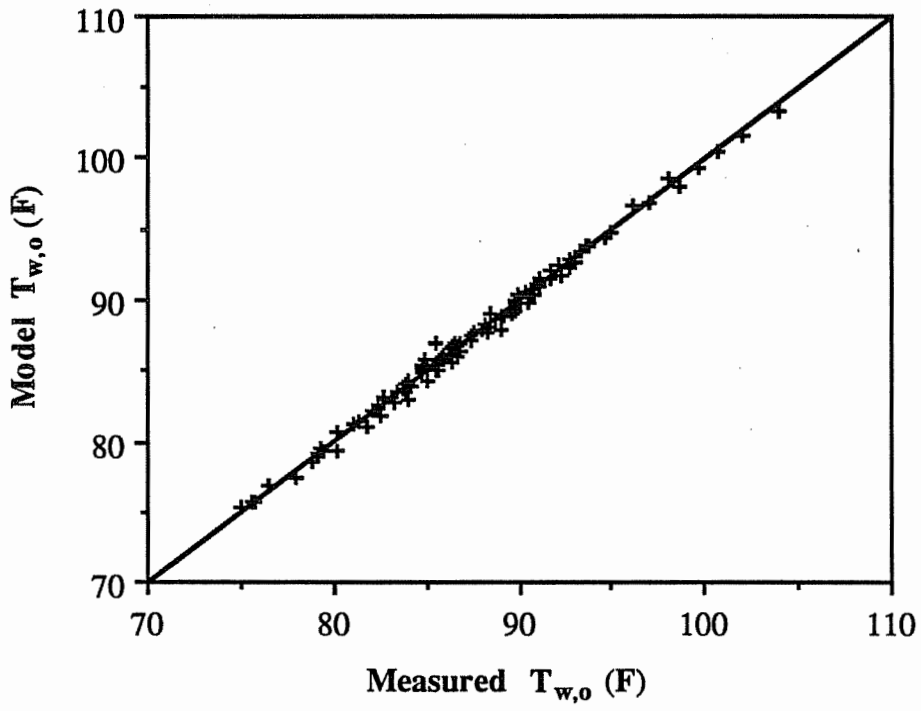

Figure 3.6. Comparisons of Leaving Water Temperature Measurements from Simpson and Sherwood [1946] with Effectiveness Model Results

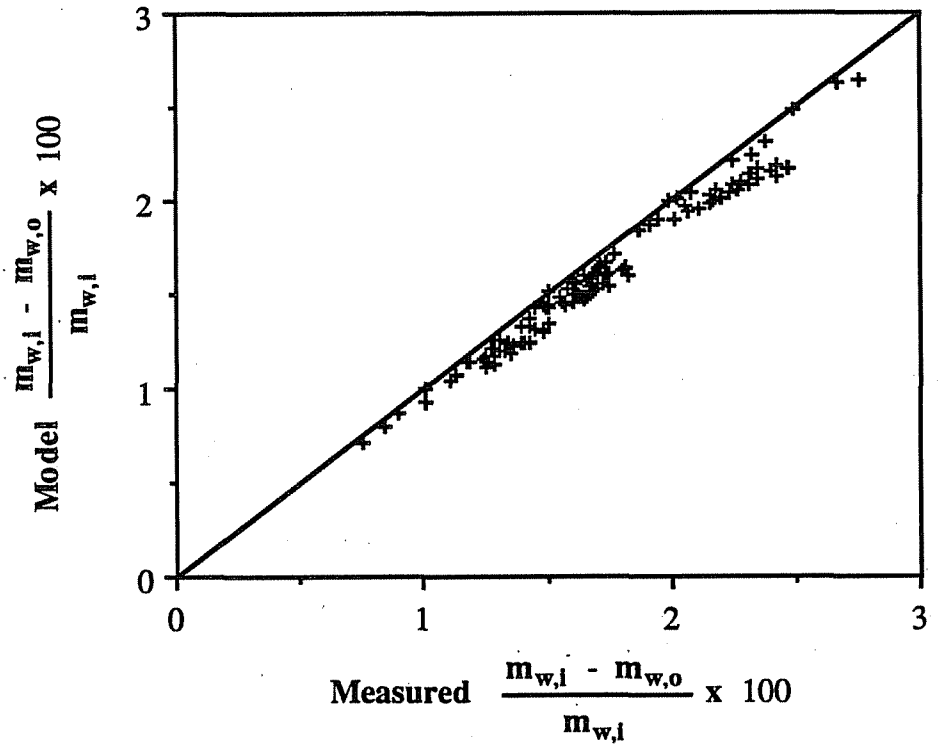

Figure 3.7. Comparisons of Relative Water Loss Measurements from Simpson and Sherwood [1946] with Effectiveness Model Results

Results of the cooling tower model were also to fit to data from the D/FW airport for a 3 day period in October. This tower has four cells, each with two-speed fans that share a common sump. D/FW measurements included the entering tower water temperature and supply water temperature to the chillers from the sump. Ambient wet bulb temperatures were available from the National Weather Service for this time period. The maximum tower air flow rates and coefficients of the Ntu correlation determined from nonlinear regression analysis were 635,000 cfm, c = 3.76, and n = -0.63. As exhibited in Figure 3.8, the model does a relatively good job of estimating the leaving cooling tower water temperature for this data. The root-mean-square of the error is approximately 1.4 degrees F. Since the differences between

entering and leaving water temperatures were in the range of 4 to 15 degrees, not nearly as good agreement was realized in terms of tower heat rejection rates. However, the agreement is within the accuracy of the measurements.

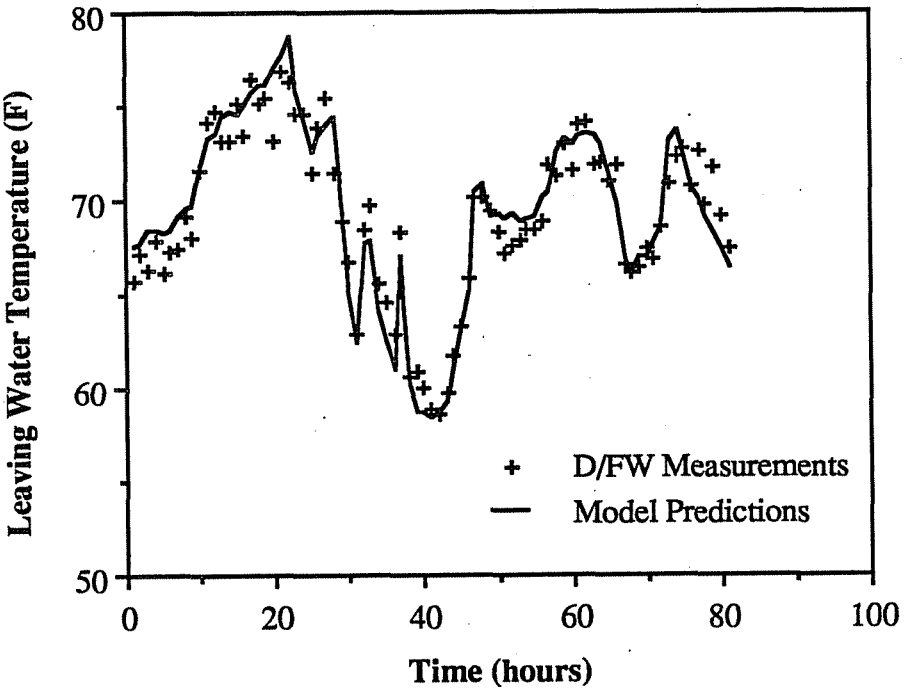

Figure 3.8. Comparisons of Leaving Water Temperature Measurements from D/FW Airport with Effectiveness Model Results

3.1.8 Potential Improvements in the Model

Theoretically, it is possible to improve the effectiveness model by accounting for the effect of water loss on the change in the water stream enthalpy in an approximate manner. Rather than totally neglecting the water loss due to evaporation in the last term of equation (3.1.1), a slightly better assumption is a constant specific enthalpy of this evaporation term throughout the tower. A corrected enthalpy is then defined as

$$h' = h - \omega C_{pw} (T_{w,i} - T_{ref}) \qquad (3.1.26)$$

With this definition, equations (3.1.11) and (3.1.13) may be replaced with

$$\frac{dh_a'}{dV} = -\frac{Ntu}{V_T}(h_a' - h_{s,w}') \tag{3.2.27}$$

$$\frac{dh_{s,w}'}{dV} = \frac{\dot{m}_a C_s' (dh_a'/dV)}{\dot{m}_w C_{pw}} \tag{3.1.28}$$

where,

$$C_s' = \left[\frac{dh_s'}{dT}\right]_{T = T_w} \tag{3.1.29}$$

Equations (3.1.26) - (3.1.29) may be solved analytically for outlet conditions given inlet conditions for a linearized C_s'. Overall, the accuracy of this analysis is no better and in many cases worse than the simpler effectiveness method. Neglecting the effect of the water loss on the enthalpy change of the water stream is a conservative assumption. On the other hand, the linearization of the saturation enthalpy between the inlet and outlet water temperatures tends to overpredict the tower heat transfer. These are relatively small, but compensating effects that result in a model with good accuracy. By including the water loss, the model becomes slightly optimistic.

The accuracy of the effectiveness model presented in this chapter depends primarily upon the temperature difference between the water stream inlet and outlet . As the inlet-to-outlet water temperature difference increases, the accuracy associated with using a linear relationship for the saturation enthalpy is reduced. Comparisons with both

detailed numerical solutions and measurements indicate that this model works well over a wide range of typical conditions. However, for more extreme conditions, it is possible to improve the accuracy of the model.

One approach for reducing the errors associated with the linearization involves dividing the cooling tower into two or more increments. The effectiveness model is then applied to each increment and the set of equations is solved for the intermediate and outlet states. With a sufficient number of increments, this model will always yield satisfactory results. This procedure is advocated by Jaber and Webb [1987]. Another approach involves choosing a better linearization than a straight line between the inlet and outlet conditions. Berman [1961] developed a correction factor to account for the curvature of the saturated air enthalpy versus temperature relationship.

Figure 3.9 shows a comparison between the detailed analysis, the effectiveness model as described in Section 3.1.3 , and the effectiveness model using the correction of Berman [1961]. Cooling tower air effectiveness is plotted as a function of the water inlet temperature for different water-to-air mass flow rates with constant ambient dry and wet bulb temperatures (80 F and 60 F). The Ntu's were determined with equation (3.1.25) using coefficients determined from the regression to the D/FW airport data. Depending upon the flow rate ratio, the accuracy of the effectiveness model is degraded with increasing temperature differences between water inlet and ambient wet bulb. As the water-to-air flow rate ratio increases, the water temperature difference decreases and the linearization is more accurate. At the low flow rate ratios, the water loss becomes more significant and compensates for greater inaccuracies in the linearization. Overall, the effectiveness model appears to give satisfactory results for temperature differences up to 50 degrees F between the water inlet and ambient wet bulb. The correction of Berman improves the results for the higher flow rate ratios, but has negative effect at

low flow rate ratios where the water loss becomes important. At low flow rate ratios and large water inlet and wet bulb temperature differences, the combination of the Berman correction and the approximate method for including water loss described above may be justified. However, the accuracy of the simpler effectiveness model is most likely sufficient over the practical operating range when considering the other uncertainties in the analysis such as inaccurate input data or the assumption of a Lewis number of unity.

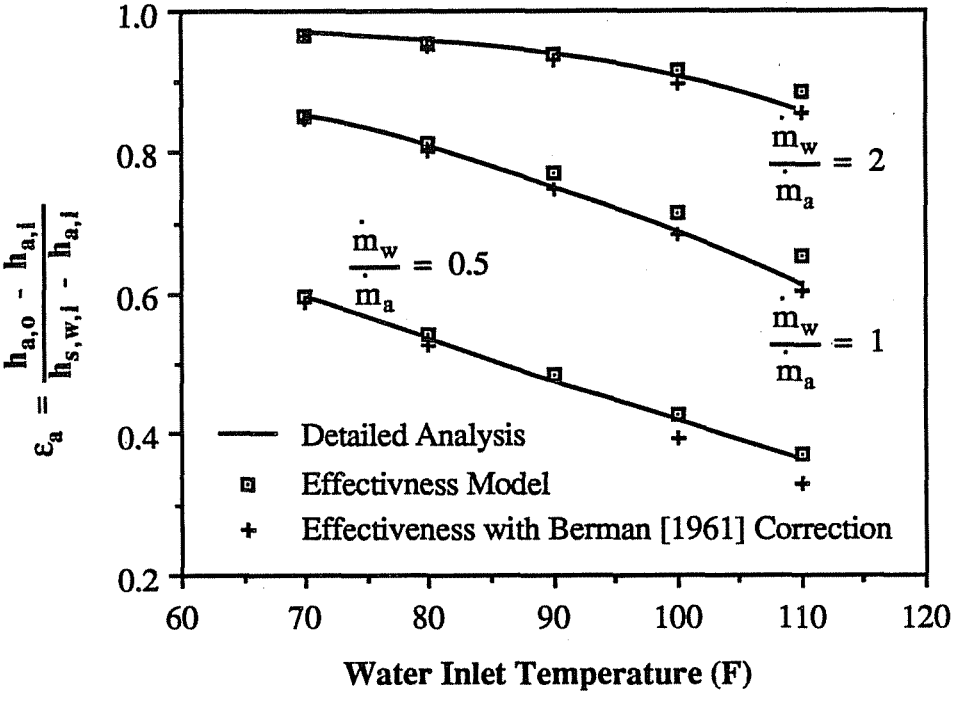

Figure 3.9. Comparisons of Detailed Model with Effectiveness Model Results for Extreme Conditions (Ambient Dry and Wet Bulb Temperature 80 F and 60 F)

3.1.8 Sump and Fan Power Analyses

In analyzing the performance of a system, it is necessary to include effects of a tower sump. Water enters a sump from each of the operating tower cells and from a water make-up source. The level of the sump is assumed to be constant, so that the

flow of water make-up is equal to the total water loss from the cells. The water volume of the sump is further assumed to be fully-mixed, so that a steady-state energy balance yields

$$\sum_{k=1}^{N_{cell}} \left(\dot{m}_{w,o} \left(T_{w,o} - T_s \right) \right)_k + \left[\dot{m}_{w,i} - \sum_{k=1}^{N_{cell}} \left(\dot{m}_{w,o} \right)_k \right] \left(T_{main} - T_s \right) = 0 \qquad (3.1.30)$$

where N_{cell} is the number of tower cells that share a common sump, T_{main} is temperature of the water make-up and T_s is the fully-mixed sump temperature. This equation is solved for the sump temperature, T_s, which is generally the supply temperature to the condenser of a centrifugal chiller in a central chilled water facility.

The cooling tower fans are assumed to obey the fan laws. Given the power requirement at maximum fan speed, the power consumption for a cooling tower consisting of N_{cell} tower cells is calculated as

$$P_t = \sum_{k=1}^{N_{cell}} \gamma_{t,k}^3 P_{t,k,des} \qquad (3.1.31)$$

where $\gamma_{t,k}$ and $P_{t,k,des}$ are the relative fan speed and design power consumption at maximum speed for the k^{th} tower cell.

As discussed in Chapter 5, the determination of optimal control points that minimize operating costs is simplified when the individual component operating costs are expressed as quadratic functions of the continuous controls and/or outputs. In the optimization process, the power consumption given by equation (3.1.31) may be approximated with a quadratic function using a second-order Taylor series expansion

about the most recent iteration point. Alternatively, it is possible to accurately correlate the power consumption of a variable-speed fan as a quadratic function of speed over its operating range. Figure 3.10 shows a comparison of the relative fan power consumption as determined with equation (3.1.31) for one cell and a quadratic function. The coefficients of the quadratic function were determined analytically by matching the power consumption determined with equation (3.1.31) at relative fan speeds of one-third, two-thirds, and full speed. The quadratic function works extremely well in correlating variable-speed fan power consumption.

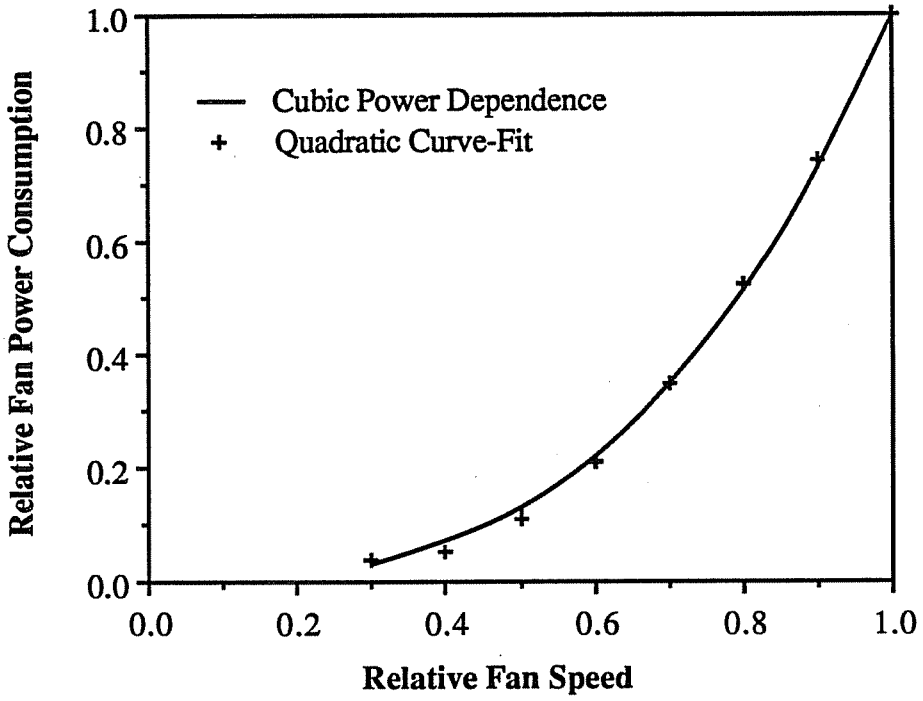

Figure 3.10. Quadratic Fit to Variable-Speed Fan Power Consumption

3.2 Condenser-Loop Pumping Requirements

The performance of a centrifugal pump is characterized by a rating curve that gives pressure rise developed by the pump and efficiency versus pump flow. The maximum

pressure rise is produced at zero flow rate, while the maximum efficiency occurs at what is considered to be the design flow. At the operating point of a pump, the pressure rise developed is equal to the total pressure drop through the system. The primary pressure losses in the condenser loop are to due to the elevation difference between the tower inlet stream and the sump and the flows through the condenser and tower nozzles. Figure 3.11 shows typical pump pressure rise and system pressure drop characteristics as a function of flow rate. The operating point of the pump occurs where the two curves intersect.

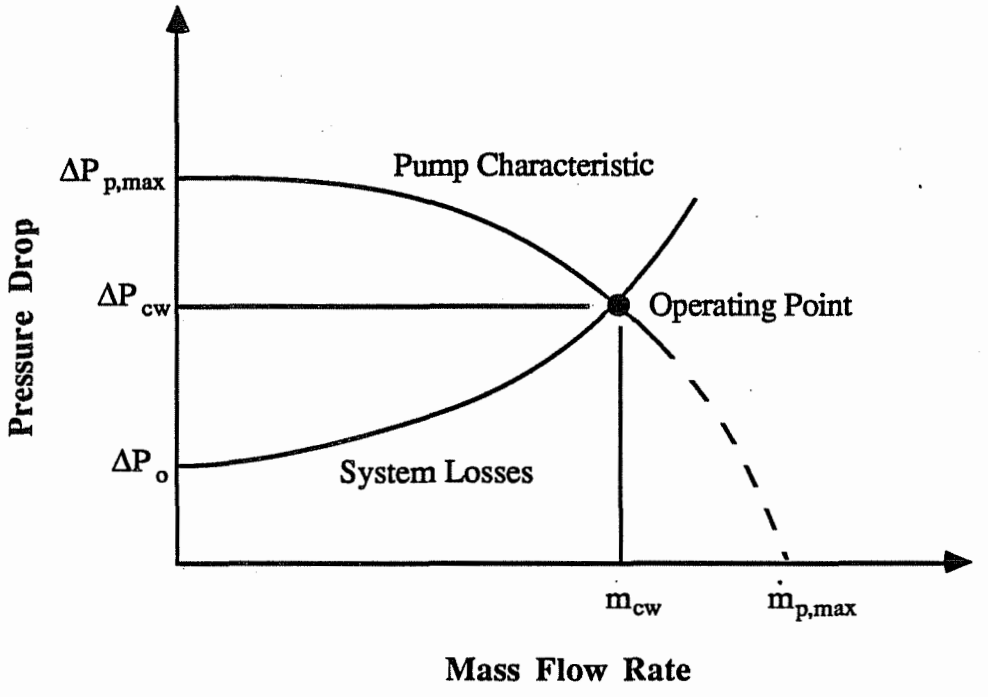

Figure 3.11. Pump Pressure Rise and System Pressure Drop Characteristics

For turbulent flow, the overall condenser water loop pressure drop takes the following form.

$$\Delta P_{cw} = \Delta P_o + \Delta P_{cw,des}\left[\frac{\dot{m}_{cw}}{\dot{m}_{cw,des}}\right]^2 \qquad (3.2.1)$$

where ΔP_o is the static pressure drop associated with the elevation change in the tower, $\dot{m}_{cw}$ is the condenser loop flow rate, and $\Delta P_{cw,des}$ is a design pressure drop for the flow components at a design condenser loop flow rate of $\dot{m}_{cw,des}$. Considering only the pressure losses within the chillers and cooling tower cells, the design condenser loop pressure drop may be expressed as

$$\Delta P_{cw,des} = \Delta P_{ch,des}\left[\frac{\dot{m}_{cw,des}}{\dot{m}_{ch,des}}\right]^2 + \Delta P_{t,des}\left[\frac{\dot{m}_{cw,des}}{\dot{m}_{t,des}}\right]^2 \qquad (3.2.2)$$

where $\dot{m}_{ch,des}$ and $\Delta P_{ch,des}$ are the flow rate and pressure drop through the chillers at specified design conditions and $\dot{m}_{t,des}$ and $\Delta P_{t,des}$ are the design flow and pressure drop for the cooling tower nozzles. The condenser loop pressure drop also depends upon the number of chillers and cooling tower cells in operation. Cooling tower cells operate in parallel and the total flow is generally divided equally between the cells. For identical chillers, the condenser flow would also be divided equally between the chillers. For parallel flow paths with identical pressure drop characteristics, the design flow rates utilized in equation (3.2.2) are simply the design values for an individual device multiplied by the number operating in parallel. The design pressure drop for the parallel components is equal to the pressure drop for an individual component at its design flow rate.

The pressure rise developed by a pump may be correlated with a simple parabolic relationship (White [1986]). In terms of the maximum pressure developed at zero

flow, $\Delta P_{p,max}$, and the maximum flow at zero pressure rise, $\dot{m}_{p,max}$, the pump pressure rise is

$$\Delta P_p = \Delta P_{p,max}\left[1 - \left(\frac{\dot{m}_{cw}}{\dot{m}_{p,max}}\right)^2\right] \tag{3.2.3}$$

Multiple pumps operating in parallel will produce a total flow capacity equal to the sum of the individual capacities at the same pressure rise. The combined pump characteristic is obtained by adding together flow capacities at fixed pressure rises. For identical parallel pumps, the maximum flow rate of equation (3.2.3) is equal to the product of the individual maximum flow rate for an individual pump and the number of pumps operating in parallel.

For a variable-speed pump, the pump characteristic changes with the pump speed. From similarity rules for centrifugal pumps, the maximum pressure rise and mass flow rate depend upon the relative pump speed according to the following relationships.

$$\Delta P_{p,max} = \gamma_p^2 \Delta P_{p,max,des} \tag{3.2.4}$$

$$\dot{m}_{p,max} = \gamma_p \dot{m}_{p,max,des} \tag{3.2.5}$$

where γ_p is the pump speed relative the maximum design speed and $\Delta P_{p,max,des}$ and $\dot{m}_{p,max,des}$ are the maximum pump pressure rise and flow rate associated with the design speed.

Equating the condenser loop pressure drop to the pump pressure rise and solving

for the total flow rate gives the following relation.

$$\dot{m}_{cw} = \dot{m}_{cw,des} \sqrt{\frac{\gamma_p^2 - \frac{\Delta P_o}{\Delta P_{p,max,des}}}{\left[\frac{\dot{m}_{cw,des}}{\dot{m}_{p,max,des}}\right]^2 + \frac{\Delta P_{cw,des}}{\Delta P_{p,max,des}}}} \tag{3.2.6}$$

For fixed-speed pumps, the relative speed in the above equation is equal to unity.

For a given mass flow rate and pressure rise, the overall pump power requirement for the condenser water loop is determined as

$$P_p = \frac{\dot{m}_{cw} \Delta P_{cw}}{\eta_p \rho_{cw}} \tag{3.2.7}$$

where ρ_{cw} is the density of the condenser water and η_p is the overall efficiency of the pump and motor. The overall pump efficiency is primarily a function of the flow rate relative to the speed of the pump (White [1986])and may be correlated with

$$\eta_p = a_0 + a_1\left[\frac{\dot{m}_{cw}}{\gamma_p \dot{m}_{p,max,des}}\right] + a_2\left[\frac{\dot{m}_{cw}}{\gamma_p \dot{m}_{p,max,des}}\right]^2 \tag{3.2.8}$$

The determination of optimal control points that minimize operating costs is simplified when the individual component operating costs are expressed as quadratic functions of the controls and/or outputs. It is possible to accurately correlate the power consumption of a variable-speed pump as a quadratic function of pump speed over its

operating range. Figure 3.12 demonstrates that a quadratic function works extremely well in correlating pump power consumption. The coefficients of the quadratic function were determined analytically by matching the power consumption determined with equation (3.2.7) at relative speeds of one-half, three-quarters, and full speed.

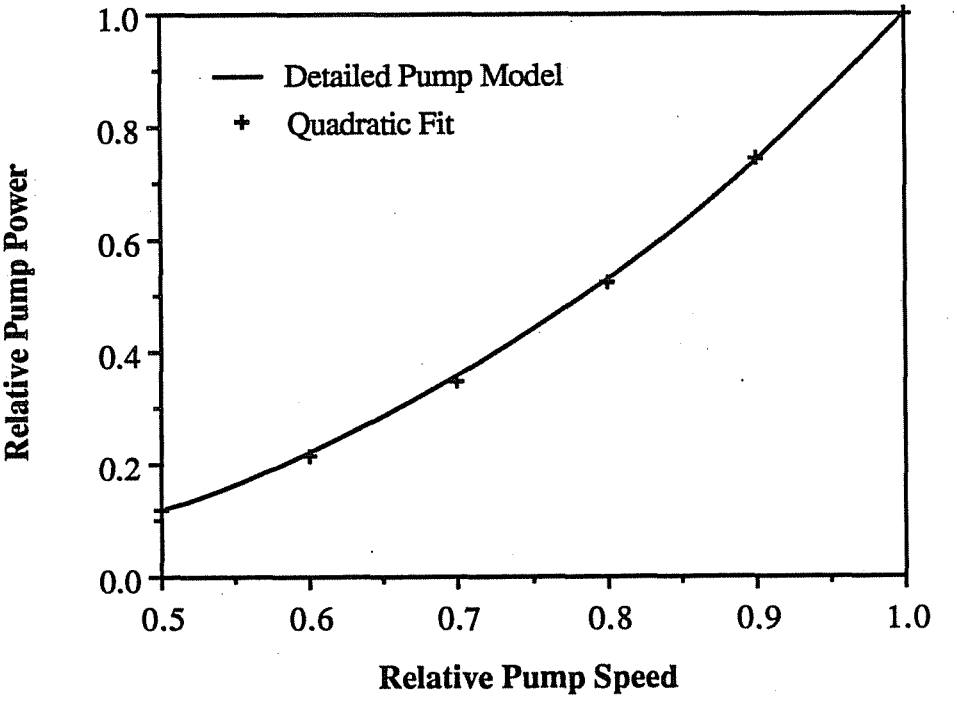

Figure 3.12. Quadratic Fit to Variable-Speed Pump Power Consumption

3.3 Summary

An effectiveness model has been presented for cooling towers. The model utilizes existing effectiveness relationships developed for sensible heat exchangers with modified definitions for number of transfer units and the capacitance rate ratio. A simple method was also developed for estimating the water loss in cooling towers. Results of the model compare well with the results of more detailed numerical solutions to the basic heat and mass transfer equations and with experimental data. The simplicity and accuracy of the effectiveness model is such that it is useful for both

design and system simulations. This modeling approach is also appropriate for other wet surface heat exchangers and is applied to cooling coils in Chapter 4.

A model was also presented for determining the condenser pump flow rate and power consumption based upon a hydraulic analysis. It was shown that the variable-speed pump power consumption may be correlated as a simple quadratic function of the relative pump speed. This was also found to be the case for variable-speed cooling tower fans. The use of quadratic functions for the component operating costs simplifies the determination of the optimal control points as described in Chapter 5.

Chapter 4
Evaporator-Side Component Models

In this chapter, models are presented for air handling and chilled water pumping equipment. An air handler consists of a cooling coil, supply air fan, and valve for modulating chilled water flow through the coil. In Section 4.1, an effectiveness model is developed for coiling coils that is similar to the cooling tower model presented in Chapter 3. The complete air handler analysis is presented in Section 4.2, while the chilled water pumping power requirements are developed in Section 4.3.

4.1 Development of an Effectiveness Model for Cooling Coils

A cooling coil is similar to a cooling tower in that energy is transferred between air and water streams due to both sensible and latent effects. The ASHRAE Equipment Guide [1983] presents a method for the design and analysis of cooling coils in which the overall heat transfer is evaluated by using log-mean temperature differences between the coolant and the surface and log-mean enthalpy differences between the surface conditions and the air stream. The use of log-mean enthalpy differences requires the assumption that the enthalpy associated with the saturated air at the surface interface is a linear function of temperature. For a given coil and entering conditions, the solution is iterative with respect to the leaving condition. For system simulation purposes, Stoecker [1975] presents an empirical model for cooling coils. This model is not useful for design and requires the determination of fifteen empirical constants from performance data.

A simple, yet fundamental model for cooling coils was proposed by Threlkeld [1970]. By assuming a linear relationship for saturation air enthalpy with respect to

both surface and water coolant temperature conditions, Threlkeld obtained an analytic solution to the heat and mass transfer equations. Threlkeld did not compare his methodology extensively either with more detailed analyses or experimental results. Elmahdy [1977] compared results of this model with experimental measurements for two different coil designs and found good agreement.

Threlkeld presented his solution for cooling coils in terms of log-mean enthalpy differences between the entering and leaving flow streams. This form is particularly useful for design purposes in which entering and leaving conditions are specified and the area requirements are to be computed. For a given coil design and entering conditions, a more convenient expression for determining the cooling capacity is based upon the coil effectiveness.

The primary difference between the analysis of cooling coils and cooling towers is associated with the fact that the air and water streams are not in direct contact. As a result, there is an additional heat transfer resistance associated with the material separating the streams and there is no loss of mass associated with the water flow. The use of multi-pass crossflow geometries also complicates the analysis of cooling coils. However, as the number of passes increases beyond about four, the performance of a crossflow heat exchanger approaches that of a counterflow.

In this section, the basic theory of a counterflow cooling coil is presented, leading to the development of an effectiveness model. A simple method for analyzing the performance of cooling coils that have both wet and dry sections is also presented. The resulting effectiveness model is compared with results of finite-difference solutions to the basic heat and mass transfer equations and manufacturers' data. In addition, functional forms for correlating performance data are presented.

4.1.1 Detailed Analysis

A schematic representation of a counterflow cooling coil in which air is cooled as a result of a flow of chilled water is shown in Figure 4.1. Assuming that the local surface temperature is less than the dewpoint of the air, then the air is both cooled and dehumidified.

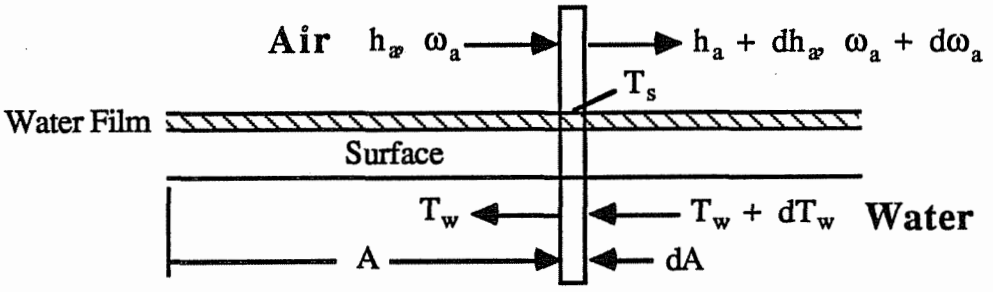

Figure 4.1. Schematic of a Counterflow Cooling Coil

Following the assumptions and development of Section 3.1.1, the equations modeling the local heat and mass transfer from the air to the chilled water for a counterflow coil without fins may be written

$$\frac{d\omega_a}{dA} = -\frac{Ntu_o}{Le_o A_o}(\omega_a - \omega_{s,s}) \tag{4.1.1}$$

$$\frac{dh_a}{dA} = -\frac{Ntu_o}{A_o}\left[(h_a - h_{s,s}) + (\omega_a - \omega_{s,s})(1/Le_o - 1)h_{g,s}\right] \tag{4.1.2}$$

$$\frac{dT_w}{dA} = \frac{\frac{dh_a}{dA} - C_{pw}(T_s - T_{ref})\frac{d\omega_a}{dA}}{\frac{\dot{m}_w}{\dot{m}_a}C_{pw}} \tag{4.1.3}$$

$$= Ntu_i (T_w - T_s) \tag{4.1.4}$$

where,

A_o = total cooling coil outside surface area

C_{pw} = constant pressure specific heat of liquid water

h_a = enthalpy of moist air per mass of dry air

$h_{g,s}$ = enthalpy of water vapor at the coil surface temperature

$h_{s,s}$ = enthalpy of saturated air at the surface temperature

$\dot{m}_a$ = mass flow rate of dry air

$\dot{m}_w$ = mass flow rate of water

Le_o = Lewis number for air stream

Ntu_o = overall air-side number of heat transfer units

Ntu_i = overall water-side number of heat transfer units

T_{ref} = reference temperature for zero enthalpy of liquid water

T_s = coil surface temperature

T_w = water temperature

ω_a = air humidity ratio

$\omega_{s,s}$ = humidity of saturated air at the coil surface temperature

In contrast to the use of mass transfer Ntu's for the cooling tower analysis, heat transfer Ntu's are utilized for the inside and outside flow streams. The Ntu's and

Lewis number are defined as

$$Ntu_i = \frac{(UA)_i}{\dot{m}_w C_{p,w}} \tag{4.1.5}$$

$$Ntu_o = \frac{h_{C,o} A_o}{\dot{m}_a C_{pm}} \tag{4.1.6}$$

$$Le_o = \frac{h_{C,o}}{h_{D,o} C_{pm}} \tag{4.1.7}$$

where,

C_{pm} = constant pressure specific heat of moist air

$(UA)_i$ = overall heat transfer conductance between water stream and outside surface

$h_{C,o}$ = convection heat transfer coefficient for air stream

$h_{D,o}$ = mass transfer coefficient for air stream

Equations (4.1.1) - (4.1.4) may be solved numerically for the air and water exit states. For given entering conditions, the solution is iterative with respect to the exit water temperature, $T_{w,o}$. For a given value of $T_{w,o}$, the equations are numerically integrated from air inlet to outlet. For sections of the coil where the local surface temperature is greater than the dewpoint of the air, no condensation occurs and equations (4.1.1) - (4.1.4) apply with $\omega_{s,s} = \omega_a$. In the following two sections, effectiveness relations are presented for both completely dry and completely wet coils.

4.1.2 Dry Coil Effectiveness

If the coil surface temperature at the air outlet is greater than the dewpoint of the incoming air, then the coil is completely dry throughout and standard heat exchanger effectiveness relationships apply. In terms of the air-side heat transfer effectiveness, the dry coil heat transfer is

$$\dot{Q}_{dry} = \varepsilon_{dry,a} \dot{m}_a C_{pm} (T_{a,i} - T_{w,i}) \tag{4.1.8}$$

where, analogous to a dry counterflow heat exchanger, the effectiveness is evaluated as

$$\varepsilon_{dry,a} = \frac{1 - \exp(-Ntu_{dry}(1 - C^*))}{1 - C^* \exp(-Ntu_{dry}(1 - C^*))} \tag{4.1.9}$$

where,

$$C^* = \frac{\dot{m}_a C_{pm}}{\dot{m}_w C_{pw}} \tag{4.1.10}$$

The overall number of transfer units for the dry coil is

$$Ntu_{dry} = \frac{Ntu_o}{1 + C^*(Ntu_o/Ntu_i)} \tag{4.1.7}$$

For finned surfaces, the air-side number of transfer units, Ntu_o, defined by equation (4.1.6) is multiplied by an overall fin efficiency factor. For air flow over finned coil

surfaces, general correlations for determining the overall heat transfer coefficient have been developed by Elmahdy [1979] for dry heat exchangers.

The exit air humidity ratio is equal to the inlet value, while the exit air and water temperatures are determined from energy balances on the flow streams as

$$T_{a,o} = T_{a,i} - \varepsilon_{dry,a}(T_{a,i} - T_{w,i}) \tag{4.1.8}$$

$$T_{w,o} = T_{w,i} + C^{*}(T_{a,i} - T_{a,o}) \tag{4.1.9}$$

The coil surface temperature at the air outlet is determined by equating the rate equation for heat transfer between the water and air streams with that between the water and the outside surface.

$$T_{s,o} = T_{w,i} + C^{*}\frac{Ntu_{dry}}{Ntu_{i}}(T_{a,o} - T_{w,i}) \tag{4.1.10}$$

If the surface temperature evaluated with the above equation is less than the inlet air dewpoint, then at least a portion of the coil is wet and the analysis in the following section must be applied.

4.1.3 Wet Coil Effectiveness

If the coil surface temperature at the air inlet is less than the dewpoint of the incoming air, then the coil is completely wet and dehumidification occurs throughout. Introducing the definition for the air saturation specific heat , C_s, from Chapter 3, assuming that C_s evaluated at the local surface temperature is equal to the value at the

local water temperature, assuming a Lewis number of unity, and neglecting the energy flow associated with condensate draining from the coil surface, equations (4.1.1) - (4.1.4) may be written

$$\frac{dh_a}{dV} = -\frac{Ntu_{wet}}{A_o}(h_a - h_{s,w}) \tag{4.1.11}$$

$$\frac{dh_{s,w}}{dA} = \frac{\dot{m}_a C_s (dh_a/dA)}{\dot{m}_w C_{pw}} \tag{4.1.12}$$

where the overall number of transfer units for a wet coil is defined as

$$Ntu_{wet} = \frac{Ntu_o}{1 + m^*(Ntu_o/Ntu_i)} \tag{4.1.13}$$

and

$$m^* = \frac{\dot{m}_a}{\dot{m}_w(C_{pw}/C_s)} \tag{4.1.14}$$

$$C_s = \left[\frac{dh_s}{dT}\right]_{T = T_w} \tag{4.1.15}$$

For finned surfaces, Ntu_o as defined by equation (4.1.6) should be multiplied by an overall fin efficiency. The air-side transfer units, Ntu_o, will differ for wet and dry coils due to different heat transfer coefficients and fin efficiencies for finned coils. There are no general correlations for heat transfer coefficients for wet coils, however ASHRAE [1985] presents data that show a relatively small difference between wet and dry

coefficients. The fin efficiency for a wet coil must account for the effects of both heat and mass transfer. Threlkeld [1970] gives a method for computing fin efficiencies for wet coils using the relationships available for dry coils.

For a constant C_s, equations (4.1.11) and (4.1.12) may be solved analytically. For a completely wet coil, the heat transfer is

$$\dot{Q}_{wet} = \varepsilon_{wet,a}\dot{m}_a(h_{a,i} - h_{s,w,i}) \tag{4.1.16}$$

where,

$$\varepsilon_{a,wet} = \frac{1 - \exp(-Ntu_{wet}(1 - m^*))}{1 - m^* \exp(-Ntu_{wet}(1 - m^*))} \tag{4.1.17}$$

Analogous to the dry analysis, the exit air enthalpy and water temperature are

$$h_{a,o} = h_{a,i} - \varepsilon_{wet,a}(h_{a,i} - h_{s,w,i}) \tag{4.1.18}$$

$$T_{w,o} = T_{w,i} + \frac{\dot{m}_a}{\dot{m}_w C_{pw}}(h_{a,i} - h_{a,o}) \tag{4.1.19}$$

The exit air temperature is determined in a manner analogous to that for determining the exit humidity ratio for the cooling tower described in Chapter 3 and as described in the ASHRAE Equipment Guide [1983].

$$T_{a,o} = T_{s,e} + (T_{a,i} - T_{s,e}) \exp(-Ntu_o) \tag{4.1.20}$$

where, the effective surface temperature is determined from its corresponding saturation enthalpy.

$$h_{s,s,e} = h_{a,i} + \frac{h_{a,o} - h_{a,i}}{1 - \exp(-Ntu_o)} \tag{4.1.21}$$

From the rate equations, the surface temperature at the air inlet is computed as

$$T_{s,i} = T_{w,o} + \frac{\dot{m}_a}{\dot{m}_w C_{pw}} \left[\frac{Ntu_{wet}}{Ntu_i}\right] (h_{a,i} - h_{s,w,o}) \tag{4.1.22}$$

If the surface temperature evaluated with the above equation is greater than the inlet air dewpoint, then a portion of the coil beginning at the air inlet is dry, while the remainder is wet.

4.1.4 Combined Wet and Dry Analysis

Depending upon the entering conditions and flow rates, only part of the coil may be wet. A detailed analysis would involve determining the point in the coil at which the surface temperature equals the dewpoint of the entering air. A method for determining the heat transfer and outlet states in this manner for a coil with dry and wet sections is given in Appendix B.

A simpler approach is to assume that the coil is either completely wet or dry. Either assumed condition will tend to underpredict the actual heat transfer. With the completely dry assumption, the latent heat transfer is neglected and the predicted heat transfer is low. With the assumption of a completely wet coil, the model predicts that

the air is humidified during the portion of the coil in which the dewpoint of the air is less than the surface temperature. The latent heat transfer to the air associated with this "artificial" mass transfer reduces the overall calculated cooling capacity as compared with the actual situation. Since both the completely dry and wet analyses underpredict the heat transfer, a simple approach is to utilize the results of the analysis that gives the largest heat transfer. The error associated with this method is generally less than 5 percent.

The steps for determining the heat transfer and outlet conditions for a cooling coil are summarized as follows:

1) Assume that the coil is completely dry and apply the analysis of Section 4.1.2.

2) If the surface temperature at the air outlet determined with the dry analysis is less than the dewpoint of the entering air, then assume that the coil is completely wet and apply the analysis of Section 4.1.3.

3) If the surface temperature at the air inlet determined with the wet analysis is greater than the entering dewpoint temperature, then a portion of the coil is dry. At this point, the analysis given in Appendix B could be used to determine the fractions of the coil that are wet and dry, and the corresponding heat transfers and outlet states. More simply, choose the result of steps 1) or 2) that yields the largest heat transfer.

4.1.5 Model Comparisons

Figures 4.2 and 4.3 show typical comparisons between results of the numerical solutions of equations (4.1.1) - (4.1.4) with a Lewis number of unity and those of the

effectiveness model described in the previous section. Air heat transfer and temperature effectivenesses are plotted versus the air-side transfer units, Ntu_o, for different water-to-air flow rate ratios. The air heat transfer effectiveness is the ratio of the actual heat transfer to the heat transfer that would occur if the exit air were saturated at temperature of the inlet water. The air temperature effectiveness is the ratio of the actual air temperature difference across the coil to the temperature difference between the inlet air and inlet water.

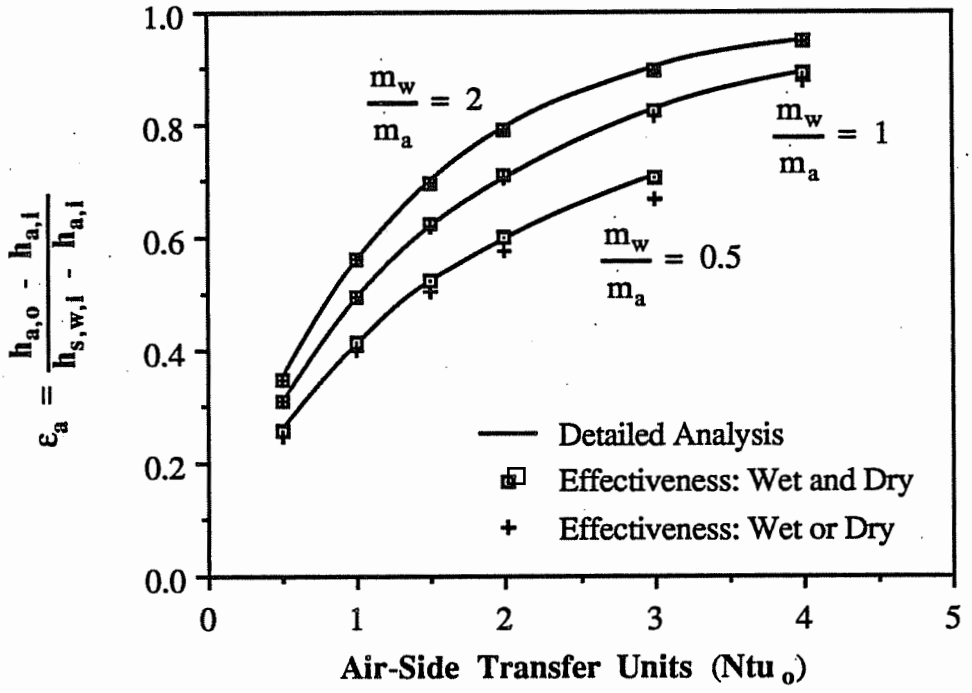

Figure 4.2. Air-Side Heat Transfer Effectiveness for Detailed and Effectiveness Models (Ambient Dry & Wet Bulb of 95 F & 68 F, Water Inlet of 41 F, $Ntu_o/Ntu_i = 2$)

As evident in Figures 4.2 and 4.3, the effectiveness model agrees very closely with the more detailed analysis. The accuracy is better than that for cooling tower analyses because the saturation enthalpy is more nearly linear in the temperature range associated with cooling coil operation. Similar agreement was found over a wide range of

conditions and coil parameters. For situations in which there were wet and dry portions of the coil, both the method of Appendix B and the simpler method of assuming the coil is either all wet or dry were utilized for the effectiveness model results. The results include conditions in which there are significant wet and dry coil sections. The differences in both the air heat transfer and temperature effectivenesses between the two methods are at most 5 percent.

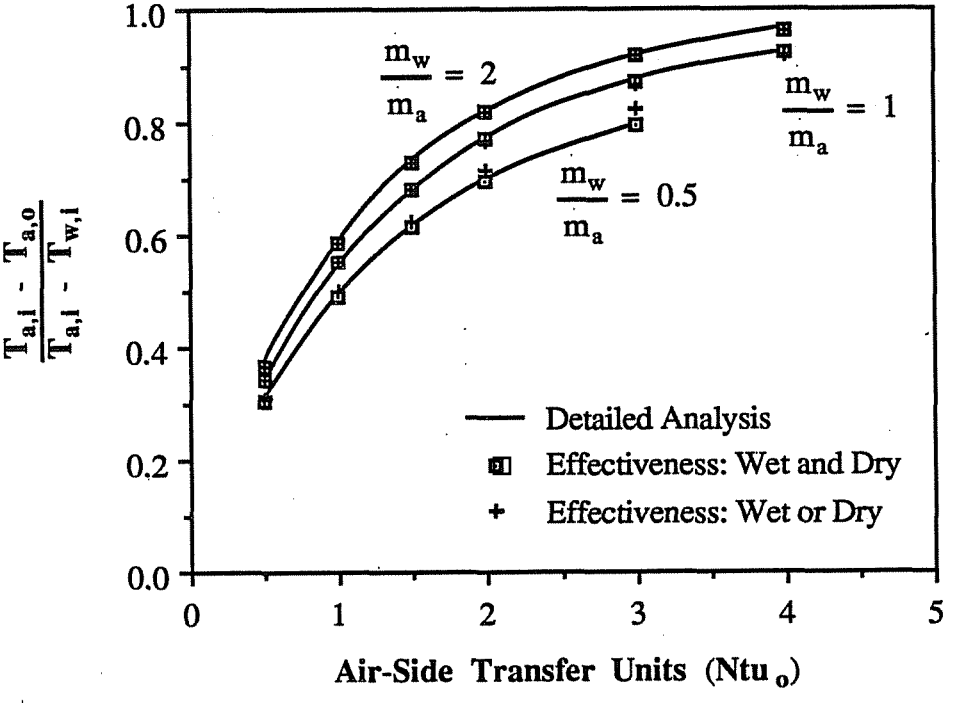

Figure 4.3. Air Temperature Effectiveness for Detailed and Effectiveness Models (Ambient Dry and Wet Bulb of 95 F and 68 F, Water Inlet of 41 F, $Ntu_o/Ntu_i = 2$)

Catalog data for the performance of a cooling coil were utilized in order to further test the accuracy of the effectiveness model. The physical characteristics of the coil and flow rates were used in order to determine heat transfer coefficients and fin efficiencies from general relationships available in the literature. For air flow over finned coil surfaces, correlations developed by Elmahdy [1979] for dry heat exchangers were utilized. Fin efficiencies for wet surfaces were determined as outlined in Threlkeld

[1970] for straight fins. Turbulent flow was assumed for the water-side heat transfer.

Table 4.1 shows representative comparisons between the model and data for a 6 row coil with 8 fins per inch of tubing for a range of conditions. The agreement between the model and the manufacturers' data is excellent.

Table 4.1
Effectiveness Model Comparisons with Cooling Coil Catalog Data

$T_{a,i}$ (F)	T_{wb} (F)	$T_{w,i}$ (F)	Velocity Water (fps)	Velocity Air (fpm)	$T_{w,o}$ (F) Data	$T_{w,o}$ (F) Model	$T_{a,i}$ (F) Data	$T_{a,i}$ (F) Model
75	60	40	4	500	47.9	47.8	48.4	48.9
75	60	44	4	700	52.0	51.9	52.7	53.0
75	60	46	2	400	55.3	55.0	52.4	53.1
80	64	40	4	500	49.7	49.7	50.5	50.8
80	64	44	2	600	59.0	58.4	56.6	56.6
80	72	40	4	500	53.8	54.1	54.3	53.8
90	72	40	4	500	53.7	54.0	55.1	55.1
90	72	46	6	600	55.4	55.6	58.6	58.6
100	80	40	6	500	53.7	54.0	57.2	56.5
100	80	40	8	700	53.1	53.7	60.4	59.3

4.1.6 Correlating Performance Data

The heat and mass transfer characteristics of a cooling coil depend primarily upon its geometry and the flow rates. In order to simulate the performance of a cooling coil in a system simulation, it is necessary to estimate the air-side and water-side transfer units as a function of the flows. General correlations exist for the air-side and water-side heat transfer coefficients and overall fin efficiencies. However, it is necessary to know specific details concerning the dimensions and configuration of the tubes and fins, which is not always readily available. It is possible to correlate the transfer units

when both inlet and outlet coil conditions are provided for a range of flows. The following forms have been found to work well.

$$Ntu_i = k_1 \left[\frac{\dot{m}_w}{\dot{m}_{w,des}} \right]^{k_2} \tag{4.1.23}$$

$$Ntu_o = k_3 \left[\frac{\dot{m}_a}{\dot{m}_{a,des}} \right]^{k_4} \tag{4.1.24}$$

where k_1, k_2, k_3, and k_4 are empirical constants that may be determined with nonlinear regression applied to differences between measurements and cooling coil model predictions of the water and air outlet temperatures. Although, the air-side transfer units differ for dry and wet coils due to different heat transfer coefficients and fin efficiencies, a single correlating function appears to work well for both cases.

Coefficients of the transfer unit equations were determined with nonlinear regression applied to the manufacturers' data presented in Table 4.1. These data cover a fairly wide range of inlet conditions and flow rates and include conditions for which the coil is completely wet and almost completely dry. The assumption that the coil was either all wet or all dry was utilized for the coil model. Figure 4.4 shows a comparison between the data and model results for the difference between outlet temperatures (both water and air) and inlet conditions. The agreement between the model results and the data is excellent.

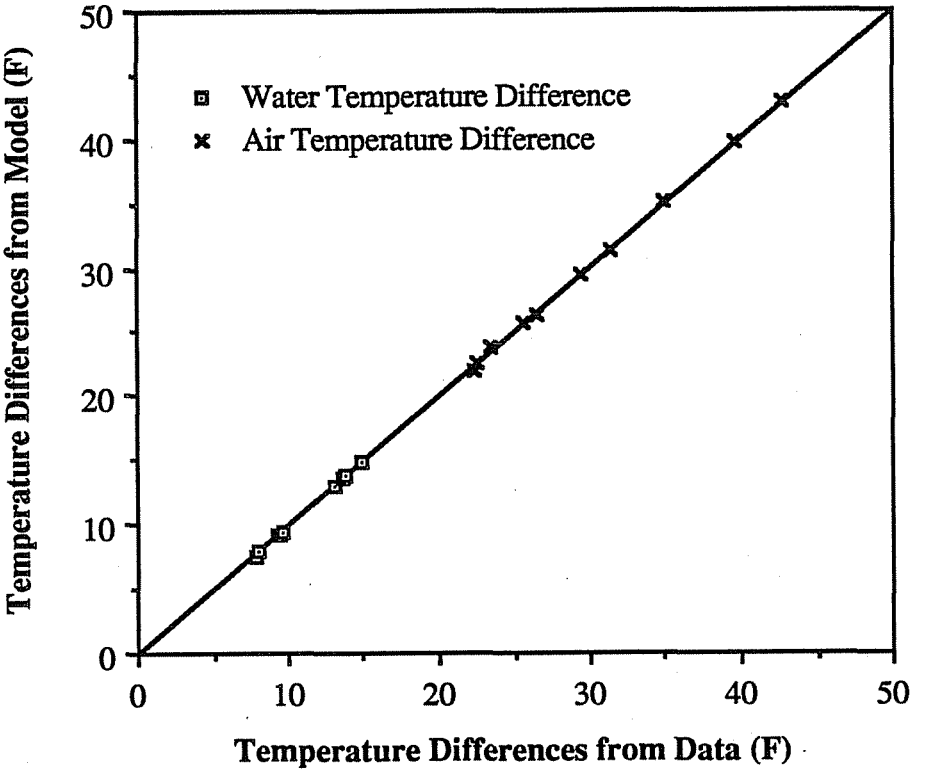

Figure 4.4. Correlation of Cooling Coil Model Results with Catalog Data

4.2 Air Handler Analysis

Local loop control of a chilled water valve modulates the flow of chilled water through the coil in order to maintain a specified supply air temperature to the zones. For a variable-air-volume (VAV) system, a local loop controller also adjusts the supply air flow in order to maintain the zone temperature (and possibly humidity) at prescribed conditions. For the purposes of this study, local loop control of the air handlers is assumed to be ideal such that specified supply air and zone temperatures (and humidity in some cases) are maintained exactly. These controls are handled as constraints in the overall optimization of the system as described in Chapter 5.

There are two possibilities for modulating the air flow in a VAV system that are considered in this study. The most efficient method involves the use of variable-speed

fan motors. The speed of the fan is adjusted to give the required air flow. The power consumption for a variable-speed air handler fan is assumed to obey the fan laws and is computed as

$$P_{ahu} = P_{ahu,des}\left[\frac{\dot{m}_{ahu}}{\dot{m}_{ahu,des}}\right]^3 \qquad (4.2.1)$$

where $\dot{m}_{ahu}$ is the supply air flow rate from the air handler and $P_{ahu,des}$ is the air handler fan power at a design flow of $\dot{m}_{ahu,des}$. Analogous to the cooling tower analysis, the air handler fan power may also be expressed as a quadratic function of the relative flow with a second-order Taylor series expansion of equation (4.2.1) or a correlation over its operating range.

A more common method for modulating supply air flow utilizes variable-pitch fan blades with fixed-speed motors. In this study, the power consumption is determined for variable-pitch fan control using a correlation from the BLAST (1981) simulation program.

$$P_{ahu} = P_{ahu,des}\left\{0.517 - 0.784\left[\frac{\dot{m}_{ahu}}{\dot{m}_{ahu,des}}\right] + 1.26\left[\frac{\dot{m}_{ahu}}{\dot{m}_{ahu,des}}\right]^2\right\} \qquad (4.2.2)$$

At part-load conditions, the power consumption is always greater for fixed-speed, variable-pitch than for variable-speed control.

In order to analyze the performance of the cooling coil, it is necessary to know the inlet enthalpy and humidity. Return air from the zones serviced by an air handler is

mixed with ambient air so that

$$h_{a,i} = X_{amb} h_{amb} + (1 - X_{amb}) h_{a,r} \tag{4.2.3}$$

$$\omega_{a,i} = X_{amb} \omega_{amb} + (1 - X_{amb}) \omega_{a,r} \tag{4.2.4}$$

where X_{amb} is the fraction of the total air handler air flow that is drawn from the ambient, h_{amb} and ω_{amb} are the enthalpy and humidity ratio associated with ambient conditions, and $h_{a,r}$ and $\omega_{a,r}$ are the enthalpy and humidity ratio of the return air from the zones. The return air conditions are determined with overall energy and mass balances.

$$h_{a,r} = h_{a,o} + \frac{\dot{Q}_{gain}}{\dot{m}_{ahu}} \tag{4.2.5}$$

$$\omega_{a,r} = \omega_{a,o} + \frac{\dot{\omega}_{gain}}{\dot{m}_{ahu}} \tag{4.2.6}$$

where $\dot{Q}_{gain}$ and $\dot{\omega}_{gain}$ are the total rate of energy and humidity gains to the ventilation stream from zones serviced by the air handler. The energy and moisture gains in a building are due to many factors that include conduction through walls, solar radiation through windows, people, lights, and equipment. In order to model these gains in detail, it is necessary to include the dynamics associated with walls and possibly the furnishings. Simulation programs such as TRNSYS [1984] contain zone models that determine energy and moisture gains in a detailed fashion. Many of the results in this

work are presented in terms of the gains to the ventilation stream. However, for the purpose of performing simulations over a cooling season, the energy and moisture gains are determined with a very simple model. The internal gains (both energy and moisture) due to people, lights, and equipment are considered to be constants that do not depend upon time. The overall conduction through walls is computed assuming an overall conductance for heat gain driven by an ambient sol-air temperature. The overall energy gains are

$$\dot{Q}_{gain} = (UA)_z(T_{sol\text{-}air} - T_z) + \dot{Q}_{int} \tag{4.2.7}$$

where $(UA)_z$ is an overall conductance, $\dot{Q}_{int}$ is the overall internal gains due to people, lights, equipment, etc., T_z is the zone temperature, and $T_{sol\text{-}air}$ is an ambient sol-air temperature determined as

$$T_{sol\text{-}air} = T_{amb} + \frac{\alpha_o}{h_o} I \tag{4.2.8}$$

where T_{amb} is the ambient dry bulb temperature, α_o and h_o are the solar absorptivity and convection coefficient for the outside of the walls, and I is the instantaneous horizontal radiation.

4.3 Chilled Water Pumping Requirements

The analysis of the pumping requirements for the chilled water loop is similar to that for the condenser loop presented in Chapter 3. The primary pressure losses in the chilled water loop are to due to the flows through the chiller and cooling coils. Commonly, the pressure drop between the chilled water supply to and return from the

air handlers is maintained at a minimum value necessary to ensure adequate flow to all air handlers in the system. For variable-speed pumping, the pump speed controller responds to changes in the air handler control valves in order to maintain the specified pressure drop. In this manner, the chilled water flow requirements of the air handlers may be met exactly (i.e. no bypass) by the pumps. For fixed-speed pumps, a bypass valve between the supply and return lines maintains the pressure drop. As the supply air temperature is increased for a given chilled water supply temperature, the water flow requirements of the air handlers are reduced and the air handler pressure drops increase. Under these circumstances, the bypass valve would open to bypass flow and reduce the pressure drop. However, for best system performance, the supply air temperatures should always be chosen to minimize the bypass flow. For systems with fixed-speed chilled water pumps, the bypass flow is considered to be zero in this study.

In the analysis of the chilled water loop, the controlled pressure drop is treated as a static (constant) pressure loss, so that the overall loop pressure drop is

$$\Delta P_{chw} = \Delta P_{ahu} + \Delta P_{evap,des}\left[\frac{\dot{m}_{chw}}{\dot{m}_{chw,des}}\right]^2 \qquad (4.3.1)$$

where ΔP_{ahu} is the static pressure drop associated with the air handlers, $\dot{m}_{chw}$ is the chilled water flow rate, and $\Delta P_{evap,des}$ is a design pressure drop for the chiller evaporator at a chilled water flow rate of $\dot{m}_{chw,des}$.

The chilled water loop pressure drop also depends upon the number of chillers in operation. For identical parallel chillers, the chilled water flow is divided equally between the chillers. In this case, the design flow rate utilized in equation (4.3.1) is simply the design value for an individual chiller multiplied by the number operating.

The design pressure drop for the parallel chillers is equal to the pressure drop for an individual component at its design flow rate.

Equating the chilled water loop pressure drop to the pump pressure rise and solving for the total flow rate gives the following relation.

$$\dot{m}_{chw} = \dot{m}_{chw,des} \sqrt{\frac{\gamma_p^2 - \dfrac{\Delta P_{ahu}}{\Delta P_{p,max,des}}}{\left[\dfrac{\dot{m}_{chw,des}}{\dot{m}_{p,max,des}}\right]^2 + \dfrac{\Delta P_{chw,des}}{\Delta P_{p,max,des}}}} \qquad (4.3.2)$$

where γ_p is the relative pump speed, $\Delta P_{p,max,des}$ is the maximum pump pressure developed at zero flow, and $\dot{m}_{p,max,des}$ the maximum flow at zero pressure rise. For fixed-speed pumps, the relative speed in the above equation is equal to unity.

For a given mass flow rate and pressure rise, the overall pump power requirement for the chilled water loop is

$$P_p = \frac{\dot{m}_{chw} \Delta P_{chw}}{\eta_p \rho_{chw}} \qquad (4.3.3)$$

where ρ_{chw} is the density of the chilled water and η_p is the overall efficiency of the pump and motor determined with a correlation of the form given by equation (3.2.8).

4.4 Summary

An effectiveness model analogous to that presented for cooling towers in Chapter 3 has been presented for cooling coils. A simple method was also developed for estimating the performance of cooling coils having both wet and dry portions. The

effectiveness relationships given in this chapter were for counterflow operation. Most cooling coils use multi-pass crossflow geometries. However, if the number of coil rows is greater than about four, then the performance of a crossflow coil approaches that of a counterflow device. The counterflow effectiveness relationship is recommended and was utilized throughout this study. However, standard effectiveness relationships for other geometries could also be applied using the definitions for Ntu and m^* given in this chapter.

Models were also presented for the air handlers and chilled water pumps. Again, it is important to note that quadratic functions work well in correlating the power consumptions of these auxiliary devices.

Chapter 5

Methodologies for Optimal Control of Systems without Storage

The optimal control problem associated with a central chilled water system may be thought of as having a two-level hierarchical structure. The first level involves local loop control in response to prescribed setpoints. An example of a first level control variable would be the compressor speed for a variable-speed chiller. The second level controls are independent variables that may be adjusted to minimize the operating costs, while still satisfying the load requirements. In the previous example, the chilled water supply temperature is a second level variable that may be adjusted independently.

The dynamics of the first level (local loop) controls must be considered in order to maintain prescribed setpoints in an efficient manner. However, for systems without significant thermal storage, the system dynamics may be neglected (Hackner [1985]) in the determination of the optimal second level control setpoints. In this study, local loop control is not considered and the first level (local loop) control is considered to be entirely dependent upon the second level setpoints.

Optimal control of a system involves minimizing the total power consumption of the chillers, cooling tower fans, condenser water pumps, chilled water pumps, and the air handling fans at each instant of time with respect to the independent continuous and discrete control while maintaining the desired zone conditions and ensuring that the control variables are within acceptable bounds. Discrete control variables are not continuously adjustable, but have discrete settings, such as the number of operating chillers, cooling tower cells, condenser water pumps, and chilled water pumps and the relative speeds for multi-speed fans or pumps. Independent continuous control

variables might include the chilled water and supply air set temperatures, relative water flow rates to the chillers (evaporators and condensers), cooling tower cells, and cooling coils, and the speeds for variable-speed fans or pumps.

In this chapter, two methodologies are presented for determining optimal values of the independent control variables that minimize the instantaneous cost of operating chilled water systems. In section 5.1, a modular component-based optimization algorithm is presented. The algorithm is implemented in a computer program that simulates the operation of a system through time, while minimizing the cost at each time increment in response to the uncontrolled (e.g. weather) variables. Each hardware component is represented as a separate subroutine in the simulation of a system. Information concerning the cost of operation of individual components and the manner in which the components are interconnected are used to perform the optimization in an efficient manner. Each component may also have constraints associated with its operation. The modular nature of this program is similar to that of the widely used TRNSYS [1984] simulation program. However, TRNSYS has no capability for performing control optimization and could not be utilized for this study.

There are three intended uses for the component-based optimization program in this study :

1) Analysis of control and design options: The program may be used as a simulation tool for comparing conventional and optimal control strategies. Conventional control strategies, such as fixed temperature setpoints, are implemented through the imposition of constraint equations. Design comparisons, such as variable versus fixed-speed equipment, may be performed for systems that are optimally controlled.

2) On-line control optimization: The algorithm may be used for on-line optimization of the simulation of an operating system using "simple" component models. The simulation could proceed in parallel with the actual system operation with the possibility of updating parameters of the component models using on-line measurements.

3) Near-optimal control algorithms: Results of the optimization program are useful for developing "simple" near-optimal control algorithms.

In Chapter 6, the component-based algorithm is applied to typical systems to study both design and control issues. Existing optimization packages proved to be extremely inefficient for these systems and had difficulties handling the nonlinear equality constraints that arose.

In section 5.2, a "simple" methodology is presented for near-optimal control. An overall empirical cost function for the total power consumption of the cooling plant is inferred from the cost functions associated with the components utilized in chilled water systems. This cost function lends itself to rapid determination of optimal control variables and may be fit to measurements using linear regression techniques. In section 5.3, results of the system-based and component based algorithms are compared.

5.1 A Component-Based Optimization Algorithm

Figure 5.1 depicts the general nature of the modular optimization problem. Each component in a system is represented as a separate set of mathematical relationships organized into a computer model. Its output variables and operating cost are functions of parameter, input, output, uncontrolled, and controlled variables. The structure of the

complete set of equations to be solved for the entire system is dictated by the manner in which the components are interconnected together.

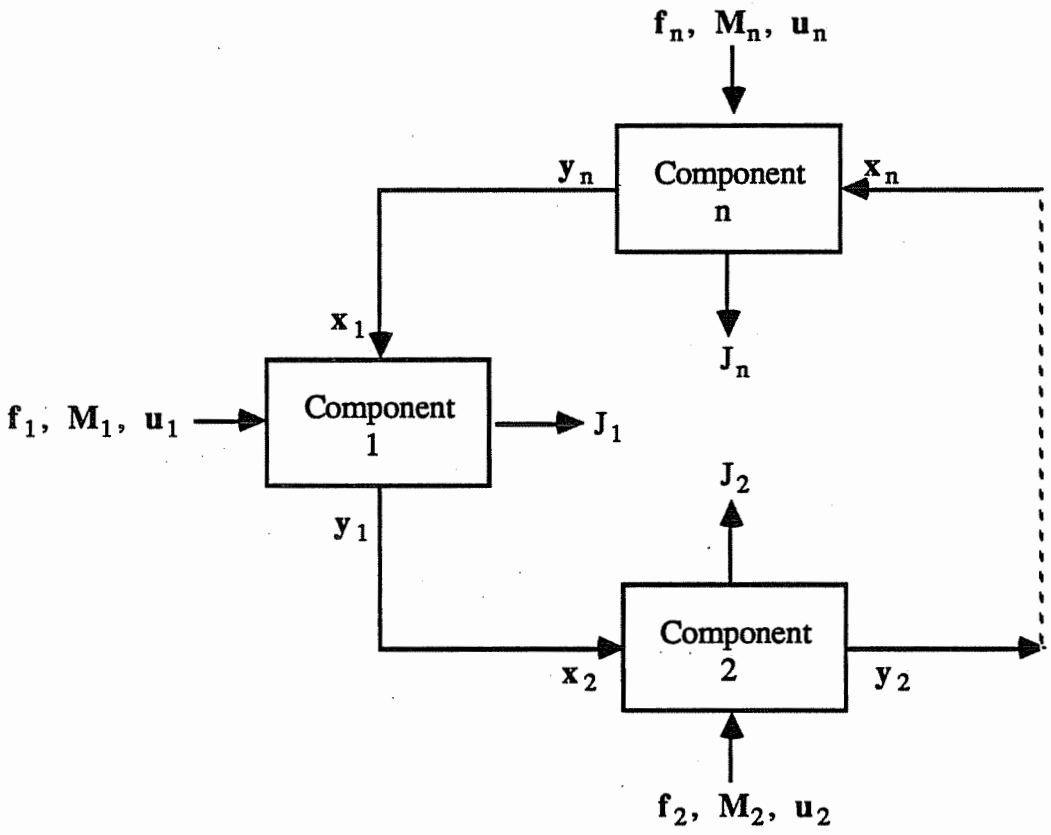

Figure 5.1. Schematic of the Modular Optimization Problem

The optimization problem is formally stated as the minimization of the sum of the operating costs of each component, J_i, with respect to all discrete and continuous controls or

Minimize

$$J(\mathbf{f},\mathbf{M},\mathbf{u}) = \sum_{i=1}^{n} J_i(\mathbf{x}_i, \mathbf{y}_i, \mathbf{f}_i, \mathbf{M}_i, \mathbf{u}_i) \qquad (5.1.1)$$

with respect to **M** and **u**, subject to equality constraints of the form

$$\mathbf{g}(\mathbf{f}, \mathbf{M}, \mathbf{u}) = \begin{bmatrix} \mathbf{g}_1(\mathbf{f}_1, \mathbf{M}_1, \mathbf{u}_1, \mathbf{x}_1, \mathbf{y}_1) \\ \mathbf{g}_2(\mathbf{f}_2, \mathbf{M}_2, \mathbf{u}_2, \mathbf{x}_2, \mathbf{y}_2) \\ \cdot \\ \mathbf{g}_n(\mathbf{f}_n, \mathbf{M}_n, \mathbf{u}_n, \mathbf{x}_n, \mathbf{y}_n) \end{bmatrix} = 0 \qquad (5.1.2)$$

and inequality constraints of the form

$$\mathbf{h}(\mathbf{f}, \mathbf{M}, \mathbf{u}) = \begin{bmatrix} \mathbf{h}_1(\mathbf{f}_1, \mathbf{M}_1, \mathbf{u}_1, \mathbf{x}_1, \mathbf{y}_1) \\ \mathbf{h}_2(\mathbf{f}_2, \mathbf{M}_2, \mathbf{u}_2, \mathbf{x}_2, \mathbf{y}_2) \\ \cdot \\ \mathbf{h}_n(\mathbf{f}_n, \mathbf{M}_n, \mathbf{u}_n, \mathbf{x}_n, \mathbf{y}_n) \end{bmatrix} \geq 0 \qquad (5.1.3)$$

where, for any component i,

$\mathbf{x}_i$ = vector of input stream variables

$\mathbf{y}_i$ = vector of output stream variables

$\mathbf{f}_i$ = vector of uncontrolled variables

$\mathbf{M}_i$ = vector of discrete control variables

$\mathbf{u}_i$ = vector of continuous control variables

J_i = operating cost

$\mathbf{g}_i$ = vector of equality constraints

$\mathbf{h}_i$ = vector of inequality constraints

Typical input and output stream variables for chilled water systems are temperature and mass flow rate. The uncontrolled variables are measurable quantities that may not be controlled, but that affect the component outputs and/or costs, such as ambient dry

bulb and wet bulb temperature.

Both equality and inequality constraints arise in the optimization of chilled water systems. One example of an equality constraint that arises when two or more chillers are in operation is that the sum of their relative loadings must be one. The simplest type of inequality constraints to handle are bounds on control variables. For example, lower and upper limits are necessary for the chilled water set temperature, in order to avoid freezing in the evaporator and to provide adequate dehumidification for the zones. Any equality constraint may be rewritten in the form of equation (5.1.2) such that when it is satisfied, the constraint equation is equal to zero. Similarly, inequality constraints may be expressed as equation (5.1.3), so that the constraint equation is greater than or equal to zero to avoid violation.

The mathematics associated with the optimization algorithm utilized in this study are well known. Special advantage is taken of the characteristic that the operating costs associated with each component in a chilled water system may be modeled with quadratic functions. A background for the development that follows is presented by Gill [1981]. In the next section, an algorithm is presented for determining optimal values of the continuous control variables for the special case where all component costs are quadratic functions and output stream variables are linear functions of the controls. This algorithm is the basis for the more general nonlinear method presented in section 5.1.2. The procedure for handling constraints is given in section 5.1.3 and the complete algorithm including the determination of the optimal discrete controls and implementation in a computer program is summarized in section 5.1.4.

5.1.1 Quadratic Costs and Linear Outputs

A simple function for which an optimum exists and may be determined analytically

is a quadratic function. In Chapter 2, it was shown that the power consumption of a chiller may be adequately represented as a quadratic function of the load and the temperature difference between leaving condenser and evaporator water temperatures. The other energy consuming components in a chilled water system are pumps and fans. As shown in Chapters 3 and 4, the power requirement of a continuously adjustable pump or fan (variable-speed or variable-pitch) may be accurately represented with a quadratic function of its control variable through either a second-order Taylor series approximation or a single quadratic correlating function. As a result, the cost of operating any of these components (chillers or auxiliary equipment) may be expressed in a general form as a quadratic function of its continuous control and/or output stream variables or

$$J_i = \mathbf{u}_i^T \mathbf{A}_i \mathbf{u}_i + \mathbf{y}_i^T \mathbf{B}_i \mathbf{y}_i + \mathbf{y}_i^T \mathbf{C}_i \mathbf{u}_i + \mathbf{p}_i^T \mathbf{u}_i + \mathbf{q}_i^T \mathbf{y}_i + r_i \qquad (5.1.4)$$

where $\mathbf{A}_i$, $\mathbf{B}_i$, and $\mathbf{C}_i$ are coefficient matrices, $\mathbf{p}_i$ and $\mathbf{q}_i$ are vectors, and r_i is a scalar constant. The coefficients of this cost function may depend upon the component operating modes (discrete controls) and uncontrolled variables.

The optimization problem is simplified if the output stream variables for each component are linear functions of the input stream and continuous control variables or

$$\mathbf{y}_i = \theta_i \mathbf{u}_i + \phi_i \mathbf{x}_i + \xi_i \qquad (5.1.5)$$

where θ_i and ϕ_i are coefficient matrices and ξ_i is a coefficient vector that may depend upon the discrete control and uncontrolled variables. The inputs to component i are outputs from other components, so that the solution for all output stream variables is of the form

$$y(f, M, u) = \tilde{\theta}u + \tilde{\xi} \tag{5.1.6}$$

where the coefficient matrix $\tilde{\theta}$ and vector $\tilde{\xi}$ depend upon the coefficients for the individual components and the interconnections between components.

The total cost of operation at any time is the sum of the individual component operating costs. With individual component costs and outputs represented by equations (5.1.4) and (5.1.5), the total cost may be reduced to

$$J(f, M, u) = u^T \tilde{A} u + \tilde{b}^T u + \tilde{c} \tag{5.1.7}$$

where,

$$\tilde{A} = A + \tilde{\theta}^T \left[B\tilde{\theta} + C \right]$$

$$\tilde{b} = p + \tilde{\theta}^T \left[2B^T \tilde{\xi} + q \right] + C^T \tilde{\xi}$$

$$\tilde{c} = r + \left[\tilde{\xi}^T B + q^T \right] \tilde{\xi}$$

$$A = \begin{bmatrix} A_1 & & \\ & A_2 & \\ & & \ddots \\ & & & A_n \end{bmatrix} \quad B = \begin{bmatrix} B_1 & & \\ & B_2 & \\ & & \ddots \\ & & & B_n \end{bmatrix} \quad C = \begin{bmatrix} C_1 & & \\ & C_2 & \\ & & \ddots \\ & & & C_n \end{bmatrix}$$

$$\mathbf{p} = \begin{bmatrix} p_1 \\ p_2 \\ . \\ p_n \end{bmatrix} \qquad \mathbf{q} = \begin{bmatrix} q_1 \\ q_2 \\ . \\ q_n \end{bmatrix} \qquad r = \sum_{i=1}^{n} r_i$$

The first-order condition for a minimizing or maximizing point requires that the Jacobian of the cost function be equal to zero. The Jacobian is a vector containing the partial derivatives of the cost function with respect to each of the control variables. For the cost function of equation (5.1.7)

$$\left[\frac{\partial J}{\partial \mathbf{u}}\right]_{\mathbf{u}^*} = \mathbf{u}^*(\tilde{\mathbf{A}} + \tilde{\mathbf{A}}^T) + \tilde{\mathbf{b}}^T = 0 \tag{5.1.8}$$

where $\mathbf{u}^*$ represents the optimal control vector. Solving for $\mathbf{u}^*$ gives

$$\mathbf{u}^* = -\left[\tilde{\mathbf{A}} + \tilde{\mathbf{A}}^T\right]^{-1} \tilde{\mathbf{b}} \tag{5.1.9}$$

In general, the cost functions that arise with chilled water systems are globally convex, so that a single global minimum exists. However, it is relatively simple to determine convexity of a quadratic equation. In order to determine whether $\mathbf{u}^*$ represents a minimum, maximum, or saddle point, it necessary to evaluate second derivatives. The second-order condition for a minimum requires that the Hessian of the cost function be positive semi-definite. The Hessian is a matrix containing partial derivatives of the transpose of the Jacobian with respect to all control variables. For the cost function of equation (5.1.7), the Hessian is simply

$$\frac{\partial}{\partial \mathbf{u}}\left(\frac{\partial J}{\partial \mathbf{u}}^{T}\right) = (\tilde{\mathbf{A}} + \tilde{\mathbf{A}}^{T}) \tag{5.1.10}$$

Positive semi-definiteness of the above Hessian implies that

$$\mathbf{u}^{T}(\tilde{\mathbf{A}} + \tilde{\mathbf{A}}^{T})\mathbf{u} \geq 0 \tag{5.1.11}$$

for all **u** not equal to zero. Simple methods exist for determining the positive semi-definiteness of symmetric Hessian matrices such as that given by equation (5.1.10).

5.1.2 Nonlinear Optimization

Some component outputs depend non-linearly upon controls or input variables and some component costs are only quadratic locally, so that an iterative technique is required to determine the optimal control values. At each iteration, an overall quadratic for the system expressed as equation (5.1.7) is formed from individual quadratic relationships for each component (eq. (5.1.4)) and a linearization of the output variables (eq. (5.1.6)).

All output variables are linearized with respect to the continuous controls using a first-order Taylor series expansion about the last iteration point, $\mathbf{u}_0$.

$$\mathbf{y(u)} \approx \mathbf{y(u_0)} + \left[\frac{\partial \mathbf{y}}{\partial \mathbf{u}}\right]_{\mathbf{u_0}} (\mathbf{u} - \mathbf{u_0}) \tag{5.1.11}$$

This equation may be written in the form of equation (5.1.6) with

$$\tilde{\theta} = \mathbf{y(u_0)} - \left[\frac{\partial \mathbf{y}}{\partial \mathbf{u}}\right]_{\mathbf{u_0}} \mathbf{u_0} \tag{5.1.12}$$

$$\tilde{\xi} = \left[\frac{\partial \mathbf{y}}{\partial \mathbf{u}}\right]_{\mathbf{u_0}} \tag{5.1.13}$$

The Jacobian of the outputs with respect to control variables is determined numerically using forward differences.

A simple estimate of the minimum point may be determined from equation (5.1.9). However, for points that are "far away" from the minimum, this may give a point that has a greater cost than the last iteration. A common procedure, that is utilized in this study, is to perform a one-dimensional search between the previous iteration and the point defined by equation (5.1.9). At the i^{th} iteration, a new estimate of the optimal control point is

$$\mathbf{u}^i = \mathbf{u}^{i-1} + s(\mathbf{u}' - \mathbf{u}^{i-1}) \tag{5.1.14}$$

where $\mathbf{u}'$ is from equation (5.1.9) and the step length, s, is determined by minimizing $J(\mathbf{u}^{i-1} + s(\mathbf{u}' - \mathbf{u}^{i-1}))$ with respect to s.

The optimal step length is approximated with polynomial interpolation. The costs at

step lengths of zero, one-half, and one are used to construct a quadratic function for the cost as a function of the step length. The optimal value of s is estimated as the minimum of this quadratic function, constrained between zero and one. In some cases, the polynomial may be a poor approximation to the real function and the estimated optimal step length may result in a cost greater than that associated with a step length of zero. Under this circumstance, the interpolation is repeated with the last computed optimal step length becoming the new step length of unity.

It is necessary to iteratively solve for the outputs of each component at each iteration of the optimization procedure with the most recent controls. A simple method that is employed in the TRNSYS [1984] program is successive substitution. Outputs are successively fed as inputs to connecting components until the values are not changing significantly. However, this method can be extremely inefficient for solving systems of equations, even if they are linear. The solution efficiency is important because the equations must be solved at each iteration of the optimization procedure and a high degree of accuracy is required for determining good numerical derivatives.

A better approach is to utilize the Newton-Raphson method applied to a set of equations that measure the residual error for the independent variables. These residual equations could be defined as differences between input values and output values that feed those inputs for one component in each recyclic loop of components. At each iteration of the Newton-Raphson procedure, new estimates of the independent variables are determined by assuming that the residual equations are globally linear using coefficients determined with a local linearization. As a result, this method converges in one iteration for linear equations. However, it is necessary at each iteration to solve a system of linear equations involving a Jacobian of residuals with respect to the independent iteration variables. The Jacobian contains the partial derivatives of each of the residual equations with respect to the independent variables and must be determined

numerically.

In the program developed in this study, an alternative method is employed that is a compromise between the methods of successive substitution and Newton-Raphson. As with Newton-Raphson, a set of residual equations are defined such that at the solution, they are identically zero. However, these equations are solved using a series of one-dimensional applications of the secant method. Consider a series of components organized in a recyclic loop. Denoting the input to one component in the loop as x and the output that feeds that input as y(x), then a residual function at the i^{th} iteration may be defined as

$$G^i = y(x^i) - x^i \tag{5.1.15}$$

A new estimate of x is determined by approximating the function with a straight line connected between the last two function values or

$$x^{i+1} = x^i - \frac{G^i}{(G^i - G^{i-1})/(x^i - x^{i-1})} \tag{5.1.16}$$

Initial values of x, y, and G are determined through successive substitution.

The advantage of this method is that it is not necessary to compute a Jacobian, so that the computation associated with updating the independent variables is much less than that for Newton-Raphson. However, since the residual equations are not coupled, convergence is slower than for Newton-Raphson. For the chilled water systems considered in this study, the coupling between recyclic loops is relatively small and the solution algorithm works well.

5.1.3 Constraints

Linear Equality Constraints

For constraints that are linear with respect to the control variables, the constraint equations may be written in the form

$$\mathbf{g(u)} = \alpha + \beta\mathbf{u} = 0 \tag{5.1.17}$$

where **g** is a vector of constraint equations, β is a coefficient matrix, and α is a coefficient vector.

A common method for solving optimization problems with linear constraints is the method of Lagrange multipliers. This method involves redefining the cost function so that at the minimum, the constraint function is automatically satisfied. The modified cost function, termed the Lagrangian, is given as

$$\tilde{J}(\mathbf{u},\lambda) = J(\mathbf{u}) + \lambda^{T}\mathbf{g(u)} \tag{5.1.18}$$

where λ is a vector of Lagrange multipliers. The modified optimization problem involves minimizing the Lagrangian with respect to both **u** and λ. The first-order conditions for a minimum require that

$$\left[\frac{\partial \tilde{J}}{\partial \mathbf{u}}\right]_{\mathbf{u}^*} = \left[\frac{\partial J}{\partial \mathbf{u}} + \lambda^{T}\frac{\partial \mathbf{g}}{\partial \mathbf{u}}\right]_{\mathbf{u}^*} = 0 \tag{5.1.19}$$

$$\left[\frac{\partial \tilde{J}}{\partial \lambda}\right]_{u^*} = g(u^*) = 0 \tag{5.1.20}$$

For the quadratic cost function and linear constraints of equations (5.1.7) and (5.1.17), these conditions yield

$$u^* = \left[\tilde{A} + \tilde{A}^T\right]^{-1}\left[\beta^T \lambda - \tilde{b}\right] \tag{5.1.21}$$

$$\lambda = \left[\beta(\tilde{A} + \tilde{A}^T)^{-1}\beta^T\right]^{-1}\left[\beta(\tilde{A} + \tilde{A}^T)^{-1}\tilde{b} - \alpha\right] \tag{5.1.22}$$

Nonlinear Equality Constraints

Nonlinear constraints are handled through linearization and the use of Lagrange multipliers. A first-order Taylor series expansion for the constraints about the last iteration point, u_o, gives

$$g(u) \approx g(u_o) + \left[\frac{\partial g}{\partial u}\right]_{u_o}(u - u_o) \tag{5.1.23}$$

The above equation may be written in the form of equation (5.1.17) with

$$\alpha = g(u_o) - \left[\frac{\partial g}{\partial u}\right]_{u_o} u_o \tag{5.1.24}$$

$$\beta = \left[\frac{\partial g}{\partial u}\right]_{u_o} \tag{5.1.25}$$

The Jacobian of the constraints with respect to control variables is determined numerically using forward differences coincidently with the computation of the Jacobian for the output stream variables with respect to controls.

With linearization applied to nonlinear constraints, the first-order condition applied to the Lagrangian cost function does not guarantee that the constraints will be satisfied at any point except the solution. More importantly, during the determination of the optimal step length, the Lagrangian does not provide a good measure of the degree to which the constraints are violated. To alleviate this problem, the optimal step length is computed using a cost function that is the sum of the original cost function and a quadratic penalty function.

$$\hat{J}(\mathbf{u}) = J(\mathbf{u}) + \mathbf{g}(\mathbf{u})^T\mathbf{g}(\mathbf{u}) \qquad (5.1.26)$$

At the i^{th} iteration, a new estimate of the optimal control point is found with equation (5.1.14), with $\mathbf{u}'$ determined from equations (5.1.21) and (5.1.22) and the step length , s, determined by minimizing $\hat{J}(\mathbf{u}^{i-1} + s(\mathbf{u}' - \mathbf{u}^{i-1})$ with respect to s.

Inequality Constraints

The only inequality constraints considered in this study are simple bounds on the control variables. These become linear equality constraints when violated and are handled with Lagrange multipliers. In order to determine the optimal control points subject to inequality constraints, the optimal control values are first determined at each iteration assuming that no inequality constraints are violated. If some control bounds are exceeded, then linear equality constraints representing these limits are added and the

optimal controls are recomputed. Additional constraints are added if violated and the process is repeated until the number of constraints is not changing or equals the number of control variables. The constrained control values represent the next iterates in the overall nonlinear optimization. It is not possible to solve a problem in which the number of constraints exceeds the number of control variables. In this situation, some of the constraints are not satisfied.

5.1.4 Algorithm Summary and Program Implementation

The steps associated with the constrained optimization of the continuous controls are summarized below.

1) Solve for component outputs with current controls.
2) Linearize outputs with respect to controls to get equation (5.1.6).
3) Determine the coefficients of the quadratic equation (5.1.7) from the component quadratic equations (5.1.4) and the linearized output equation (5.1.6).
4) Determine the control point associated with a step length of unity with equations (5.1.21) and (5.1.22).
5) Estimate optimal step length with polynomial interpolation applied to minimizing $\hat{J}(\mathbf{u}^{i-1} + s(\mathbf{u}' - \mathbf{u}^{i-1})$ with respect to s, where the augmented cost function is defined by equation (5.1.26).
6) Determine next estimate of control point, $\mathbf{u}^i$, with equation (5.1.14).
7) If $\hat{J}(\mathbf{u}^i) > \hat{J}(\mathbf{u}^{i-1})$ then set $\mathbf{u}' = \mathbf{u}^i$ and go to step 5.
8) If no controls exceed their bounds or the number of constraints equals the number of controls then go to step 11.
9) Add equality constraints for any controls that exceed bounds unless the number of constraints equals the number controls.

10) Determine a constrained optimum with equations (5.1.21) and (5.1.22) and go to step 8.

11) If the change in cost from the last iteration is greater than a specified tolerance, then go to step 1.

The complete optimization algorithm is implemented in a computer program that can simulate the optimal operation of a system through time (Braun [1988]). The system is described through input data that specifies the components, their parameters, and their interconnections in a manner similar to that for the TRNSYS [1984] simulation program. At each simulation timestep, data for the uncontrolled variables (e.g., weather, schedules) are read and the constrained nonlinear optimization of the continuous control variables is performed for each feasible combination of discrete controls with the combination giving the minimum being the optimal control. Not all possible combinations of discrete controls are feasible. For instance, the operation of more than one condenser or chilled water pump might be non-optimal under all conditions when only one chiller is on, so that these combinations would not be worth considering. In the implementation of the optimization algorithm for this study, the feasible combinations of discrete modes are specified as input data. In the event that the optimization algorithm were implemented for on-line optimal control, then a better approach for determining the optimal discrete control modes at each time interval would be to order the feasible combinations of modes and only allow a single change (up or down) between combinations within the list.

The complete mathematical description of a specific optimization problem depends upon the choice of the independent controls and the constraints imposed upon the system. Generally the supply air temperature for each air handler is considered to be an

independent (adjustable) control variable. In this case, the local loop controller varies the air and water flow through the cooling coil in order to maintain that setpoint, along with the desired temperature in the zone. However, in terms of the optimization algorithm, it is more straightforward to consider the relative air and water flow rates to the cooling coil as control variables, with an equality constraint that forces the zone temperature to be maintained. One advantage of this formulation is that the power consumption of the air handler may be represented as a quadratic function of the speed in a simple manner. It is also easier to handle bounds on the fan speed as compared with the supply air setpoint, since the fan speed has a natural upper and lower bound, while physical constraints on the setpoint vary according to the coil entering air and water conditions and design.

5.2 A System-Based Algorithm for Near-Optimal Control

The methodology for determining optimal values of control variables described in the previous section could be used for on-line optimal control of chilled water systems. However, in order to calibrate the models for a specific plant, measurements would be required for outputs and power consumptions for each component in the system. Also, depending upon the number of control variables, the computational requirements may be restrictive. An alternative approach for near-optimal control described in this section involves correlating the overall system power consumption with a single function that allows for a rapid determination of optimal control variables and requires measurements of only total power over a range of conditions.

5.2.1 System Cost Function

The concept of utilizing quadratic functions for the power consumptions of individual components can be extended to the system as a whole. In the vicinity of any

optimal control point, the system power consumption may be approximated with a quadratic function of the continuous control variables according to equation (5.1.7). However, the quadratic relationship changes with changes in the operating modes (i.e. discrete controls) and uncontrolled variables. It will be shown that a quadratic function also correlates power consumption in terms of the uncontrolled variables over a wide range of conditions, so that the following cost function may be applied for determining optimal control points.

$$J(\mathbf{f},\mathbf{M},\mathbf{u}) = \mathbf{u}^T\hat{\mathbf{A}}\mathbf{u} + \hat{\mathbf{b}}^T\mathbf{u} + \mathbf{f}^T\hat{\mathbf{C}}\mathbf{f} + \hat{\mathbf{d}}^T\mathbf{f} + \mathbf{f}^T\hat{\mathbf{E}}\mathbf{u} + \hat{g} \qquad (5.2.1)$$

where $\hat{\mathbf{A}}$, $\hat{\mathbf{C}}$, and, $\hat{\mathbf{E}}$ are coefficient matrices, $\hat{\mathbf{b}}$ and $\hat{\mathbf{d}}$ are coefficient vectors, and $\hat{g}$ is a scalar. The empirical coefficients of the above cost function depend upon the operating modes, so that it is necessary to determine these constants for feasible combinations of discrete control modes. Once again, many mode combinations may be unfeasible or clearly non-optimal under all conditions and therefore need not be considered. Some advantage may also be taken of the symmetry in the quadratic terms of equation (5.2.1). Both $\hat{\mathbf{A}}$ and $\hat{\mathbf{C}}$ may be expressed as symmetric matrices, so that only the upper (or lower) triangular coefficients need be determined.

5.2.2 Near-Optimal Control Algorithm

One advantage of the cost function of equation (5.2.1) is that a solution for the optimal control vector that minimizes the cost may be determined analytically by applying the first-order condition for a minimum. Equating the Jacobian of equation (5.2.1) with respect to the control vector to zero and solving for the optimal control, (with symmetric $\hat{\mathbf{A}}$), gives

$$\mathbf{u}^* = \mathbf{k} + \mathbf{K}\mathbf{f} \tag{5.2.2}$$

where,

$$\mathbf{k} = -\frac{1}{2}\hat{\mathbf{A}}^{-1}\hat{\mathbf{b}}$$

$$\mathbf{K} = -\frac{1}{2}\hat{\mathbf{A}}^{-1}\hat{\mathbf{E}}$$

The cost associated with the unconstrained control of equation (5.2.2) is

$$J^* = \mathbf{f}^T\Theta\mathbf{f} + \sigma^T\mathbf{f} + \tau \tag{5.2.3}$$

where,

$$\Theta = \mathbf{K}^T\hat{\mathbf{A}}\mathbf{K} + \hat{\mathbf{E}}\mathbf{K} + \hat{\mathbf{C}}$$

$$\sigma = 2\mathbf{K}\hat{\mathbf{A}}\mathbf{k} + \mathbf{K}\hat{\mathbf{b}} + \hat{\mathbf{E}}\mathbf{k} + \hat{\mathbf{d}}$$

$$\tau = \mathbf{k}^T\hat{\mathbf{A}}\mathbf{k} + \hat{\mathbf{b}}^T\mathbf{k} + g$$

The control defined by equation (5.2.2) results in a minimum power consumption if and only if the Hessian of the cost function is a positive-definite matrix or in the case of equation (5.2.1), if $\hat{\mathbf{A}}$ is positive definite. If this condition holds and if the system power consumption correlates with equation (5.2.1), then equation (5.2.2) dictates that

the optimal continuous control variables vary as a near linear function of the uncontrolled variables. However, a different linear relationship applies to each feasible combination of discrete control modes. In the implementation of the algorithm, the minimum cost associated with each mode combination is computed from equation (5.2.3). The costs for each combination are compared in order to identify the minimum. Simple bounds on the continuous control variables may be handled as outlined in section 5.1.3.

5.2.3 Parameter Estimation

The total number of empirical coefficients in equation (5.2.1) that need to be determined for each feasible set of modes is

$$N_{coef} = N_u^2 - \frac{N_u(N_u - 1)}{2} + N_u + N_f^2 + \frac{N_f(N_f - 1)}{2} + N_f + N_f N_u + 1 \quad (5.2.4)$$

where N_u is the number of continuous control variables and N_f is the number uncontrolled variables.

One approach for determining these constants would be to apply regression techniques directly to measured total power consumption. Since the cost function is linear with respect to the empirical coefficients, linear regression techniques may be utilized. A set of experiments could be performed on the system over the expected range of operating conditions. In some cases, the quadratic cost function may only be an accurate index near the optimal control points, so that it would be necessary to repeat the experiments in the vicinity of the control defined by equation (5.2.2). Possibly, the regression could be performed on-line using least-squares recursive parameter updating (Ljung [1983]).

Another approach for estimating coefficients of the empirical system model would involve regression to results of a simulation of the system. By using mechanistic models for the individual components, data over a limited range of conditions would be sufficient to calibrate the coefficients of the models. The use of the component-based optimization algorithm as a simulation tool would ensure a good fit near the optimal control points.

Rather than fitting empirical coefficients of the system cost function of equation (5.2.1), the coefficients of the optimal control equation (5.2.2) and the minimum cost function of equation (5.2.3) could be determined directly with regression applied to optimal control results. At a given set of conditions, optimal values of the continuous control variables could be estimated through trial-and-error variations in the system or with the component-based optimization algorithm. Only $(N_f + 1)$ independent conditions would be necessary to determine coefficients of the linear control law given by equation (5.2.2). The coefficients of minimum cost function could then be determined from system measurements with the linear control law in effect. The total number of coefficients to determine with this approach is less than that for direct regression to power measurements.

$$N_{coef} = N_u(N_f + 1) + N_f^2 - \frac{N_f(N_f - 1)}{2} + N_f + 1 \qquad (5.2.5)$$

The disadvantage of this approach is that there is no direct way to handle constraints on the controls.

5.2.4 Application to Chilled-Water Systems

In order to apply the system-based optimization technique, it is necessary to identify

both the control variables for which the optimization is to be performed and the uncontrolled variables that effect the system performance through time. Using the component-based optimization algorithm described in this chapter, it is shown in Chapter 6 that the important uncontrolled variables are the total chilled water load and ambient wet bulb temperature. Additional secondary uncontrolled variables that could be important if varied over a wide range would be the individual zone latent to sensible load ratios and the ratios of individual sensible zone loads to the total sensible loads for all zones.

Chapter 6 also identifies control simplifications that reduce the number of independent control variables and simplify the optimization. These simplifications and their implications are summarized as follows.

1) Variable-Speed Tower Fans: Operate all tower cells at identical fan speeds. The only tower control variable is fan-speed which is equivalent to air flow relative to the maximum possible flow.

2) Multi-Speed Tower Fans: Increment lowest tower fans first when adding tower capacity. Reverse for removing capacity. With this sequencing, a single independent tower control variable is the relative tower air flow.

3) Variable-Speed Pumps: The sequencing of variable-speed pumps should be directly coupled to the sequencing of chillers, to give peak pump efficiencies for each possible combination of operating chillers. Multiple variable-speed pumps should be controlled to operate at equal fractions of their maximum speed. With this sequencing arrangement, a single independent control variable for the condenser pump is the flow relative to the maximum possible flow.

4) Chillers: Multiple chillers should have identical chilled water set temperatures and the evaporator and condenser water flows for multiple chillers should be divided according to the chillers relative cooling capacities. The independent chiller control variables are a single chilled water temperature and the number of chillers operating.

5) Air Handlers: All parallel air handlers should have identical supply air setpoint temperatures. As a result, only a single setpoint control variable applies to all air handlers.

Using these general results, a reduced set of independent control variables are: 1) supply air set temperature, 2) chilled water set temperature, 3) relative tower air flow, 4) relative condenser water flow, and 5) the number of operating chillers.

The supply air and chilled water setpoints are continuously adjustable control variables. However, since the chilled water flow requirements are dependent upon these controls, there may be discrete changes in power consumption associated with varying these controls, if there are discrete control changes in the pump operation. For the same total flow rate, the overall pumping efficiency changes with the number of operating pumps. However, this has a relatively small effect upon the overall power consumption, so that the discontinuity may be neglected in fitting the overall cost function to changes in the control variables.

For variable-speed cooling tower fans and condenser water pumps, the relative tower air and condenser water flows are continuous control variables. Analogous to the chilled water flow, the overall condenser pumping efficiency changes with the number of operating pumps, so that there may be a discontinuity in the power

consumption associated with continuous changes in the overall relative condenser water flow. This discontinuity may also be neglected in fitting the overall cost function to changes in this control variable.

With variable-speed pumps and fans, the only significant discrete control variable is the number of chillers operating. A chiller mode defines which of the available chillers are to be on-line. The optimization problem involves determining optimal values of only four continuous control variables for each of the feasible chiller modes. The chiller mode giving the minimum overall power consumption represents the optimum. In order for a chiller mode to be feasible, it must be possible to operate the specified chillers safely within their capacity and surge limits. In practice, abrupt changes in the chiller modes should also be avoided. Large chillers should not be cycled on or off, except when the savings in associated costs with the change is significant.

For fixed-speed cooling tower fans and condenser water pumps, there are only discrete possibilities for the relative flows. One method of handling these variables is to consider each of the discrete combinations as separate modes. However, for multiple cooling tower cells with multiple fan speeds, the number of possible combinations may be large. A simpler approach, that works well in this case, is to treat the relative flows as continuous control variables and to select the discrete relative flow that is closest to that determined with the continuous optimization. At least three relative flows (discrete flow modes) are necessary for each chiller mode in order to fit the quadratic cost function. The number of possible sequencing modes for fixed-speed pumps is generally much more limited than that for cooling tower fans, with at most two or three possibilities for each chiller mode. In fact, with many current designs, individual pumps are physically coupled with chillers and it is impossible to operate greater or fewer pumps than the number of chillers operating. Thus, it is generally best

to treat the control of fixed-speed condenser water pumps with a set of discrete control possibilities, rather than using a continuous control approximation.

The methodology for near-optimal control of a chilled water system may be summarized as follows.

1) Change the chiller operating mode if at the limits of chiller operation (surge or capacity).
2) For the current set of conditions (load and wet bulb), estimate the feasible modes of operation that would avoid limits on the chiller and condenser pump operation.
3) For the current operating mode, determine optimal values of the continuous controls with equation (5.2.2).
4) Determine a constrained optimum, if controls exceed their bounds.
5) Repeat steps 3 and 4 for each feasible operating mode.
6) Change the operating mode if the optimal cost associated with the new mode is significantly less than that associated with the current mode.
7) Change the values of the continuous control variables. When treating multiple-speed fan control with a continuous variable, use the discrete control closest to the optimal continuous value.

If the linear optimal control equation (5.2.2) is directly fit to optimal control results, then there is no direct way of handling the constraints. A simple solution is to constrain the individual control variables as necessary and neglect the effects of the constraints on the optimal values of the other controls and the minimum cost function. The variables of primary concern with regard to constraints are the chilled water and supply air set temperatures. These controls must be bounded for proper comfort and safe operation

of the equipment. On the other hand, the cooling tower fans and condenser water pumps should be sized so that the system performs efficiently at design loads and constraints on control of this equipment should only occur under extreme conditions.

There is a strong coupling between optimal values of the chilled water and supply air temperature, so that decoupling these variables in evaluating constraints is generally not justified. However, when either control is operating at a bound, optimization results indicate that the optimal value of the other "free" control is approximately bounded at a value that depends only upon the ambient wet bulb temperature. The optimal value of this "free" control (either chilled water or supply air setpoint) may be estimated at the load at which the other control reaches its limit. Coupling between optimal values of the chilled water and condenser water loop controls is not as strong, so that interactions between constraints on these variables may be neglected.

5.3 Comparisons

Braun [1987] correlated the power consumption of the Dallas/Fort Worth airport chiller, condenser pumps, and cooling tower fans with the quadratic cost function given by equation (5.2.1) and showed good agreement. Since the chilled water loop control was not considered, the chilled water setpoint was treated as a known uncontrolled variable. The discrete control variables associated with the four tower cells with two-speed fans and the three condenser pumps were treated as continuous control variables. The optimal control determined by the near optimal equation (5.2.2) also agreed well with that determined using a non-linear optimization applied to a detailed simulation of the system.

In order to evaluate results of the system-based methodology for a complete system that includes the air handlers, the component-based optimization was applied to an example system, as described in Chapter 6. Coefficients of the optimal control and

minimum system cost function were fit to results of the component-based optimization over a range of conditions. Figures 5.2 - 5.5 show comparisons between the controls as determined with the component-based and system-based methods for a range of loads, for a relatively low and high ambient wet bulb temperature (60 F and 80 F).

In Figures 5.2 and 5.3, optimal values of the chilled water and supply air temperatures are compared. The near-optimal control equation provides a good fit to the optimization results for all conditions considered. The chilled water temperature was constrained between 38 F and 55 F, while the supply air setpoint was allowed to float freely. Figures 5.2 and 5.3 show that for the conditions where the chilled water temperature is constrained, the optimal supply air temperature is also nearly bounded at a value that depends upon the ambient wet bulb.

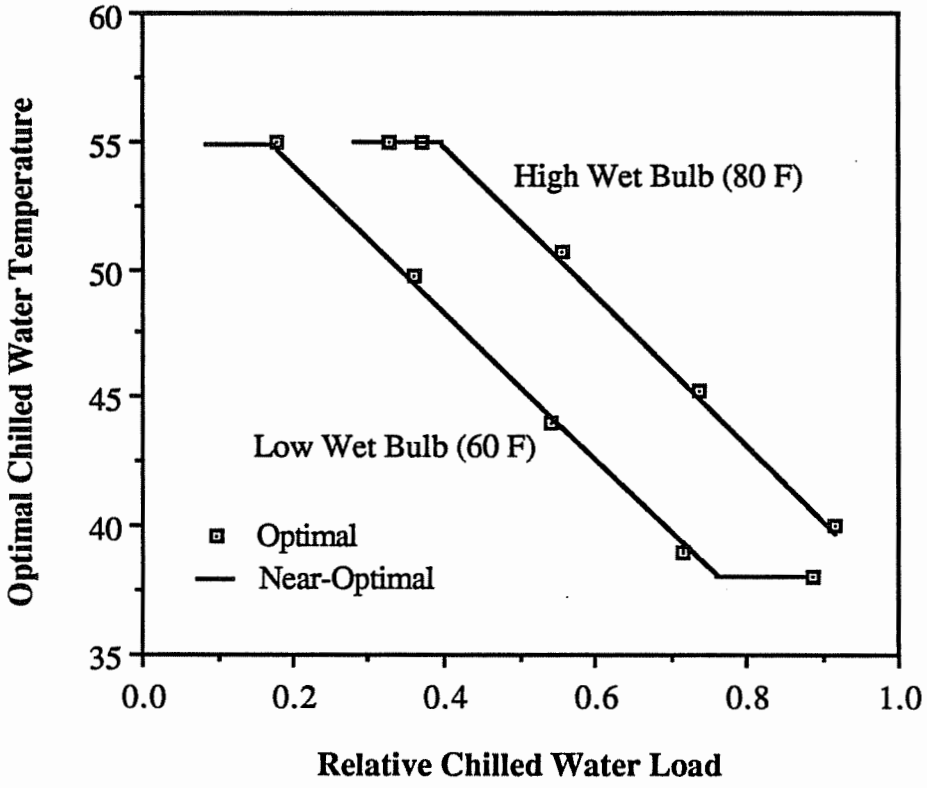

Figure 5.2. Comparisons of Optimal Chilled Water Temperature

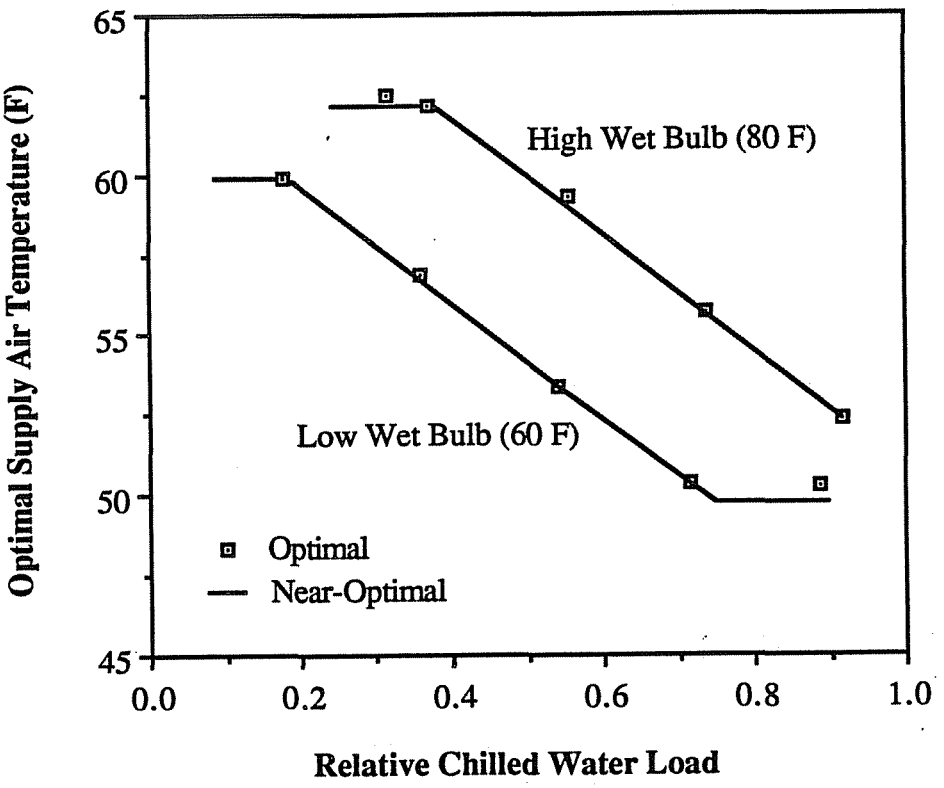

Figure 5.3. Comparisons of Optimal Supply Air Temperature

Optimal relative cooling tower air and condenser water flow rates are compared in Figures 5.4 and 5.5. Although the optimal controls are not exactly linear functions of the load, the linear control equation provides an adequate fit. The differences in these controls result in insignificant differences in overall system power consumption, since as shown in Chapter 6, the optimum is extremely flat with respect to these variables. The nonlinearity of the condenser loop controls is partly due to the constraints imposed upon the chilled water set temperature. However, this effect is not very significant.

Figures 5.4 and 5.5 also suggest that the optimal condenser loop control is not very sensitive to the ambient wet bulb temperature. However, the cooling tower considered is representative of that at D/FW airport and operates at high effectiveness. For a lower effectiveness tower, the sensitivity of the control to ambient wet bulb is greater.

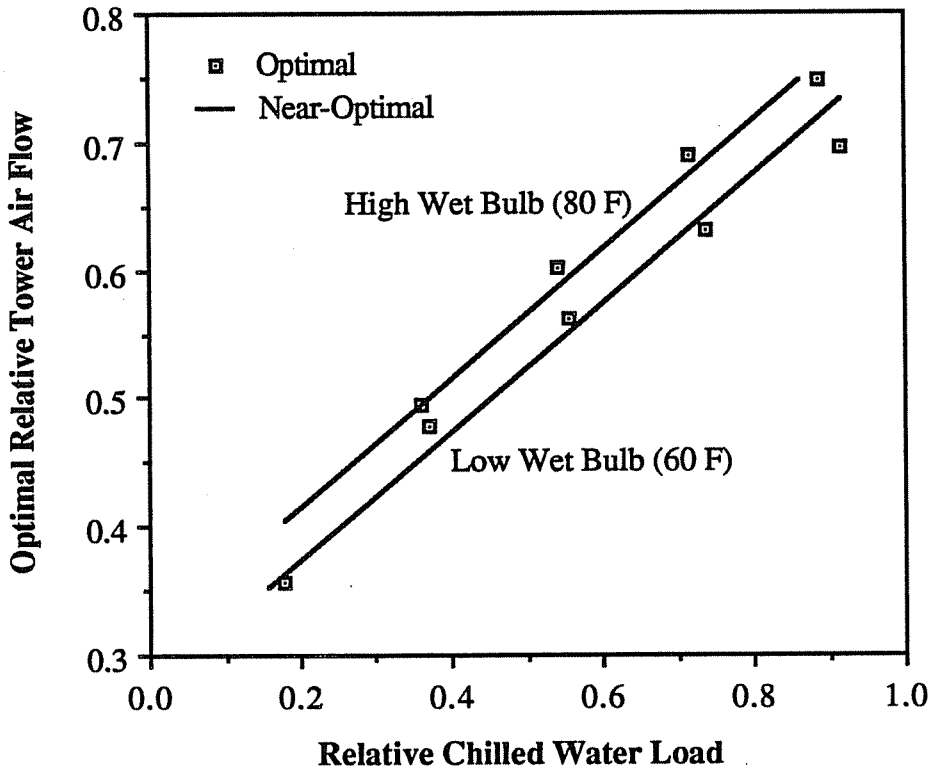

Figure 5.4. Comparisons of Optimal Tower Control

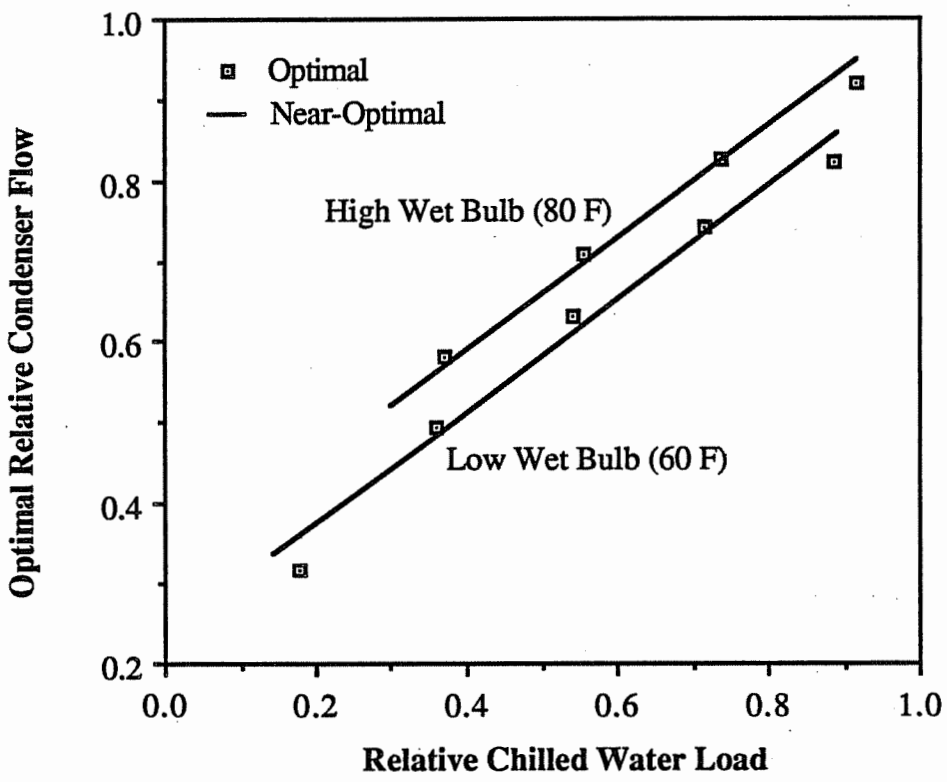

Figure 5.5. Comparisons of Optimal Condenser Pump Control

In order to determine the optimal discrete mode of operation, it is necessary to have a reasonably accurate model of the minimum cost of operation for each mode. Figure 5.6 shows a comparison between the optimal system coefficient of performance (COP) determined with the component-based optimization algorithm and the near-optimal quadratic cost function of equation (5.2.3). The differences between the results are very small over a wide range of chilled water loads and ambient wet bulbs. This model works well, even though it does not explicitly consider the constraints on the chilled water temperature that are exhibited at low and high loads in Figure 5.2.

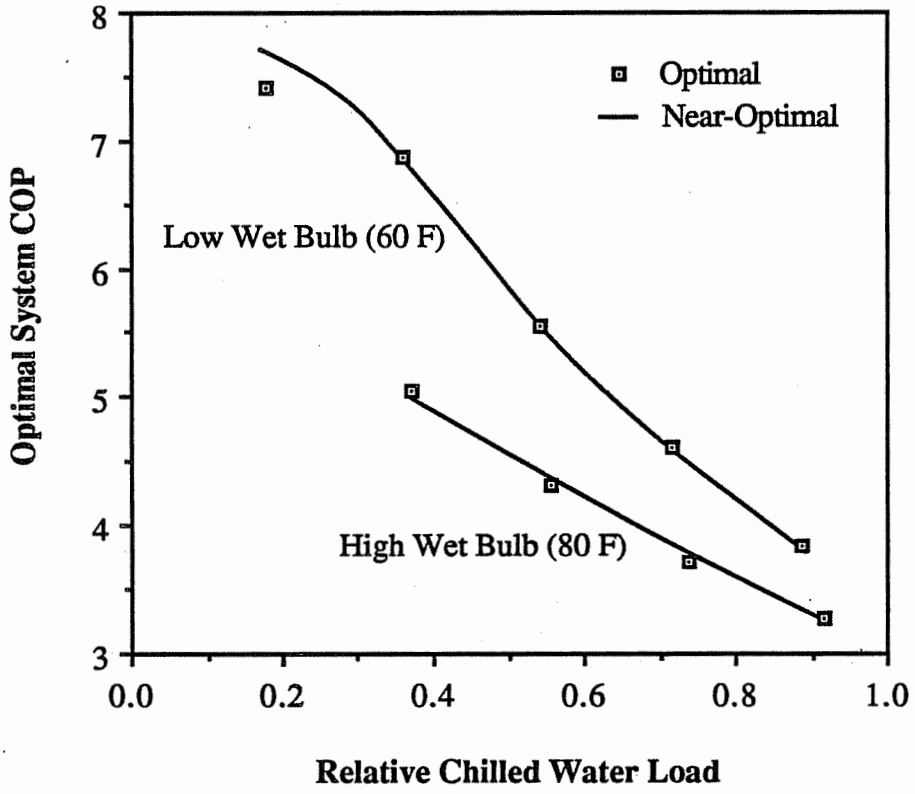

Figure 5.6. Comparisons of Optimal System Performance

5.4. Summary

Two methodologies have been presented for determining optimal control points of chilled water systems. A component-based non-linear optimization algorithm was developed as a simulation tool for investigating optimal system performance. Results of this algorithm implemented in a computer program, led to the development of a simpler system-based methodology for near-optimal control.

The advantage of the component-based algorithm over the system-based approach is that it provides a "true" solution to the optimization problem, including any nonlinear constraints. Each of the components in the system is represented as a separate subroutine with its own parameters, controls, inputs, and outputs. Models of

components may be either mechanistic or empirical in nature, so that the methodology is useful for evaluating both system design or control characteristics. In Chapter 6, this methodology is applied to typical chilled water systems to study both design and control issues.

The component-based algorithm takes advantage of the quadratic cost behavior of the components found in chilled water systems in order to solve the optimization problem in an efficient manner. However, in order to utilize this methodology as a tool for on-line optimization, it is necessary to have detailed performance data for each of the individual system components. The system-based near-optimal control methodology presented in this chapter utilizes an overall system cost function in terms of the total chilled water load and ambient wet bulb temperature. This cost function leads to a set of linear control laws for the continuous control variables in terms of these uncontrolled variables. Separate control laws are required for each feasible combination of discrete controls and the costs associated with each combination are compared to identify the optimum. The overall procedure is simple enough so as to be implementable either manually or on-line using microcomputers. For manual control applications, charts such as those that appear in Figures 5.2 - 5.6 could be used to determine optimal control as a function of load and wet bulb.

Chapter 6

Applications to Systems without Storage

In this chapter, the modeling and optimization techniques described in previous chapters are applied to chilled water systems without storage. The results that are presented arise from both specified controls applied to individual component and subsystem modeling and optimal control results determined with the component-based algorithm described in Chapter 5.

6.1 System Description

Figure 1.1 showed a general schematic of the variable air volume (VAV) system considered in this study. The central cooling facility, which consists of multiple centrifugal chillers, cooling towers, and pumps, provides chilled water to a number of air handling units in order to cool air that is supplied to building zones. General descriptions of the components and modeling assumptions were given in Chapters 2, 3, and 4. All energy consuming components in the system are assumed to be electrically driven.

At any given time, it is possible to meet the cooling needs with any number of different modes of operation and setpoints. Optimal control of a system involves minimizing the total power consumption of the chillers, cooling tower fans, condenser water pumps, chilled water pumps, and the air handling fans at each instant of time with respect to the independent continuous and discrete control variables. Chapter 5 describes a method for determining optimal values of these control variables. The discrete control variables considered in this chapter include the number of operating chillers, cooling tower cells, condenser water pumps, and chilled water pumps and the

relative speeds for multi-speed fans or pumps. The independent continuous control variables considered include the chilled water and supply air set temperatures, relative water flow rates to multiple chillers (both evaporators and condensers) and multiple cooling tower cells, and the speeds for variable-speed cooling tower fans and chilled and condenser water pumps.

In addition to the independent optimization control variables, there are also local loop (dependent) controls associated with the chillers, air handlers, and chilled water pumps. All local loop controls are assumed to be ideal, such that their dynamics are not considered. Each chiller is considered to be controlled such that the specified chilled water set temperature is maintained. The air handler local loop control involves control of both the coil water flow and fan air flow in order to maintain the prescribed supply air setpoint and zone temperature. The total requirement for the chilled water flow to the air handlers is dictated by the chilled water and supply air setpoints and the load. Control of the chilled water pumps is implemented through a local loop control that maintains a constant pressure difference between the main supply and return pipes for the air handlers. The setpoint for this pressure difference is chosen to ensure adequate distribution of flow to all air handlers and is not considered an optimization variable.

The optimal control variables change through time in response to uncontrolled variables. The uncontrolled variables are measurable quantities that may not be controlled, but that affect the component outputs and/or costs, such as the load and ambient dry and wet bulb temperature.

The results presented in this study are primarily representative of the Dallas/Fort Worth (D/FW) airport cooling system. However, characteristics of the systems studied by Lau [1985] and Hackner [1985] are also utilized. Table 6.1 summarizes the different component characteristics considered in this study. The loads employed throughout are representative of the D/FW system, so that components studied by Lau

and Hackner are scaled for D/FW conditions. Appendix C gives the parameter values associated with the individual component models. The ventilation air flow is taken to be 10% of the design air flow for the air handler under all circumstances. The use of an economizer or "free" cooling cycles were not considered in this study. These modes of operation would occur at low ambient wet bulb temperatures, such that the cooling loads could be met without operating the chillers.

The base system makes use of the component characteristics associated with the first choice for each component type in Table 6.1. For the most part, this corresponds to the current D/FW system. However, detailed data were not available for the performance of the air handlers. As a result, the air handler performance characteristics from manufacturers data used by Hackner [1985] were utilized in the base system. Except where otherwise noted, all pumps and fans are considered to be operated with variable-speed motors. Although combinations of components from Table 6.1 other than that associated with the base system were considered, results are only presented for the base system, except when alternative systems yield different conclusions.

Many of the results presented in this chapter are for steady-state conditions and are given as a function of load at ambient dry and wet bulb temperatures of 80 F and 70 F. For the purpose of performing simulations over a cooling season, optimal costs of operation are correlated in terms of the load and ambient conditions using the form given by equation (5.2.3). The result is integrated over time in response to time-varying load and weather conditions. In those cases where cooling season results are presented, weather data for May through October in Dallas, Texas and Miami Florida were utilized. Two different constant internal gains to the zones were considered: one-third and one-half of the maximum chiller cooling capacity. Only conditions where the ambient wet bulb temperature was greater than 60 F were considered in the

determination of plant operating costs.

Table 6.1
Summary of System Component Characteristics

Component	Component Characteristics
Chillers	1) D/FW variable-speed chiller 2) D/FW fixed-speed chiller 3) Lau (1985) chiller scaled to D/FW loads 4) Hackner (1985) chiller scaled to D/FW loads
Cooling Towers	1) D/FW tower characeristics 2) Lau (1985) tower scaled to D/FW loads 3) Hackner (1985) tower scaled to D/FW loads
Pumping	1) D/FW system and pump characteristics 2) 20% greater system and pumping head at design conditions than 1) 3) 20% lower system and pumping head at design conditions than 1)
Air Handlers	1) Hackner (1985) scaled to D/FW loads 2) 20% greater fan power requirements at design conditions than 1) 3) 20% lower fan power requirements at design conditions than 1)
Loads	1) 20% of zone loads are latent 2) 15% of zone loads are latent 3) 25% of zone loads are latent

6.2 Control Guidelines for Multiple Components in Parallel

For some of the independent control variables, it is possible to determine control guidelines that when implemented yield near-optimal performance. These guidelines simplify the optimization process, in that these independent control variables may be reduced to dependent variables. They are also useful to plant engineers as "rules of

thumb" for improved control practices. In this section, both component modeling and optimization techniques are used to identify control guidelines associated with multiple components arranged in parallel.

6.2.1 Multiple Cooling Tower Cells

The power consumption of a chiller is sensitive to the condensing water temperature, which is, in turn, affected by both the condenser water and cooling tower air flow rates. Increasing either of these flows reduces the chiller power requirement, but at the expense of an increase in the pump or fan power consumption.

Braun [1987] and Nugent [1988] have shown that for variable-speed fans, the minimum power consumption results from operating all cooling tower cells under all conditions. The power consumption of the fans depends upon the cube of the fan speed. Thus, for the same total air flow, operating more cells in parallel allows for lower individual fan speeds and overall fan power consumption. An additional benefit associated with full-cell operation is lower water pressure drops across the spray nozzles, which results in lower pumping power requirements. However, at very low pressure drops, inadequate spray distribution may adversely affect the thermal performance of the cooling tower. Another economic consideration is the greater water loss associated with full-cell operation.

Most current cooling tower designs utilize multiple-speed, rather than continuously adjustable variable-speed fans. In this case, it is not optimal to operate all tower cells under all conditions. The optimal number of cells operating and individual fan speeds will depend upon the system characteristics and ambient conditions. However, simple relationships exist for the best sequencing of cooling tower fans as capacity is added or removed. When additional tower capacity is required, then in almost all practical cases,

the tower fan operating at the lowest speed (including fans that are off) should be increased first. Similarly, for removing tower capacity, the highest fan speeds are the first to be reduced.

These guidelines are derived from evaluating the incremental power changes associated with fan sequencing. For two-speed fans, the incremental power increase associated with adding a low-speed fan is less than that for increasing one to high speed if the following condition is satisfied.

$$\gamma_{t,low}^{3} < (1 - \gamma_{t,low}^{3}) \qquad (6.2.1)$$

or

$$\gamma_{t,low} < 0.79 \qquad (6.2.2)$$

where $\gamma_{t,low}$ is the relative fan speed at low speed. If the low speed is less than 79% of the the high fan speed, then the incremental power increase is less for adding a low-speed as opposed to a high-speed fan. In addition, if the low speed is greater than 50% of the high speed, then the incremental increase in air flow is greater (and therefore better thermal performance) for adding the low-speed fan. Most commonly, the low speed of a two-speed cooling tower fan is between one-half and three-quarters of full speed. In this case, tower cells should be brought on-line at low speed before any operating cells are set to high speed. Similarly, the fan speeds should be reduced to low speed before any cells are brought off-line.

For three-speed fans, the sequencing logic is not as obvious. However, for the special case where low speed is greater than or equal to one-third of full speed and the

difference between the high and intermediate speeds is equal to the difference between the intermediate and low, then the best strategy is to increment the lowest fan speeds first when adding tower capacity and decrement the highest fan speeds when removing capacity. Typical three-speed combinations that satisfy this criteria are 1) one-third, two-thirds, and full speed or 2) one-half, three-quarters, and full speed.

Another issue related to control of multiple cooling tower cells having multiple-speed fans concerns the distribution of water flow to the individual cells. Typically, the water flow is divided equally among the operating cells. However, the overall thermal performance of the cooling tower is best when the flow is divided such that the ratio of water to air flow rates is identical for all cooling tower cells. In comparing equal flow rates to equal flow rate ratios, at worst, a five percent difference between the heat transfer effectivenesses for a combination of two tower cells, one operating a one-half and the other at full speed was found. Depending upon the conditions, these differences generally result in less than a one percent change in the chiller power. These differences should also be contrasted with the lower water pressure drop across the spray nozzles (lower pumping power) associated with equally divided flow. In addition, the performance differences are smaller for greater than two-cell operation, when a majority of cells are operating at the same speed. Overall, equal water flow distribution between cooling tower cells is near-optimal.

6.2.2 Multiple Chillers

Multiple chillers are normally configured in a parallel manner and typically controlled to give identical chilled water supply temperatures. For the parallel chiller combinations considered in this study, controlling for identical set temperatures was found to be either optimal or near-optimal. Besides the chilled water setpoint, additional control variables are the relative chilled and condenser water flow rates.

Simple guidelines may be established for distributing these flows.

In general, the relative condenser water flows to each chiller should be controlled to give identical leaving condenser water temperatures for all chillers. This condition approximately corresponds to relative condenser flow rates equal to the relative loads on the chillers. Figure 6.1 shows results for four different sets of two chillers operated

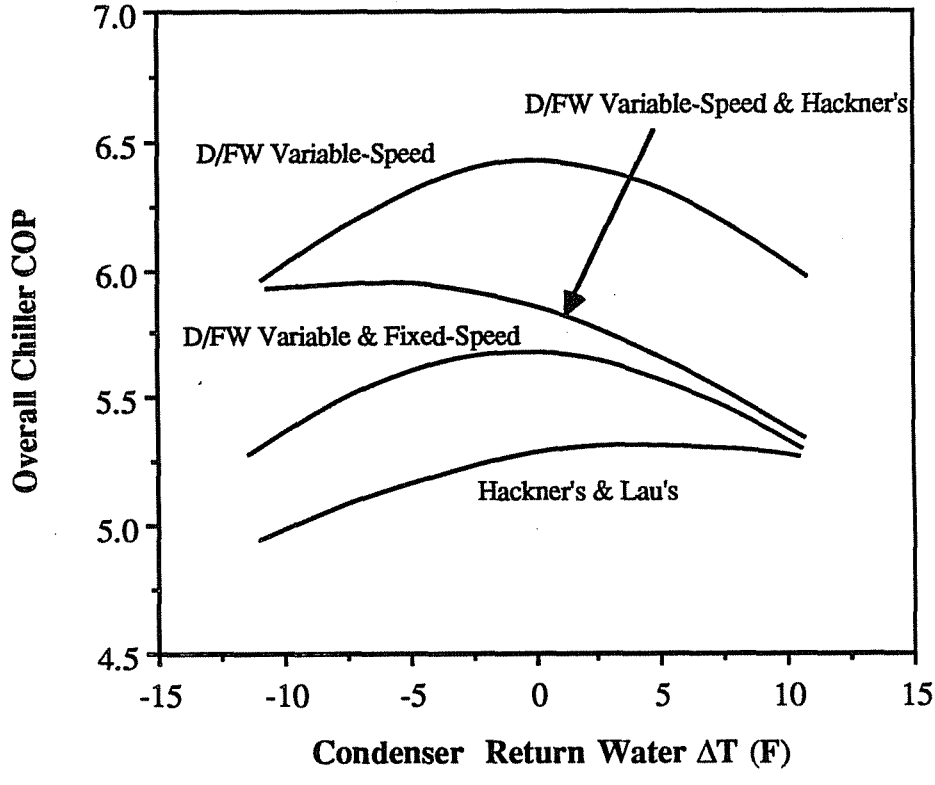

Figure 6.1. Effect of Condenser Water Flow Distribution for Two Chillers in Parallel

in parallel. The overall chiller coefficient of performance (COP) is plotted versus the difference between the condenser water return temperatures for equal loadings on the chillers. For the identical D/FW variable-speed chillers, the optimal temperature difference is almost exactly zero. This was found to be the case for all identical chillers considered in this study. For the non-identical chillers of Figure 6.1, equal leaving

condenser water temperatures result in chiller performance that is close to the optimum. Even for the D/FW variable and fixed-speed chiller combination, which have very different performance characteristics, the penalty associated with the use of identical condenser leaving water temperatures is insignificant. Similar results were obtained for unequal loadings on the chillers.

For given chilled water return and supply temperatures, the relative chilled water flow to each chiller is equal to its relative loading. Consider the problem of determining the optimal relative loadings for N_{ch} chillers in parallel. The relative condenser water flows are assumed to be controlled to give identical return water temperatures. The optimization problem is one of minimizing the total chiller power consumption or

$$P_{ch} = \sum_{i=1}^{N_{ch}} P_{ch,i} \tag{6.2.3}$$

with respect to the relative loadings, $f_{L,i}$, with the constraint

$$\sum_{i=1}^{N_{ch}} f_{L,i} = 1 \tag{6.2.4}$$

By forming the Lagrangian and applying the first-order condition for a minimum or maximum, it can be shown that the point of minimum or maximum overall power occurs where the derivatives of the individual chiller power consumptions with respect to their relative loadings are equal.

$$\frac{\partial P_{ch,i}}{\partial f_{L,i}} = \frac{\partial P_{ch,j}}{\partial f_{L,j}} \qquad \text{for all i, j} \tag{6.2.5}$$

This condition, along with the constraint of equation (6.2.4) are sufficient to determine the relative loadings. For identical chillers, these equations are satisfied for all chillers loaded equally or

$$f_{L,i} = \frac{1}{N_{ch}} \qquad \text{for } i = 1 \text{ to } N_{ch} \tag{6.2.6}$$

For chillers with different cooling capacities, but identical part-load characteristics, the constrained optimality conditions are satisfied when each chiller is loaded according to the ratio of its capacity to the sum total capacity of all operating chillers. For the i^{th} chiller,

$$f_{L,i} = \frac{Q_{cap,i}}{\sum_{i=1}^{N_{ch}} Q_{cap,i}} \qquad \text{for } i = 1 \text{ to } N_{ch} \tag{6.2.7}$$

where $Q_{cap,i}$ is the cooling capacity of the i^{th} chiller.

The relative loadings determined with equations (6.2.6) or (6.2.7) could result in either minimum or maximum power consumptions. With the second-order necessary condition for a minimizing point, it is possible to show that these points represent a minimum when the derivative of the COP with respect to relative loading is less than zero. In other words, the chillers are operating at loads greater than the point at which the maximum COP occurs. Typically, but not necessarily, the maximum COP occurs

at loads that are about 40 - 60% of a chillers cooling capacity. In this case, and with loads greater than about 50% of cooling capacity, the control defined by equations (6.2.6) and (6.2.7) results in a minimum power consumption.

Figure 6.2 shows the effect of the relative loading on chiller COP for different sets of identical chillers loaded at approximately 70% of their overall capacities. Three of the chillers have maximum COP's when evenly loaded, while the fourth (D/FW fixed-speed) obtains a minimum at that point. The part-load characteristic of the D/FW fixed-speed chiller is unusual in that the maximum COP occurs at its capacity (see Chapter 2). This chiller was retrofit with a different refrigerant and drive motor which caused its capacity to be derated from 8700 tons to 5500 tons. As a result, the evaporators and condensers are oversized for its current capacity.

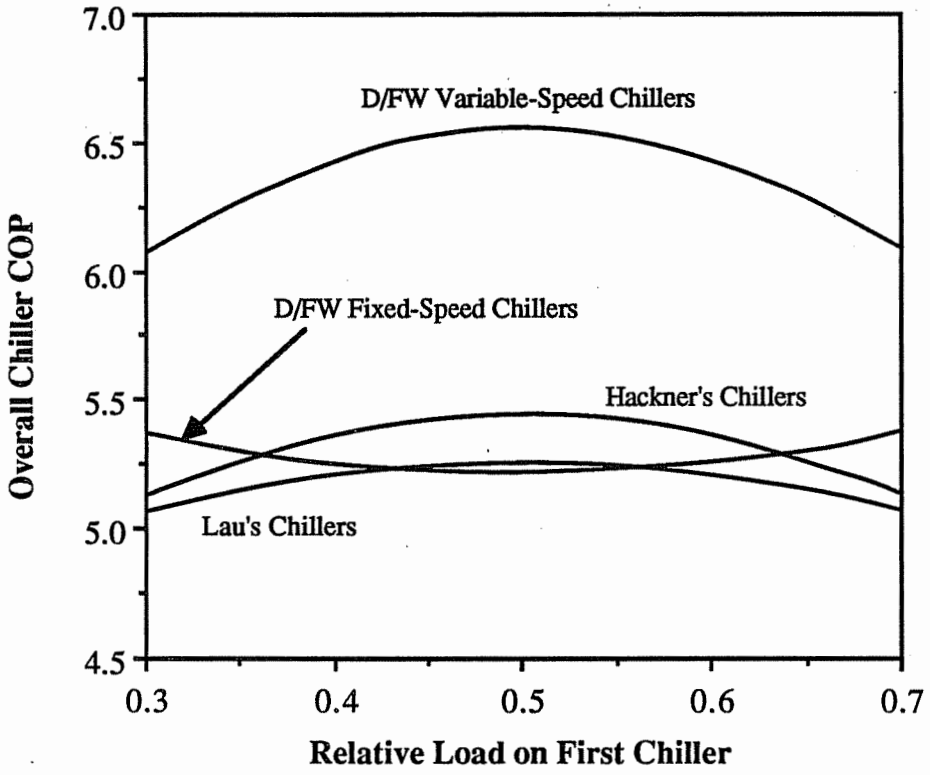

Figure 6.2. Effect of Relative Loading for Two Identical Parallel Chillers

The effect of loading on non-identical chillers was also investigated. The minimum power consumption was realized with near-even loading for all combinations considered, except for those involving the D/FW fixed-speed chiller. The best strategy for this particular fixed-speed chiller in combination with other chillers is to load it as heavily as possible, since its performance is best at full load.

One of the important issues concerning control of multiple chillers is chiller sequencing. Sequencing involves determining the conditions at which specific chillers are brought on-line or off-line. The optimal sequencing of chillers depends primarily upon their part-load characteristics. Chillers should be brought on-line at conditions where the total power of operating with the additional chiller would be less than without it. Optimization results indicate that the optimal sequencing of chillers may not be decoupled from the optimization of the rest of the system. The characteristics of the system change when a chiller is brought on-line or off-line due to changes in the system pressure drops and overall part-load performance. The optimal point for switching chiller operation may differ significantly from switch points determined if only chiller performance were considered at the conditions before the switch takes place.

6.2.3 Multiple Air Handlers

In a large system, a central chilled water facility may provide cooling to several buildings, each of which may have a number of air handling units in parallel. If the supply air setpoints of each of the air handlers were considered to be a unique control variable, the optimization problem would become quite complicated. However, the error associated with using identical supply air temperatures for all air handlers is relatively small as compared with the optimal solution, even when the loading on the various cooling coils differs significantly. As a result, the number of control variables in the optimization process may be reduced by one less than the number of air handlers.

Figure 6.3 shows a comparison between individual and identical setpoint control values for a system with two identical air handlers. The system coefficient of performance (COP) associated with optimal control is plotted versus the relative loading on one air handler. The difference between individual and identical setpoint control is not significant over the practical range of relative loadings. This result is most easily explained by considering the limits on the relative loadings. For the case of equal loadings on the air handlers, the optimal control setpoints are equal for identical air handlers. In the other extreme, where all of the load is applied to one air handler, then the supply air temperature of the unloaded air handler has no importance, since its power consumption is zero. Between the two extremes, the error associated with assuming identical setpoints is relatively small. This result also extends to many air handlers in parallel and to non-identical designs.

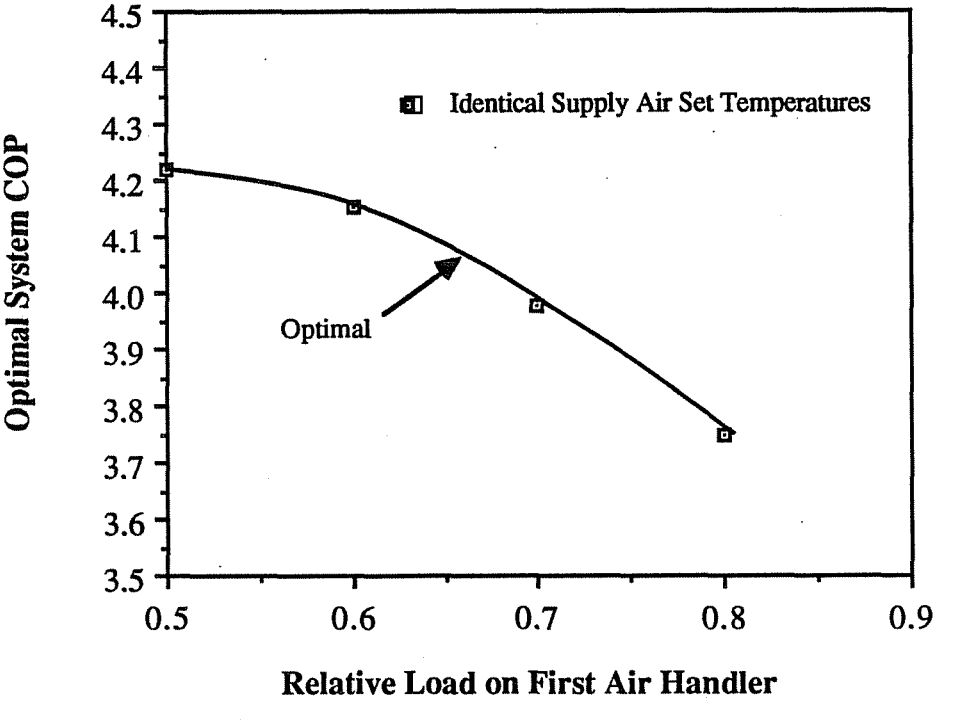

Figure 6.3. Comparison of Optimal System Performance for Individual Supply Air Setpoints with that for Identical Values

Although the number of control variables is reduced by considering only a single supply air set temperature, the overall operating cost still depends upon the performance and loadings on the individual air handlers. However, for the purpose of determining optimal control, air handlers may be combined into a single effective air handler under the conditions that all zones are maintained at the same air temperature and the heat transfer characteristics of the coils are similar. The required air flow as a fraction of the design air flow for the i^{th} air handler in parallel, $\gamma_{ahu,i}$, may be expressed in terms of an overall air flow ratio as

$$\gamma_{ahu,i} = \frac{f_{ahu,i}}{f_{ahu,des,i}} \gamma_{ahu} \tag{6.2.8}$$

where γ_{ahu} is the ratio of the total required air flow to the total design air flow, $f_{ahu,i}$ is the ratio of air flow for the i^{th} air handler to the total air flow for all air handlers, and $f_{ahu,des,i}$ is the ratio of design air flow for the i^{th} air handler to the total design air flow for all air handlers. If all air handlers have identical supply air and zone air temperature setpoints, then $f_{ahu,i}$ is also equal to ratio the sensible loading on the zones supplied by i^{th} air handler to the total sensible zone loads, $f_{sens,i}$. In this case, the total air handler power consumption for variable-speed fans is

$$P_{ahu} = \gamma_{ahu}^{3} \sum_{i=1}^{N_{ahu}} P_{ahu,des,i} \left[\frac{f_{sens,i}}{f_{ahu,des,i}} \right]^3 \tag{6.2.9}$$

where $P_{ahu,des,i}$ is the power consumption for the i^{th} air handler at it's design air flow.

As a result, all the air handlers may be combined into one air handler having the sum total area, water flow, air flow, and loading, with the power computed according

to equation (6.2.9). For the near-optimal control algorithm described in Chapter 5, it is necessary to include the relative zone sensible loads ($f_{sens,i}$) as uncontrolled variables in the empirical system cost function, if they change significantly.

6.2.4 Multiple Pumps

A common control strategy for sequencing both condenser and chilled water pumps is to bring pumps on-line or off-line with chillers. In this case, there is a condenser and chilled water pump associated with each chiller. For fixed-speed pumps, this strategy is not optimal. At the point at which a chiller is brought on-line in parallel and assuming that the pump control does not change, there is a reduction in the pressure drop and subsequent increase in flow rate for both the condenser and chilled water loops. The increased flow rates tend to improve the overall chiller performance. However, if the pumps are operating near their peak efficiency before the additional chiller is brought on-line, then there is a drop in the pump efficiency when adding the additional chiller while holding the pump control constant. Most often, the improvements in chiller performance offset the degradation in pump performance, so that there is no need for an additional pump at the chiller switch point.

Figure 6.4 shows the optimal system performance for different combinations of chillers and fixed-speed pumps in parallel as a function of load for a given wet bulb. The optimal switch point for a second pump occurs at a much higher load (~0.62) than the switch point for adding or removing a chiller (~0.38). If the second pump were sequenced with the second chiller, then the optimal switch would occur at the maximum chiller capacity and approximately a 10% penalty in performance would result at this condition. The optimal control for sequencing fixed-speed pumps depends upon the load and the ambient wet bulb temperature and should not be directly coupled to the

chiller sequencing.

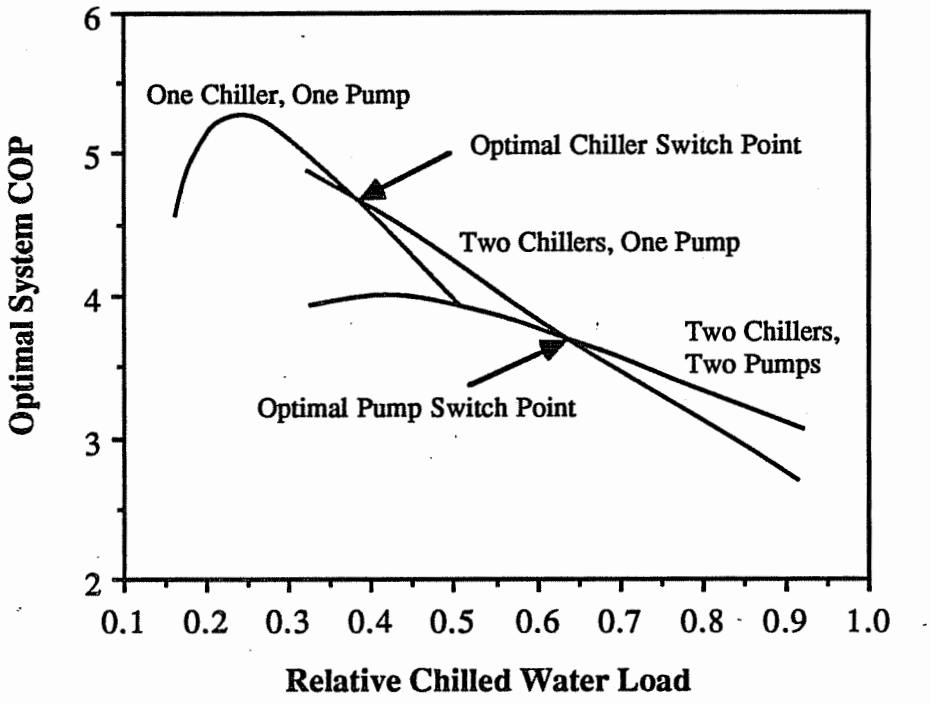

Figure 6.4. Effect of Chiller and Pump Sequencing on Optimal System Performance

The sequencing of variable-speed pumps is more straightforward than that for fixed-speed pumps. For a given set of operating chillers and tower cells (i.e. given system pressure drop characteristics), variable-speed pumps have relatively constant efficiencies over their range of operation. As a result, the best sequencing strategy is to select pumps so as to operate near their peak efficiencies for each possible combination of operating chillers. Since the system pressure drop characteristics change when chillers are added or removed, then the sequencing of variable-speed pumps should be directly coupled to the sequencing of chillers. For identical variable-speed pumps oriented in parallel, the best overall efficiency is obtained if they operate at identical speeds. For non-identical pumps, near-optimal efficiency is realized if they operate at equal fractions of their maximum speed.

6.3 Sensitivity Analyses and Control Characteristics of Subsystems

In this section, the sensitivity of the optimal system performance to the uncontrolled and controlled variables is studied.

6.3.1 Effects of Load and Ambient Conditions

For a given system in which the relative loadings on each zone are relatively constant, the optimal control variables are primarily a function of the total sensible and latent gains to the zones, along with the ambient dry and wet bulb temperatures. Figure 6.5 shows the effect of these uncontrolled variables on the total operating costs. For a given load and wet bulb temperature, the effect of the ambient dry bulb temperature is insignificant, since air enthalpies depend primarily upon wet bulb temperatures and the performance of wet surface heat exchangers are driven primarily by enthalpy differences. Typically, the zone latent gains are on the order of 15-25% of the total zone gains. In this range, Figure 6.5 shows that the effect of changes in latent gains has a relatively small effect upon the system performance for given total load. Consequently, results for overall system performance and optimal control may be correlated in terms of only the ambient wet bulb temperature and total chilled water load. In the event that the load distribution between zones changes significantly through time, then this must also be included as a correlating variable.

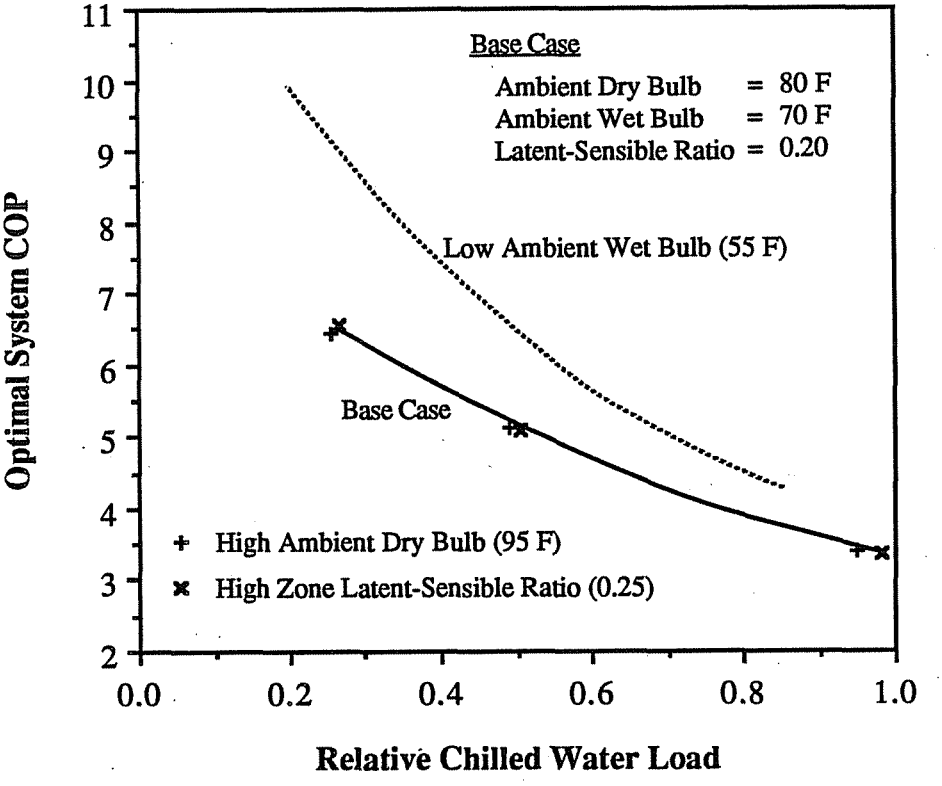

Figure 6.5. Effect of Uncontrolled Variables on Optimal System Performance

6.3.2 Condenser Water Loop

The primary controllable variables associated with heat rejection to the environment are the condenser water and tower air flow rates. Figures 5.4 and 5.5 showed how optimal values of these flow rates vary with both total chiller load and ambient wet bulb temperature. Both optimal air and water flows increase with load and wet bulb temperature. Higher condensing temperatures and reduced chiller performance result from either increasing loads or wet bulb temperatures for a given control. Increasing the air and water flow under these circumstances reduces the chiller power consumption at a faster rate than the increases in fan and pump power.

Figures 6.6 shows the sensitivity of the total power consumption to the tower fan and condenser pump speed. Contours of constant power consumption are plotted

versus fan and pump speeds. Near the optimum, power consumption is not sensitive to either of these control variables, but increases more quickly away from the optimum. The rate of increase in power consumption is particularly large at low condenser pump speeds. There is a minimum pump speed necessary to overcome the static head associated with the height of the water discharge in the cooling tower above the takeup from the sump. As the pump speed approaches this value, the condenser flow approaches zero and the chiller power increases dramatically. It is generally better to have too high rather than too low a pump speed. The "flatness" near the optimum indicates that it is not necessary for an extremely accurate determination of the optimal control.

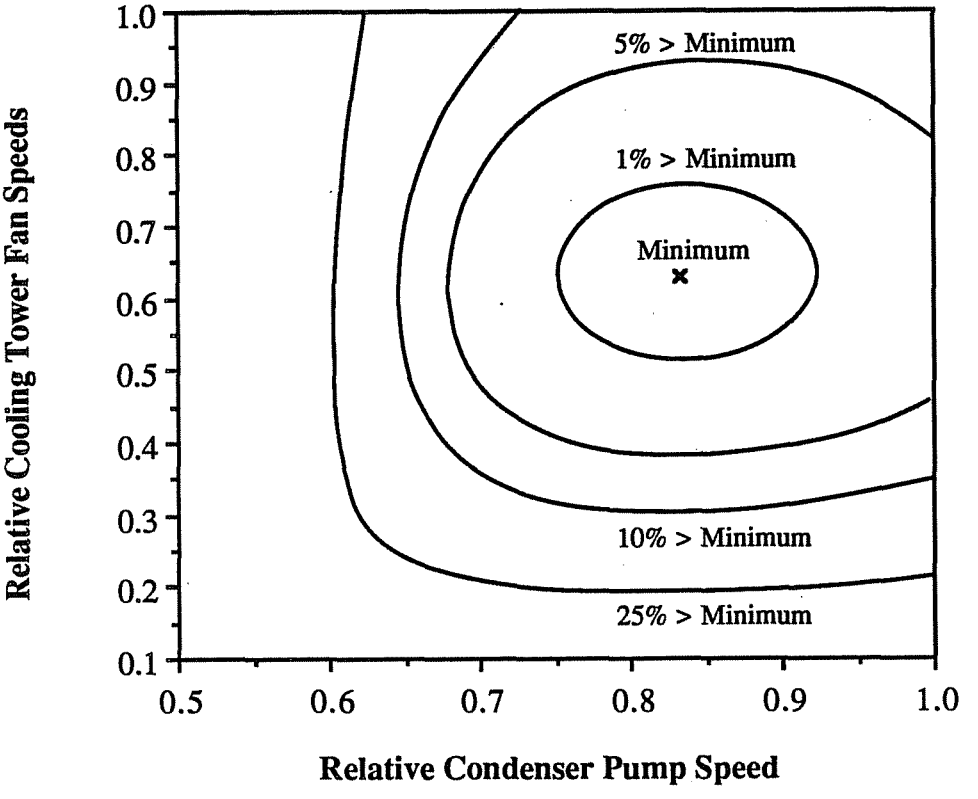

Figure 6.6. Power Contours for Condenser Loop Control Variables

6.3.2 Chilled Water Loop

Figures 5.2 and 5.3 showed the dependence of the optimal chilled water and supply air set temperatures on the load and wet bulb. Both the optimal chilled water and supply air temperatures decrease with increasing load for a fixed wet bulb temperature. This behavior occurs because the rate of change in air handler fan power with respect to load changes is larger than that for the chiller at the optimal control points. As the wet bulb temperature increases for a fixed load, the optimal set temperatures also increase. There are two primary reasons for this result: 1) For a given load, the chiller power depends primarily upon the temperature difference between the leaving condenser and chilled water temperatures. The condenser temperature and chiller power consumption increase with increasing wet bulb temperature and the optimal chilled water temperature increases in order to reduce the temperature difference across the chiller. 2) In the absence of humidity control, optimal supply air and chilled water temperatures increase with decreasing sensible zone loads for constant total chiller load. In addition, the sensible to total load ratio decreases with increasing wet bulb temperature for constant total load.

Figure 6.7 shows the sensitivity of the system power consumption to the chilled water and supply air set temperatures for a given load and wet bulb temperature. Within about 3 degrees F of the optimum, the power consumption is within 1% of the minimum. Outside of this range, the sensitivity to the setpoints increases significantly. The penalty associated with operation away from the optimum is greater in the direction of smaller differences between the supply air and chilled water setpoints. As this temperature difference is reduced, the required flow of chilled water to the coil increases and the chilled water pumping power is larger. For a given chilled water or supply air temperature,the temperature difference is limited by the heat transfer

characteristics of the coil. Below this limit, the required water flow and pumping power would approach infinity if the pump output were not constrained. It is generally better to have too large rather than too small a temperature difference between the supply air and chilled water setpoints.

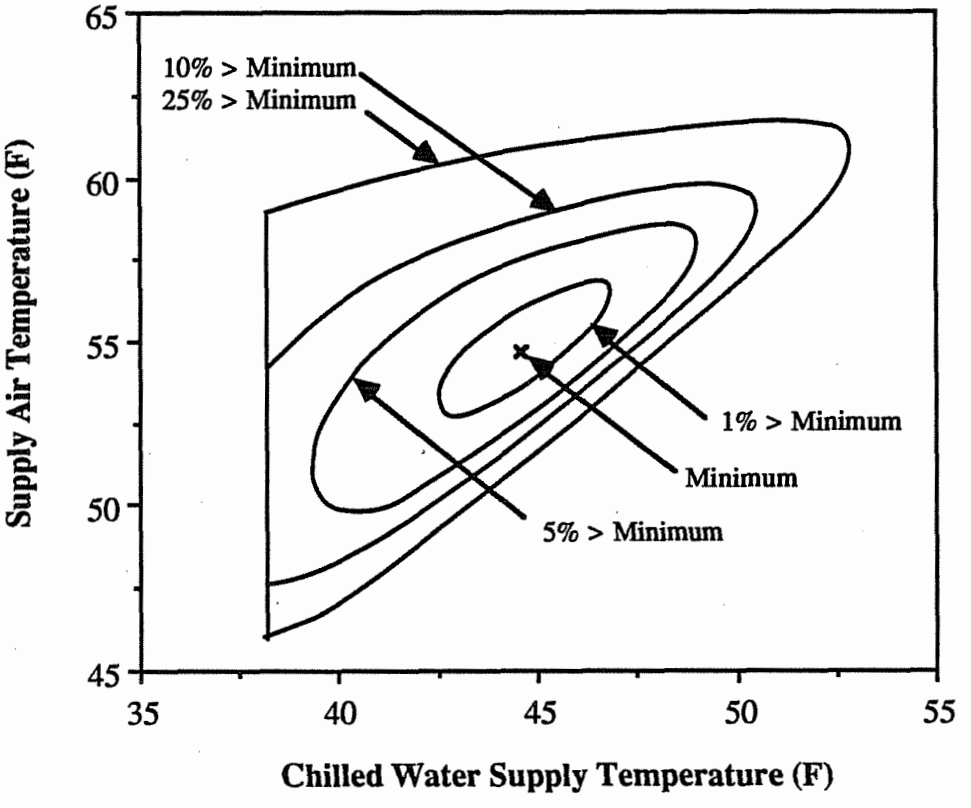

Figure 6.7. Power Contours for Chilled Water and Supply Air Temperatures

6.4 Optimal versus "Alternative" Control Strategies

There is no general strategy that has been established for controlling chilled water systems. Most commonly, the chilled water and supply air set temperatures are constants that do not vary with time. In some applications, these setpoints vary according to the ambient dry bulb temperature. Generally, there is an attempt to control the cooling tower and condenser water flow in response to changes in the load and

ambient wet bulb. One strategy for controlling these flow rates is to maintain constant temperature differences between the cooling tower outlet and the ambient wet bulb (approach) and between the cooling tower inlet and outlet (range), regardless of the load and wet bulb. In some applications, humidity along with temperature is controlled within the zones. In this section, the performance of some of these control strategies is compared with that of an optimally controlled system.

6.4.1 Conventional Control Strategies

Fixed values of chilled water and supply air setpoints and tower approach and range that are optimal or near-optimal over a wide range of conditions do not exist. In addition, it is not obvious how to choose values that work best overall. One simple, yet reasonable approach is to determine fixed values that result in near-optimal performance at design conditions. Figure 6.8 shows a comparison between the performance associated with optimal control and 1) fixed chilled water and supply air temperature setpoints (40 and 52 F) with optimal condenser loop control, 2) fixed tower approach and range (5 and 12 F) with optimal chilled water loop control, and 3) fixed setpoints, approach, and range. The results are given as a function of load for a fixed wet bulb temperature. Since the fixed values were chosen to be appropriate at design conditions, the differences in performance as compared with optimal control are minimal at high loads. However, at part-load conditions, Figure 6.8 shows that the savings associated with the use of optimal control become very significant. Optimal control of the chilled water loop results in greater savings than that for the condenser loop for part-load ratios less than about 50%.

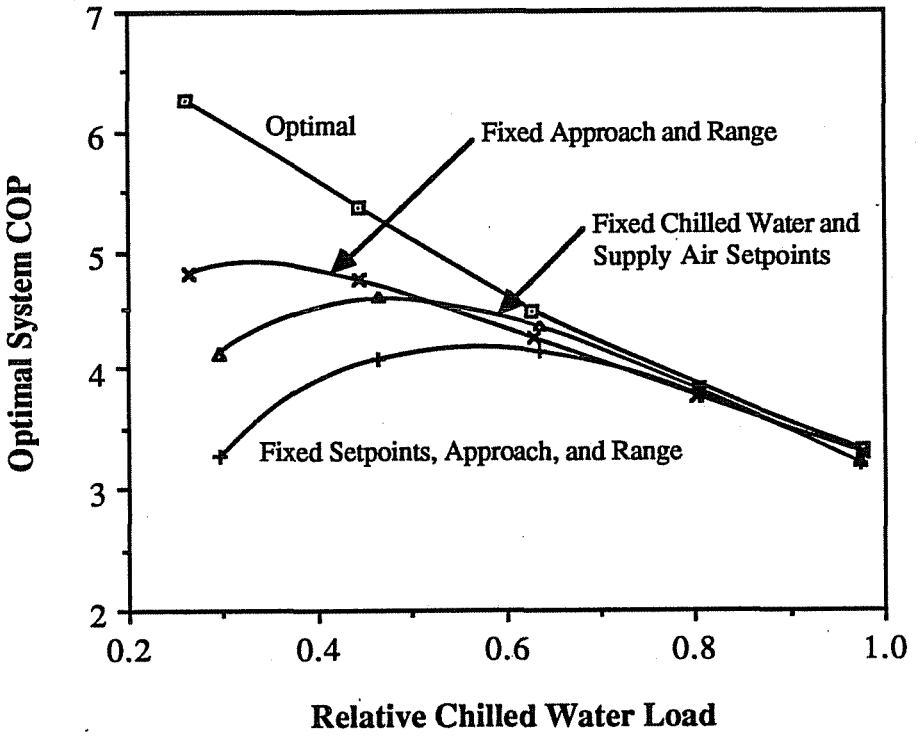

Figure 6.8. Comparisons of Optimal Control with "Conventional" Control Strategies

The overall savings over a cooling season for optimal control depends upon the time variation of the load. If the cooling load were relatively constant, then fixed values of temperature setpoints, approach, and range could be chosen to give near-optimal performance. Table 6.2 summarizes cooling season operating costs for the conventional control strategies relative to optimal control for two different load characteristics in both Dallas and Miami. The low and high internal gains are approximately one-third and one-half of the maximum cooling requirement of the system. In Dallas, the maximum total operating cost difference of approximately 17% occurs for fixed setpoints, approach, and range with low internal gains. The difference is reduced to 7% for the high internal gains, since the system operates at a more uniform load near the design conditions. There is approximately twice the penalty

associated with the use of fixed chilled water and supply air setpoints as compared with fixed tower approach and range for low internal gains, but the penalties are equal for the high internal gains. The results for the Miami climate are similar to those for Dallas.

Table 6.2
Cooling Season Results for Optimal vs. Conventional Control

Control Description	Cost Relative to Optimal Control			
	Low Internal Gains		High Internal Gains	
	Dallas	Miami	Dallas	Miami
fixed temperature setpoints	1.09	1.10	1.03	1.03
fixed approach and range	1.05	1.06	1.03	1.03
fixed setpoints, approach, range	1.17	1.19	1.07	1.07

6.4.2 Humidity Control

In a variable air volume system, it is generally possible to adjust the chilled water temperature, supply air temperature, and air flow rate in order to maintain both temperature and humidity. In constraining the room humidity, the number of "free" control variables in the optimization is reduced by one. For a given chilled water temperature, there is at most one combination of the supply air temperature, air flow rate, and water flow rate that will maintain both the room temperature and humidity.

ASHRAE [1981] defines acceptable bounds on the room temperature and humidity for human comfort. For a zone that is being cooled, the equipment operating costs are minimized when the zone temperature is at the upper bound of the comfort region. However, operation at the humidity upper limit does not minimize costs. Figure 6.9 compares costs and humidities associated with fixed and free floating zone humidities as a function of the load. Over the range of loads for this system, the free floating humidity operates within the comfort zone at lower costs and humidities with the largest

differences occurring at the high loads. Operation at the upper humidity bound results in lower latent loads, but the addition of this humidity control constraint requires higher supply air temperatures than that associated with free floating humidities. In turn, the higher supply air temperature results in greater air handler power consumption. In effect, the addition of any constraint reduces the number of free control variables by one and results in operation at a higher cost. In the determination of optimal control points, the humidity should be allowed to float freely, unless it falls outside the bounds of human comfort.

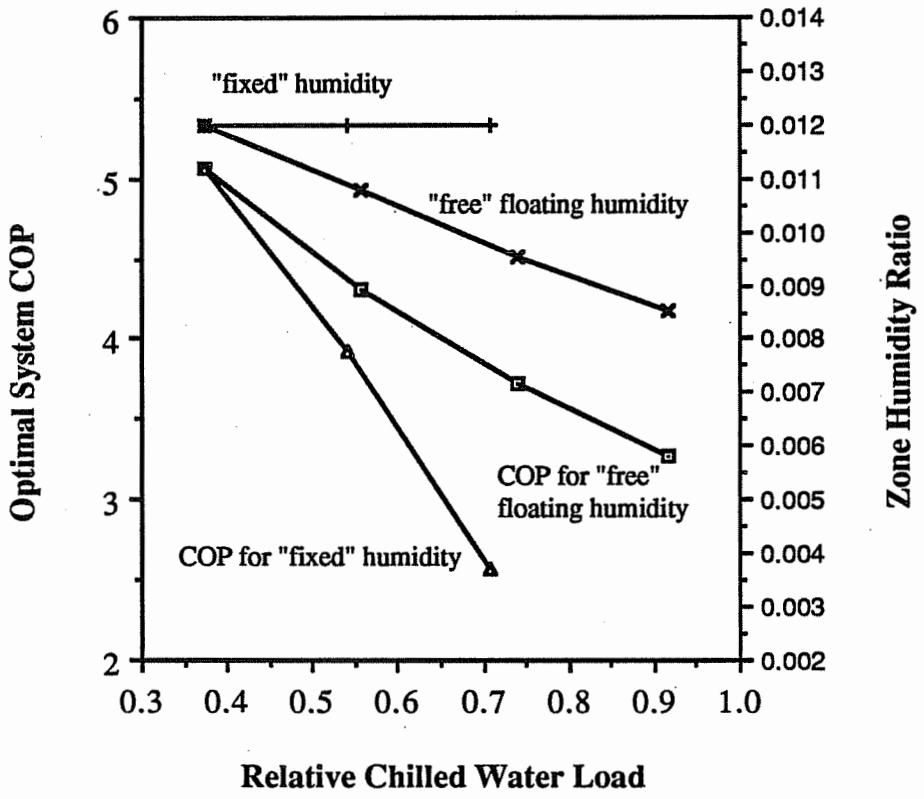

Figure 6.9. Comparison of "Free" Floating and "Fixed" Humidity Control

6.5 Comparisons of Alternative System Configurations under Optimal Control

In order to compare the operating costs associated with different system designs, it is most appropriate that each be optimally controlled. In this section, alternative system configurations are compared in terms of their optimal system performance.

6.5.1 Variable versus Fixed-Speed Equipment

The part-load performance of a centrifugal chiller depends upon the method by which its capacity is modulated. As noted earlier, the Dallas/Fort Worth primary chiller was originally operated at a constant speed and the cooling capacity was modulated with the use of pre-rotation inlet vanes and outlet diffuser vanes. The chiller was subsequently retrofit with a variable-speed electric motor and the vane control was disconnected.

In general, the part-load performance of a chiller is better for variable-speed as compared with vane control. In this study, the performance of the D/FW chiller was measured for both types of capacity modulation for nearly identical conditions as described in Chapter 2. Figures 2.13 and 2.14 showed the performance for the variable and fixed-speed control, while Figure 2.15 gave a direct comparison of their performance. Figure 6.10 gives a comparison between the overall optimal system performance for both types of control. At part-load conditions, the performance associated with the variable-speed control is significantly better. However, the power requirements are similar at conditions associated with the peak loads. This is expected, since at this condition, the vanes are wide open and the speed under variable-speed control approaches that of the fixed-speed operation.

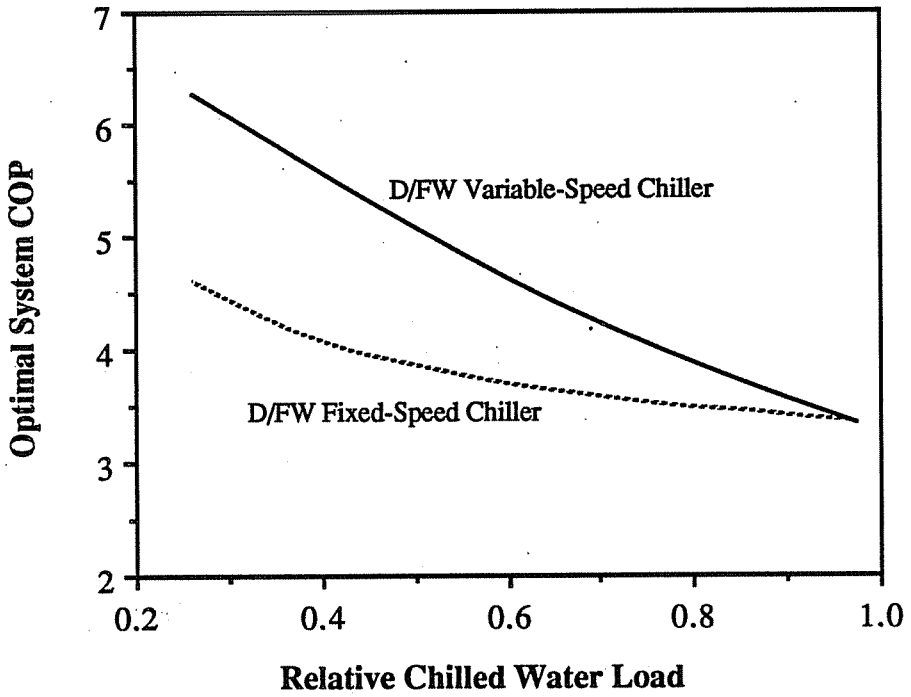

Figure 6.10. Optimal System Performance for Variable and Fixed-Speed Chillers

Part of the improvement with variable-speed chiller control may result from the unique characteristics of the D/FW chiller. The capacity of this chiller was derated, so that the evaporator and condenser are oversized at the current capacity relative to the original design capacity. As a result, the performance is more sensitive to penalties associated with part-load operation of the compressor than to heat exchange improvements that occur with lower loads.

The most common design for cooling towers utilizes multiple tower cells in parallel that share a common sump. Each tower cell has a fan that may have one, two, or possibly three operating speeds. Although multiple cells, having multiple fan settings offers a wide flexibility in the control, the use of variable-speed tower fans can provide additional improvements in the overall system performance.

Figure 6.11 compares optimal system performance for single-speed, two-speed,

and variable-speed tower fans as a function of load for a given wet bulb. There are four tower cells for this system. All cells operate for the variable-speed fan results under all conditions, while cells are isolated for discrete fan control results when their fans are off. The discrete changes in the control of the multi-speed fans causes the discontinuities in the slopes of the curves in Figure 6.11. The flexibility in the control with one or two-speed fans is most limited at low loads. Below about 70% of full-load conditions, the difference between one-speed and variable-speed fans becomes very significant. With two-speed fans, the differences are on the order of 3 - 5% over the entire range.

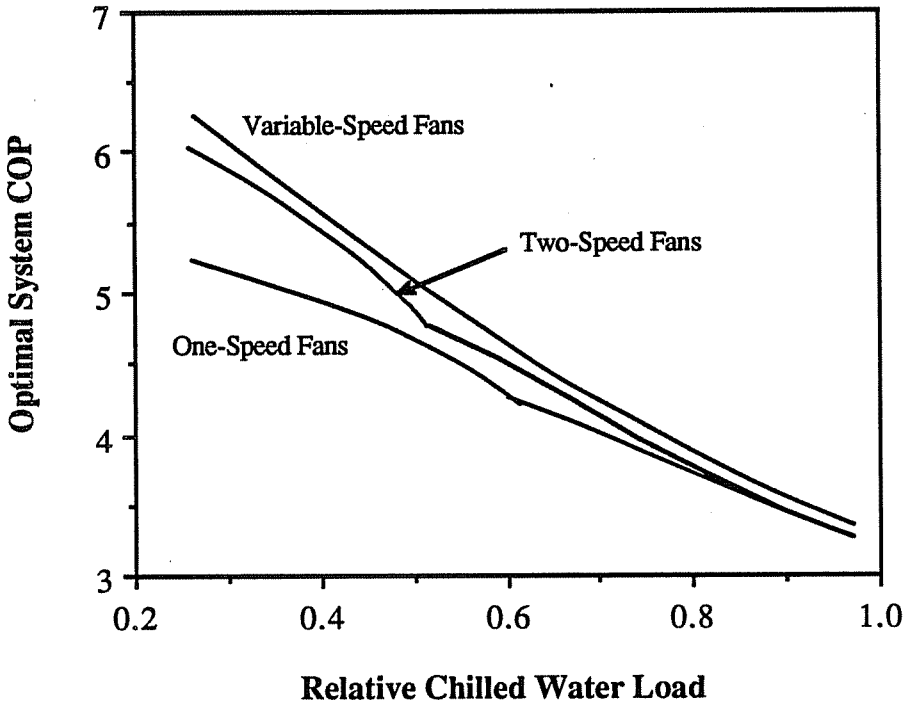

Figure 6.11. Comparison of One-Speed, Two-Speed, and Variable-Speed Cooling Tower Fans (Four Cells)

If a fixed-speed pump is sized to give proper flow to a chiller at design conditions, then it is oversized for part-load conditions and the system will have higher operating

costs than with a variable-speed pump having the same design capacity. The use of a smaller fixed-speed pump for low load conditions improves the flexibility in control and can reduce the overall power consumption. Figure 6.12 gives the optimal system performance for variable-speed and fixed-speed pumps applied to both the condenser and chilled water flow loops. The "large" fixed-speed pumps are sized for design conditions, while the "small" pump has one-half the flow capacity of the large. Below about 60% of full-load conditions, the use of variable-speed pumps shows a very significant improvement over single fixed-speed pumps. With the addition of "small" fixed-speed pumps, the improvements with variable-speed become significant at about 40% of the maximum load.

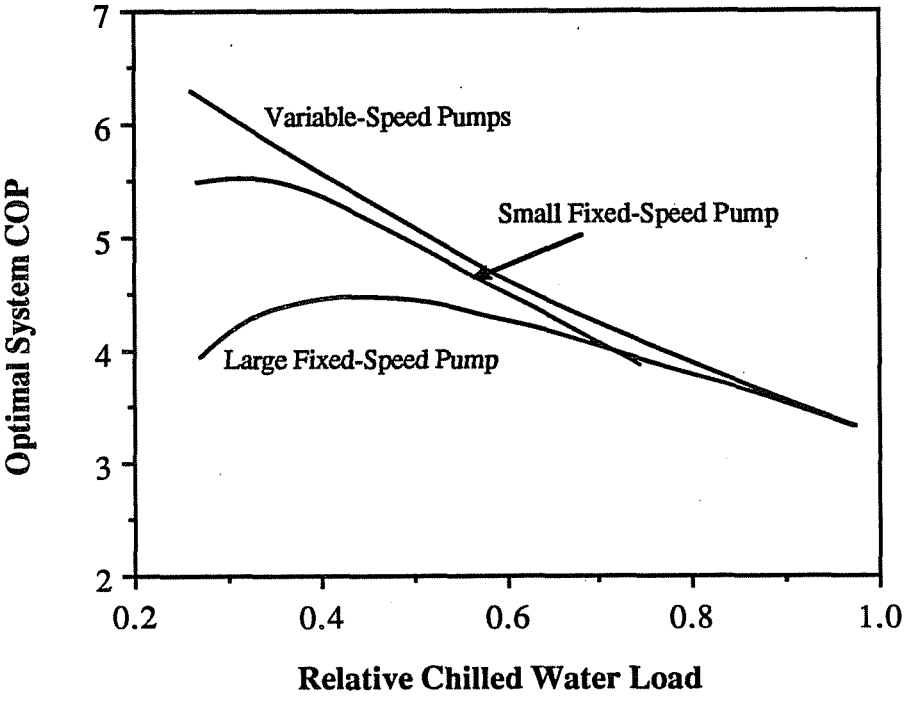

Figure 6.12. Comparison of Variable and Fixed-Speed Pumps

The overall savings over a cooling season associated with the use of variable-speed equipment depends upon the time variation of the load. Table 6.3 summarizes cooling

season operating costs for the fixed-speed equipment relative to all variable-speed for low and high internal gains in both Dallas and Miami. Included in this table are results for fixed-speed air handler fans with variable-pitch blades to control the air flow. The results do not differ significantly between the Dallas and Miami climates. The largest differences for all situations are seen in comparing the fixed-speed to the variable-speed chillers (13% to 18%). The use of individual fixed-speed pumps or fans in the system carries a penalty of about 3 - 10% depending upon the load characteristics. Overall, the use of all fixed-speed equipment results in operating costs that are 26 - 43% higher than for all variable-speed drives.

Table 6.3
Cooling Season Results for Variable vs. Fixed-Speed Equipment

Configuration	Cost Relative to All Variable-Speed Equipment			
	Low Internal Gains		High Internal Gains	
	Dallas	Miami	Dallas	Miami
fixed-speed chiller	1.16	1.18	1.14	1.13
fixed-speed tower fans	1.06	1.06	1.05	1.05
fixed-speed pumps	1.10	1.09	1.05	1.04
fixed-speed air handler fans	1.07	1.07	1.04	1.04
all fixed-speed equipment	1.42	1.43	1.29	1.26

6.5.2 Series versus Parallel Chillers

Multiple chillers are typically arranged in parallel and the chilled and condenser water flows are divided between the chillers according to their loading. Alternatively, it is possible to arrange chillers in series, so that the total chilled and condenser water flows pass through each evaporator and condenser. Two possible arrangements for series chillers are series-parallel and series-counterflow. In the series-parallel

arrangement, the chilled and condenser water flows are in parallel, in that these streams enter the same chiller. For the series-counterflow configuration, the streams enter at opposing chillers.

For the same total flow, multiple chillers operate more efficiently in series rather than in parallel. Figure 6.13 gives a comparison between the chiller coefficients of performance for parallel and series arrangements of two identical chillers as a function of the relative loading on the first chiller for identical entering temperatures and flow rates. Both series arrangements require significantly less power than the parallel chillers, the best arrangement being series counterflow. For the same total flow, the heat transfer coefficients are higher and leaving water temperature differences are lower for the individual chillers in series orientations than for parallel.

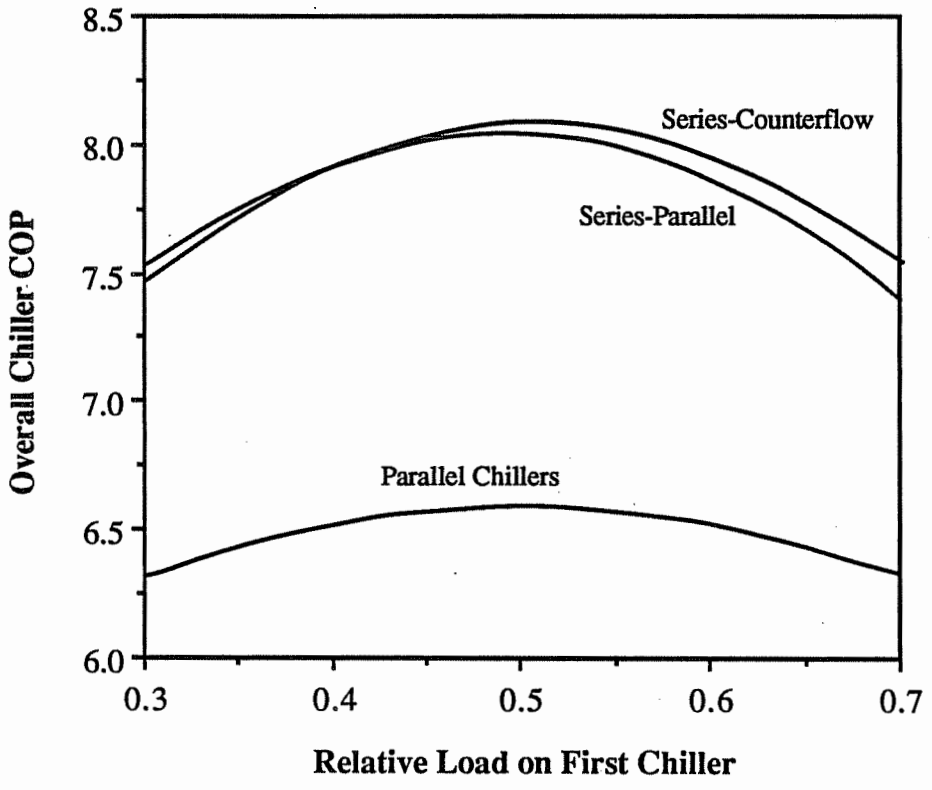

Figure 6.13. Comparison of Chiller Performance for Parallel and Series Configurations

Although the chillers perform more efficiently in series rather than parallel, there are significant increases in water stream pressure drops across both the evaporators and condensers for the series arrangement. For two identical chillers, the ratio of the pressure drop across either the evaporator or condenser for a series arrangement as compared with that for parallel is approximately 8-to-1 for identical flow rates. The difference in the overall system performance for series versus parallel depends upon the magnitude of evaporator and condenser pressure drops as compared with the other pressure losses in the chilled and condenser water loops. Figure 6.14 compares the optimal system performance for series and parallel chillers as a function of load for a given wet bulb. For this system, the tradeoffs between improved chiller performance and increased pressure drops balance such that overall system performance is similar for both configurations. Reducing the evaporator and condenser pressure drops by 20% did not have a significant effect upon this result.

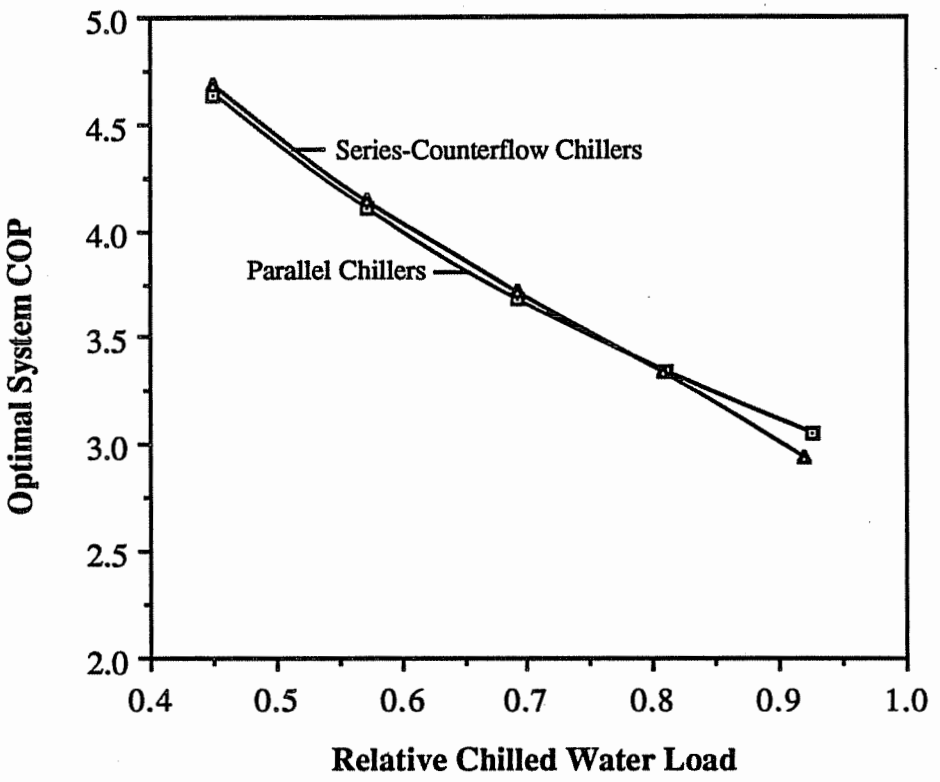

Figure 6.14. Optimal System Performance for Series and Parallel Chillers

6.6 Summary

Optimization techniques were applied to the control of chilled water systems. The important uncontrolled variables that effect system performance and optimal control variable settings were identified as the total chilled water load and ambient wet bulb temperature. Additional secondary uncontrolled variables that could be important if varied over a wide range would be the individual zone latent to sensible load ratios and the ratios of individual sensible zone loads to the total sensible loads for all zones.

Control guidelines that reduce the number of independent control variables and simplify the optimization were also identified. These general results were utilized in Chapter 5 to develop a "simple" methodology for near-optimal control of chilled water systems without storage. The guidelines are also useful to plant engineers for

improved control practices and are summarized as follows.

1) Variable-Speed Tower Fans: Operate all tower cells at identical fan speeds.

2) Multi-Speed Tower Fans: Increment lowest tower fans first when adding tower capacity. Reverse for removing capacity.

3) Variable-Speed Pumps: The sequencing of variable-speed pumps should be directly coupled to the sequencing of chillers, to give peak pump efficiencies for each possible combination of operating chillers. Multiple variable-speed pumps should be controlled to operate at equal fractions of their maximum speed.

4) Chillers: Multiple chillers should have identical chilled water set temperatures and the evaporator and condenser water flows for multiple chillers should be divided according to the chillers relative cooling capacities.

5) Air Handlers: All parallel air handlers should have identical supply air setpoint temperatures.

No general simplifications could be found for the optimal sequencing of chillers and fixed-speed pumps. It is necessary to evaluate the overall system performance in order to determine the optimal points for adding or removing chillers. In general, it is not optimal to sequence fixed-speed pumps with chillers.

Additional results and conclusions concerning both control and design under optimal control of chilled water systems are summarized as follows.

1) Depending upon the load characteristics, fixed values of chilled water and supply air setpoints and cooling tower approach and range resulted in approximately 7 - 19% greater cooling season operating costs than that for optimal control in Dallas and Miami.

2) In the determination of optimal control points, the humidity should be allowed to float freely, unless it falls outside the bounds of human comfort. In effect, the addition of any constraint reduces the number of free control variables by one and results in operation at a higher cost.

3) Depending upon the load characteristics, the cooling season operating costs were approximately 26 - 43% greater for all fixed-speed equipment as compared with all variable-speed in Dallas and Miami. The most significant difference was attributed to the chiller.

4) The performance of multiple chillers is enhanced by orientation in series rather than parallel. However, the increase in pumping power requirements for series chillers offsets the chiller improvements and the overall performance for the two configurations is similar.

Chapter 7

Methodologies for Optimal Control of Systems with Storage

There are several advantages associated with the use of thermal storage in large cooling systems. From a design point of view, the use of storage can increase the peak cooling capacity of a system, thereby reducing the size and initial cost of chillers, cooling towers, and air handlers. For existing systems, introducing storage can allow operation at more favorable part-load conditions. However, the most important applications of storage are for 1) shifting the load from times of high to times of low utility electric rates and 2) limiting the peak system power consumption in the presence of utility demand charges.

There are two types of storage that are presently being installed for chilled water systems: water and ice. Typically, both storage types are arranged in parallel between the chillers and the air handlers in the chilled water loop. These systems generally operate in different modes that allow for charging (cool-down) and discharging of storage and for direct cooling in which the storage is isolated and the chillers meet the load directly. In an ice system, a chiller produces ice during the charging mode and a brine solution is pumped between the storage and air handlers during discharge. A water storage system relies on stratification in order to achieve good performance. Cold water from the chillers is fed to the bottom of storage during the charging cycle. During discharge, this chilled water is pumped to the air handlers and warm return water from the air handlers is added to the top of storage. The stratification of storage is produced by the cold supply to the bottom and warm return to the top.

In this chapter, a methodology is outlined for determining the optimal control of a fully-stratified chilled water storage system. This methodology is utilized as tool for

analyzing the control of these systems. A simpler near-optimal control strategy is developed from the results of the detailed analysis. In order to implement either the optimal or near-optimal control, it is necessary to forecast the cooling load requirements. Time-series techniques are applied to the development of a model for forecasting the cooling requirements of buildings.

7.1 Optimization of Systems with Storage

Optimal control of a system with thermal storage involves minimizing the integral of the operating costs, while satisfying required constraints. There are capacity limits associated with each piece of equipment in the plant. If sensible energy storage is utilized, then there are upper and lower limits on the temperature of storage in order to provide proper comfort and avoid freezing. The general form of the optimization problem is

Minimize

$$J = \int_{t_0}^{t_f} L\,(\mathbf{x}(t), \mathbf{u}(t), \mathbf{f}(t), t)\,dt \qquad (7.1.1)$$

subject to

$$\frac{d\mathbf{x}}{dt} = \phi\,(\mathbf{x}, \mathbf{u}, \mathbf{f}) \qquad (7.1.2)$$

$$\mathbf{x}(t) \;\varepsilon\; \mathbf{X}$$

$$\mathbf{u}(t) \;\varepsilon\; \mathbf{U}$$

where J is the total cost of the process between the times t_o and t_f, L is the instantaneous cost at time t, **x** is a vector of state variables, **u** is the vector of control variables, **f** is a vector of uncontrolled variables, and **X** and **U** are constraint sets associated with the state and control variables. The instantaneous operating cost at any time is the product of the total system power consumption and the cost of electricity or

$$L(\mathbf{x}(t), \mathbf{u}(t), \mathbf{f}(t), t) = R(t)\, P(\mathbf{x}(t), \mathbf{u}(t), \mathbf{f}(t)) \qquad (7.1.3)$$

where P is power consumption and R is the cost of electricity.

The solution of the optimal control problem gives a vector of control functions for a continuous representation or sequences of values for the discrete case. This solution can either be expressed as a function of time, $\mathbf{u}^*(t)$, in open-loop control, or alternatively as a function of the state variables, $\mathbf{u}^*(\mathbf{x})$, for closed-loop control.

One approach for solving the optimal control problem expressed by equations 7.1.1 and 7.1.2 that evolved from the calculus of variations was introduced by Pontryagin [1962]. The minimum principle provides a set of necessary conditions which the optimal control, $\mathbf{u}^*$, must satisfy if it exists. One limitation of this approach is that constraints on the state and control variables are often difficult to handle. It is also possible to determine a local minimum as a solution.

Alternatively, the optimization problem may be solved in a discrete manner using dynamic programming (Bellman [1957]). This method handles constraints on both state and control variables in a straightforward manner. This method also guarantees a global minimum. The major limitations are associated with large memory and computation requirements when many state variables are involved. In this study, dynamic programming is utilized to study the optimal control of chilled water systems with storage.

7.1.1 Dynamic Programming

Dynamic programming may be applied as a numerical technique for determining global solutions to dynamic optimization problems. The method involves discretization of the problem with respect to both time and state variables. The discrete-time representation of the optimization problem becomes

Minimize

$$J = \sum_{k=0}^{K} L(\mathbf{x}(k), \mathbf{u}(k), \mathbf{f}(k), k) \tag{7.1.4}$$

subject to

$$\mathbf{x}(k) = \phi(\mathbf{x}(k-1), \mathbf{u}(k-1), \mathbf{f}(k-1)) \tag{7.1.5}$$

$$\mathbf{x}(k) \in \mathbf{X}$$

$$\mathbf{u}(k) \in \mathbf{U}$$

The integral cost function has been converted to a sum of individual stage costs from 0 to K, while the state equations are represented in difference form.

The heart of dynamic programming is Bellman's principle of optimality. The principle can be stated as follows:

> Suppose the sequence of optimal controls, $\mathbf{u}^*(k)$, $k = 0, 1, \ldots, K$, optimizes $J(\mathbf{u})$. Define a subproblem:

$$J_m = \sum_{k=m}^{K} L\,(\mathbf{x}(k), \mathbf{u}(k), \mathbf{f}(k), k)$$

with the initial state at stage m equal to that associated with the original optimal control, $\mathbf{x}(m) = \mathbf{x}^*(m)$. Then the solution to the original optimal control problem from stage m to K, $\mathbf{u}^*(k)$, k = m, m+1,..., K also optimizes $J_m(u)$.

This fairly simple principle leads to an iterative functional equation for determining optimal control termed the dynamic programming equation.

$$I(\mathbf{x}(m), m) = \min\{L(\mathbf{x}(m), \mathbf{u}(m), \mathbf{f}(m)) + I(\mathbf{x}(m+1), m+1)\} \qquad (7.1.6)$$

I(x(m), m) is defined as the minimum cost-to-go from state x at stage m to K. The dynamic programming equation is related to the principle of optimality in that the minimum cost-to-go from any state x(m) is found by minimizing the sum of the stage cost for the present stage, m and the minimum cost in going to the end of the process from the resulting state at the next stage, m+1.

Equation 7.1.6 may be used in a numerical scheme for determining optimal control. The state variables are discretized within the constraint set establishing a network of paths between successive stages and possible states. Figure 7.1 shows a possible network for a single state variable with specified initial and final conditions for 5 stages. For clarity in Figure 7.1, the change in state from one stage to the next is limited to one state increment. The problem is solved for all stages by beginning at the end of the process and working towards the beginning. For the network of Figure 7.1, an initial cost-to-go of zero is assumed at the final state, x(K), K = 5. At stage K-1,

the minimum cost-to-go for each possible state is simply the stage cost associated with the path from that state to the final state. At any stage k, the minimum cost-to-go for any state, according to equation 7.1.6, is associated with the path having the smallest sum of the stage cost and cost-to-go of the next state. At the 0^{th} stage, the minimum cost- to-go is the cost associated with the optimal path through the network.

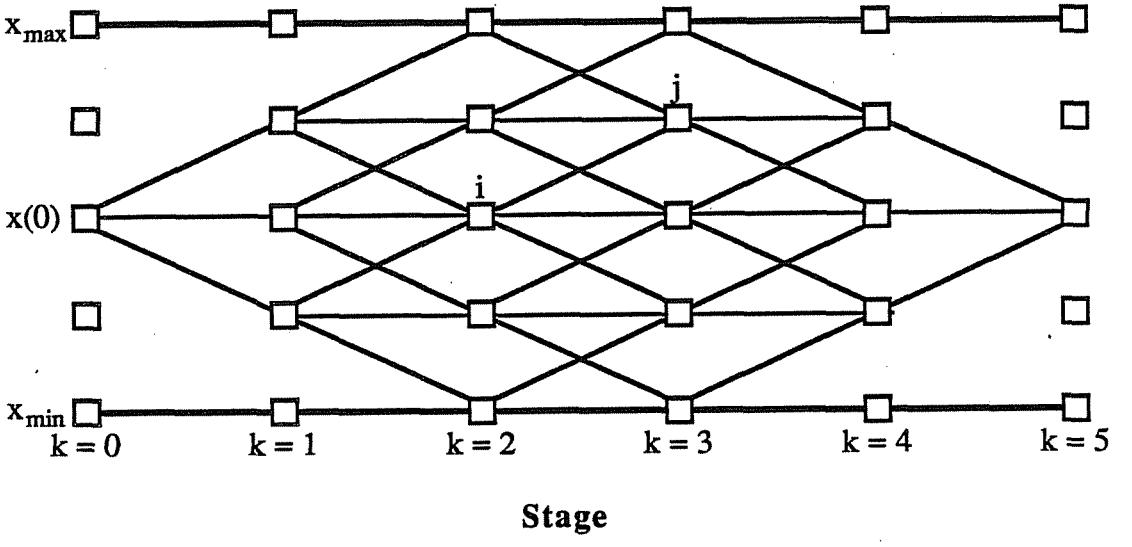

Figure 7.1. Dynamic Programming Network

There are many possible controls that will take the system from any state i to any other state j, one stage ahead. The minimization of equation 7.1.6 dictates that the stage cost be a minimum associated with optimal control between the two states. For any path from i to j, this stage cost optimization problem may be formally stated as

Minimize

$$J_{i\text{-}j}(k) = L(\mathbf{x}(k), \mathbf{u}(k), \mathbf{f}(k), k) \qquad (7.1.7)$$

subject to

$$\mathbf{x}_j(k+1) = \phi(\mathbf{x}_i(k), \mathbf{u}(k), \mathbf{f}(k)) \tag{7.1.8}$$

Depending upon the number of stages and state variables, the computational and memory requirements associated with the use of dynamic programming may be excessive. The number of nodes in a dynamic programming network is equal to the number stages times the number of state variable increments together raised to a power equal to the number state variables. For a problem with 10 stages having 3 state variables, each discretized with 10 increments, the number of network nodes would be 10,000. Morin (1979) provides a review of improvements in the the dynamic programming procedures that address this problem.

One such improvement, utilized in this study, involves application of dynamic programming in an iterative scheme in which bounds on the state variables are reduced at each iteration in the vicinity of the last computed optimal solution. Initially, the network is coarse and encompasses the total range of acceptable state variables. At each iteration, an optimal path is determined through the network and the size of the network is reduced for the next iteration. At each iteration and at each stage, the number of state variables is constant and bounds on the network are defined equidistant above and below the states along the last computed optimal path. In the limit, the size of the network approaches zero along the optimal control path.

7.1.2 Application to Systems with Fully-Stratified Water Storage

Figure 7.2 shows a schematic of a chilled water storage oriented in parallel between the chillers and air handler equipment. There are five primary modes of operation

associated with control of storage that are considered in this study:

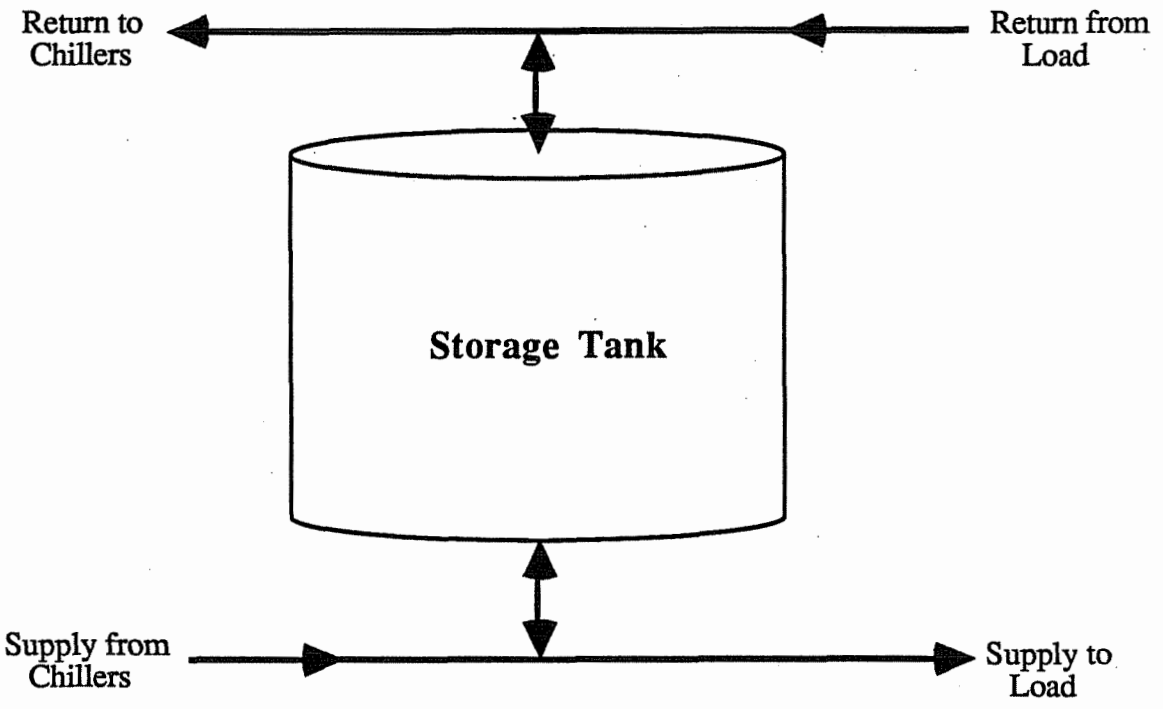

Figure 7.2. Parallel Configuration for Thermal Storage

1) Direct Cooling: The cooling load is met completely by chilled water supplied from the chillers and there is no flow to or from storage. All independent control variables are "free" in the control optimization.

2) Partial Charge: Chilled water from the chillers is provided to meet the load and to lower the temperature of storage. In this mode, the chilled water supply temperature is controlled to be a constant. All other independent control variables are "free" in the control optimization.

4) Partial Discharge: Chilled water is supplied from both the chillers and storage to

meet the load. In this mode, the return water from the load is controlled to be constant. All other independent control variables are "free".

4) Full Charge: There is no cooling load requirement (i.e. air handlers are off) and the chillers are operating solely to charge the storage. The chilled water supply temperature is controlled to be constant and all other independent control variables are "free".

5) Full Discharge: The cooling load is met completely by water supplied from storage and the chillers and condenser loop equipment is off. The return water from the load is controlled to be a constant.

The use of constant inlet temperatures to storage during charging and discharging is common practice. The storage capacity is proportional to the difference between the load water return temperature for discharging and the chilled water supply temperature for charging. However, there are practical limits on these temperatures. The limit on the chilled water supply in order to avoid freezing problems in the evaporator is approximately 40 F. A load water return temperature of 60 F during discharge is approximately the upper limit necessary to insure proper dehumidification at the cooling coils for the load. The constant values of chilled water supply temperature for charging and load water return temperature for discharging were chosen as 40 and 60 F, respectively.

Neglecting heat gains from the environment, conduction, and mixing at the inlets, the energy equation for charging or discharging storage is

$$\frac{\partial T}{\partial t} = -v\frac{\partial T}{\partial x} \tag{7.1.9}$$

where T is temperature, t is time, x is position measured from the inlet, and v is the velocity of the fluid. The fully-stratified model represented by equation (7.1.9) has a known analytic solution. Given an initial temperature distribution at time t, the solution of this hyperbolic partial differential equation for the distribution at time $t + \Delta t$ and position x is

$$T(t + \Delta t, x) = T(t, x - v\Delta t) \qquad \text{for } x > v\Delta t \tag{7.1.10}$$

$$T(t + \Delta t, x) = T_i(t + \Delta t - x/v) \qquad \text{for } x < v\Delta t \tag{7.1.11}$$

where $T_i(\tau)$ is the inlet temperature (i.e. chiller supply or load return) at any time τ. For fluid that was within the storage at time t, equation (7.1.10) states that the distribution at time $t + \Delta t$ is a copy of the original distribution moved by an amount $v\Delta t$. For fluid that enters the storage during the time period, equation (7.1.11) shows that the temperature distribution downstream of the inlet is a history of the inlet conditions.

The use of constant inlet temperatures to the storage during charging and discharging simplifies the storage model and the overall optimization problem. In this case, the storage has two distinct temperature zones and the state of storage is represented by the position of the front between cold fluid supplied from the chillers and warm fluid returned from the load. If *x* represents the distance of this front above the bottom of storage relative to the height of storage, then it follows from equation (7.1.11) that a discrete state equation for storage at stage k may be expressed as

$$x\,(k+1) = x\,(k) + v\,\Delta t \tag{7.1.12}$$

where v is the velocity of the fluid relative to the tank height measured in the x direction. The relative position of the front may also be thought of as the relative storage charge. At a value of 0, the storage is empty in terms of its ability to provide cooling to the load. At a value of 1, the storage is fully charged. In terms of the rate at which energy is removed from storage, the relative fluid velocity is

$$v = \frac{\dot{Q}_s}{(T_{charge} - T_{discharge})\,Cap_s} \tag{7.1.13}$$

where $\dot{Q}_s$ is the energy discharge (positive) or charge (negative) rate of storage, T_{charge} is the chilled water supply temperature in the charging mode (40 F), $T_{discharge}$ is the load water return temperature in the discharging mode (60 F), and Cap_s is the thermal capacitance of storage. From an energy balance, the required chiller cooling rate is

$$\dot{Q}_{ch} = \dot{Q}_L - \dot{Q}_s \tag{7.1.14}$$

where $\dot{Q}_L$ is the total building cooling load rate.

In the dynamic programming algorithm, the state variable (i.e. relative charge level) is discretized between 0 and 1. Between any two states on the dynamic programming network, it is necessary to determine the optimal stage cost. For a given mode of operation at a given stage, the minimum power consumption of the equipment depends primarily upon the total cooling load, ambient wet bulb temperature, and the storage charging or discharging rate. The load and wet bulb are considered to be known (forecasted) uncontrolled variables. The required storage charge or discharge rate is

computed from equations (7.1.12) and (7.1.13) using the known states. Rather than perform the stage optimization within the dynamic programming algorithm, minimum power requirements from steady-state optimizations were correlated for each mode of operation using the form of equation (5.2.3). The optimal stage cost between any two states, for stage k is

$$J^*_{i\text{-}j}(k) = R(k)\left\{P^*_{i\text{-}j}(\dot{Q}_L(k), T_{wb}(k), \dot{Q}_{s,i\text{-}j}(k))\right\}\Delta t \qquad (7.1.15)$$

where R is the cost of electricity and $P^*_{i\text{-}j}$ is the minimum average power consumption between states i and j evaluated at a load, wet bulb, and storage discharge (or charge) rate of $\dot{Q}_L$, T_{wb}, and $\dot{Q}_{s,i\text{-}j}$

There are limits associated with operation of the equipment that must be considered. If the required chiller cooling rate is greater than the capacity of the chiller, then it is not possible to make the transition between the two states and an infinite stage cost is assigned. There is also a minimum cooling rate required to avoid compressor surge. However, in the full discharge mode, the chillers are off and the required chiller cooling is zero. If storage is being discharged and the required cooling rate determined with equation (7.1.14) is less than the minimum chiller cooling rate, then the chiller is assumed to operate a portion of the time during that stage at its minimum capacity in the partial discharge mode and is considered to be off the rest of the time with the system in the full discharge mode. The average rate of power consumption for the stage is then

$$P^* = P^*(\dot{Q}_L, T_{wb}, \dot{Q}_L - \dot{Q}_{ch,min})\frac{\Delta t_{on}}{\Delta t} + P^*(\dot{Q}_L, T_{wb}, \dot{Q}_L)\left[1 - \frac{\Delta t_{on}}{\Delta t}\right] \qquad (7.1.16)$$

where $\dot{Q}_{ch,min}$ is the minimum chiller cooling capacity and Δt_{on} is the time period for operation of chillers at their minimum capacity determined as

$$\Delta t_{on} = \frac{\dot{Q}_L - \dot{Q}_{s,i-j}}{\dot{Q}_{ch,min}} \Delta t \qquad (7.1.17)$$

Similarly, if the system is operating in the charge (partial or full) or direct mode and the required chiller load is less than the minimum allowable, then the chillers are considered to operate at their minimum capacity for the time necessary to meet the total load requirement and are off the remainder of the stage.

There are also considered to be additional limits associated with minimum and maximum rates of charging and discharging storage. The maximum charging or discharging rate is limited by the maximum chilled water pump flow and the supply temperatures to storage during charging or discharging. The minimum rates are due to limits on the control valves that distribute the flow between storage and the air handlers during charging and between storage and the chillers during discharging. If the required charging or discharging rate is greater than the maximum, then it is not possible to make the transition between the two states on the dynamic programming network and an infinite stage cost is assigned. If the required charging or discharging rate is less than the minimum rate, then the system is assumed to operate a period of the time during that stage in the partial charging or discharging mode at the minimum rate and the remainder in the direct cooling mode.

7.1.3 Results for Fully-Stratified Storage

The methodology described in the previous section was applied to a fully-stratified chilled water storage system in order to answer two questions: 1) What is the

magnitude of cost savings associated with the use of optimally controlled storage in the absence of time-of-day or peak demand utility rates? and 2) Is it necessary to perform "true" optimal control for systems having time-of-day rates or do simpler control strategies work "well enough"? In order to study these issues, one-day (24-hour) simulations were performed for known load distributions and ambient wet bulb conditions. Only steady-periodic solutions were considered so that the final state equalled the initial state. Both the load and wet bulb were varied according to a sinusoidal function as

$$f(t) = \frac{f_{max} + f_{min}}{2} + \frac{f_{max} - f_{min}}{2} \sin\left[\frac{2\pi}{24}(t - 12)\right] \qquad (7.1.18)$$

where f(t) is the value of the uncontrolled variable (load or wet bulb) at time t and f_{min} and f_{max} are the minimum and maximum values that occur at 6 a.m. and 6 p.m., respectively. The effects of different minimum and maximum values were considered. In some cases, the cooling system was assumed to be off at night (6 p.m. to 6 a.m.), such that the load during this time was zero. The system considered was the base system described in Chapter 6.

In the absence of time-of-day electric utility rates and if the peak load is less than the capacity of the chiller, then the optimal control strategy for all 24 hour load and wet bulb patterns considered was to operate in the direct mode for all times. In other words, storage provided no benefit for this system. For no night-time load, thermal storage provided at most a 5% reduction in the overall power consumption for the system and loads considered.

One of the reasons that storage provides little or no operating cost savings when

there are no special time-of-day utilities rates is due to the fact that this system operates most efficiently in the direct mode. For charging of storage, the chillers operate at a fixed chilled water supply, while for discharging, the return temperature from the load is constant. In the direct mode, these variables are optimized as a function of the load and wet bulb temperature. Undoubtably, storage would provide some additional benefit if the chilled water supply and load water return temperatures during charging and discharging were also "free" control variables in the optimization. However, this complicates the dynamic optimal control problem considerably by introducing many state variables and would be difficult to implement in practice.

Figures 7.3 and 7.4 show how the optimal charge level of storage and chiller loading vary over a day for different storage sizes with time-of-day electric rates. The cost of electricity is assumed to be \$0.15/kW-hr for the hours from 8 a.m. to 8 p.m. and \$0.05/kW-hr for the rest of the day. The ambient wet bulb varied between 65 and 75 F, while the minimum and maximum loads were 1500 and 4000 tons. The storage charge level is defined as the fraction of the tank that is filled with chilled water at 40 F, with the remainder of the tank at 60 F. Two different storage sizes were considered for these results: 1500 and 2000 ton-hours/deg. F. The no storage results shown in Figure 7.4 represent the total building load and would be the load on the chiller if there were no storage or if the system always operated in the direct cooling mode.

In the presence of time-of-day rates, Figure 7.3 shows that the optimal charge level reaches a maximum at the time at which the rates increase and realizes a minimum when the rates decrease. The smaller storage capacity is insufficient to meet the load during the period of high utility rates. As a result, the storage is completely discharged when the utility rates are lowered. Between the hours of about 8 a.m. to 1 p.m., this system operates primarily in the direct cooling mode and the storage remains near its full charge. Since the storage is undersized, then the chiller must operate sometime during

the high rate period. The optimal time to operate the chiller is during the first part of the high rate period when the ambient wet bulb is lower and the system performs more efficiently.

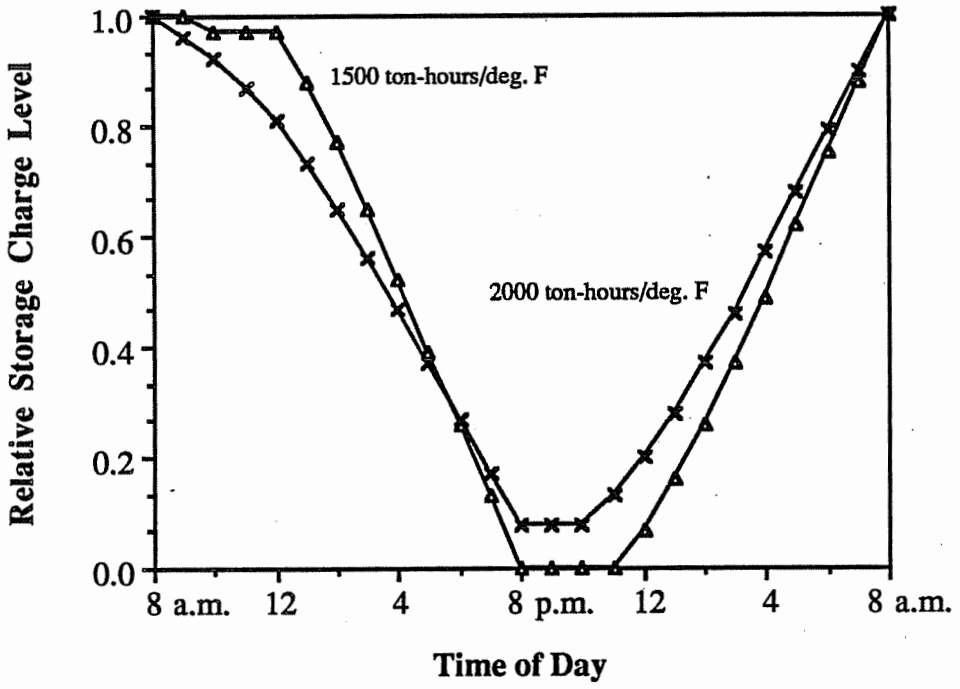

Figure 7.3. Optimal Storage Charge Level for One Day with Time-of-Day Electric Rates

The system with the larger storage has excess capacity and operates in the full discharge mode for the entire high rate period and reaches a minimum charge level when the rates are reduced. As evident from Figure 7.4, there is no load on the chillers (i.e. chillers off) for this system between 8 a.m. and 8 p.m. After the rates are reduced, both the small and large storage systems operate in the direct cooling mode for a period of time before charging the storage. During the charging period, the chillers are loaded at a fairly constant rate until the maximum storage charge is reached at the time when the rates increase.

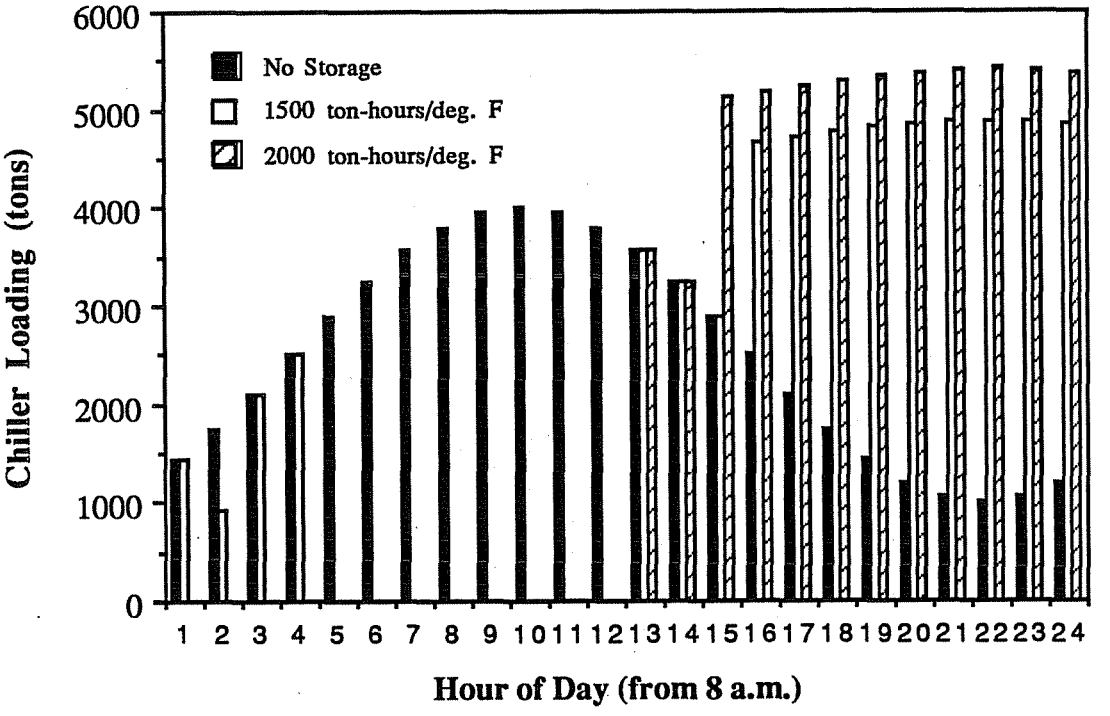

Figure 7.4. Optimal Chiller Loading for One Day with Time-of-Day Electric Rates

From the results of dynamic programming applied to systems with storage, some simple guidelines may be established for "near-optimal" control when time-of-day utility rates are in place.

1) Begin the period of high rates with the storage fully charged.

2) During high-rate hours, the system should operate in the full discharge mode for a period of time necessary for the storage to completely discharge, if possible. If the storage capacity is not sufficient to meet the load when rates are high, then the system should operate in the direct mode for the remaining time. The direct mode on-peak operation should occur during times when the wet bulb temperature is

lowest, generally during the morning and early afternoon hours.

3) During low-rate hours, the chillers may operate at their capacity to charge storage during the time when the wet bulb temperature is lowest for near-optimal performance. For the remainder of the time, the system should operate in the direct cooling mode.

Table 7.1 compares the cost of operation associated with optimal control, the near-optimal control strategy outlined above and a non-optimal, more conventional control strategy. In the non-optimal strategy, the system operates in the full discharge mode from the start of the on-peak utility rate period. If the storage is completely discharged during this period, then the system operates in the direct mode to meet the load until the electric rates decrease. The storage is then charged at full capacity until fully charged. The advantage of this control strategy is that it does not require forecasting of the cooling loads or ambient wet bulb. The disadvantage is that the chillers may operate at high cooling loads during times when the wet bulb is higher.

Table 7.1 shows that the near-optimal control strategy results in operating costs that are close to those for optimal control. However, depending upon the storage capacity in relation to the load, the non-optimal strategy gives costs that can be significantly greater. All three controls give similar results at large storage capacities, since the system always operates in the discharge mode when rates are high and operates in the charging mode at full capacity for a significant portion of the time when rates are low. The conventional strategy also works well when the variation in the wet bulb temperature is small.

Table 7.1 One-Day Operating Cost Comparisons for Systems with Thermal Storage

System Description	Daily Operating Costs ($) Optimal	Near-Optimal	Conventional
24 hour load min. and max loads: 1500, 4000 tons storage capacity: 1500 ton-hours/deg. F	2686	2727	3095
24 hour load min. and max. loads: 1500, 4000 tons storage capacity: 2000 ton-hours/deg. F	2489	2497	2564
12 hour load min. and max loads: 1000, 5000 tons storage capacity: 1500 ton-hours/deg. F	2167	2301	2625
12 hour load min. and max loads: 1000, 5000 tons storage capacity: 2000 ton-hours/deg. F	1943	2066	2095

7.3 Models for Forecasting Building Cooling Requirements

In order to implement optimal or near-optimal control of thermal storage, it is necessary to forecast cooling load requirements. In this section, measurements from the Dallas/Fort Worth airport are utilized to develop a time-series model for forecasting cooling loads.

Building cooling loads are functions of many variables such as ambient temperature, solar radiation, occupancy of people, lighting, computers, etc. All of these heat gains are periodic functions having a dominant period of 24 hours. There are also random components in the loads resulting from the stochastic nature of the weather and the way that the buildings and the distribution system are utilized. Therefore, a

combined deterministic plus stochastic model is appropriate for load forecasting.

The procedure for fitting a combined model to a data set is a three step process. A purely deterministic model is defined through regression to the data. Next, a stochastic time-series model is fit to the residual errors associated with the deterministic model. In this step, the proper time-series model order is defined. Finally, parameters of the combined deterministic plus stochastic model are estimated simultaneously.

For on-line optimal control of the equipment, it would be advantageous to utilize on-line recursive parameter estimation for the forecasting model. Recursive parameter estimation is most easily carried out with linear models (i.e. the model is linear in the unknown parameters). For that reason, this study was restricted to linear time-series models termed AR (auto-regressive) models. A good background to material presented in this section is found in Pandit and Wu [1983].

7.2.1 Time-Series Models

A time series is a sequence of observed data ordered in time. The statistical methodology dealing with the analysis of such a data sequence is termed time-series analysis. A time-series model expresses the dependence of the present observation as a sum of two independent parts: one dependent upon preceding observations and the other an independent random sequence. The simple auto-regressive model of order n (AR(n)) is given by

$$X_t = \sum_{i=1}^{n} \phi_i X_{t-1} + e_t \qquad (7.2.1)$$

where X_t is the current (zero mean) output of the system, X_{t-i} is the output i steps previous, ϕ_i is i^{th} parameter of the model, and e_t can be thought of either as a random

input to the system or the one-step ahead prediction error of the model. At time t-1, the best forecast of an observation for time t is obtained by evaluating the expected value of the right-hand side. The expected value of a random variable with a zero mean is zero, thus the one-step ahead prediction for the model defined by equation (7.2.1) at time t-1 is

$$\hat{X}_t = \sum_{i=1}^{n} \phi_i X_{t-1} \qquad (7.2.2)$$

From equations (7.2.1) and (7.2.2), it should be evident that e_t is the error associated with the one-step ahead forecast of the model. This is true for all time series models. In order to estimate parameters of the model for a given set of data, the sum of the squares of the one-step ahead prediction errors (e_t's) is minimized with respect to the unknown ϕ's using linear regression. For a given model, greater than one-step ahead forecasts are determined with equation (7.2.2) applied recursively to known and forecasted values.

A more general time-series model that utilizes both previous observations and errors is termed an auto-regressive moving average model (ARMA). Pandit and Wu [1983] have defined a rational method for determining the order of an ARMA model that provides an adequate fit to the data. However, a nonlinear regression is required in order to determine the coefficients of the model. Theoretically, an ARMA model can be represented by an AR model of infinite order. However, in practice, only a finite AR model is necessary. The advantage of using AR models is that linear regression techniques may be utilized. This is especially important for load forecasting in the context of on-line optimal control, when coefficients of the model are updated using

recursive parameter estimation techniques.

Periodic trends in the data may be removed by the use of a trigonometric polynomial of order m, having the form

$$P(t) = \sum_{j=1}^{m} a_j \sin(j\omega t) + \sum_{j=1}^{m} b_j \cos(j\omega t) \tag{7.2.3}$$

where ω is the frequency and the a's and b's are unknown coefficients that are fit with a linear least squares method applied to the data.

A combined model can also be expressed in a linear form. The combined model for a zero mean output, Y_t, is the sum of the deterministic and stochastic models.

$$Y_t = \sum_{j=1}^{m} a_j \sin(j\omega t) + \sum_{j=1}^{m} b_j \cos(j\omega t) + \sum_{i=1}^{n} \phi_i X_{t-1} + e_t \tag{7.2.4}$$

But, by definition

$$X_t = Y_t - \sum_{j=1}^{m} a_j \sin(j\omega t) + \sum_{j=1}^{m} b_j \cos(j\omega t) \tag{7.2.5}$$

Substituting equation (7.2.5) into (7.2.4) gives

$$Y_t = \sum_{j=1}^{m} a'_j \sin(j\omega t) + \sum_{j=1}^{m} b'_j \cos(j\omega t) + \sum_{i=1}^{n} \phi_i Y_{t-1} + e_t \tag{7.2.6}$$

where a'_j and b'_j are different coefficients than those appearing in equation (7.2.4).

All the empirical coefficients of equation (7.2.6) can be fit to data with linear least-squares methods. For one-time parameter estimation from a batch of measurements, the data is typically averaged and the average is subtracted from the data before the fitting process. Parameters of this model may also be fit using on-line recursive parameter estimation as outlined by Ljung [1983].

7.2.2 Application to Forecasting Cooling Loads

Simple AR models given by equation (7.2.1) were fit with approximately three days of cooling load data in March from the D/FW airport for a sampling interval of 1 hour. Results of this analysis are summarized in Table 7.2.

Table 7.2
AR Model Fit to March D/FW Data (1 hour sampling)

Parameter	AR(1)	AR(2)	AR(3)	AR(4)	AR(5)
ϕ_1	0.881	0.870	0.886	0.8496	0.8140
ϕ_2		0.009	0.060	0.0748	0.0930
ϕ_3			-0.059	0.1390	0.1510
ϕ_4				-0.2290	-0.1010
ϕ_5					-0.1500
rms(tons)	334	334	334	329	327

At first glance, it might appear that an AR(1) model is adequate for this data set. The reduction in the root-mean sum of squares of the 1-step prediction errors is insignificant when going from AR(1) to AR(2). However, the AR(4) model does show some additional improvement. This behavior results from the large degree of randomness

exhibited in the data on a small time scale. A four-hour history is useful in overcoming the short-term fluctuations and to incorporate the larger time scale variations in the data. Comparisons of the one-step and five-step ahead predictions with the data are shown in Figures 7.5 and 7.6. The AR(4) model does reasonably well for the one hour prediction, but falters badly with five hour forecasts. Similar results were obtained with an ARMA(3,2) model fit to this data.

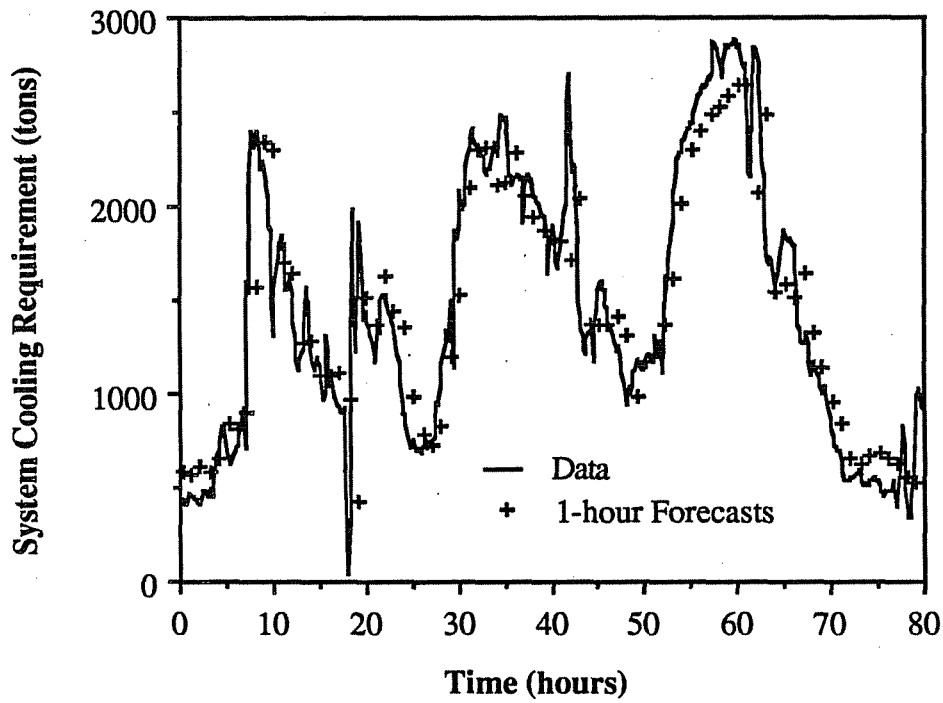

Figure 7.5. One-Hour Forecasts of March D/FW Cooling Load Data for AR(4) Model

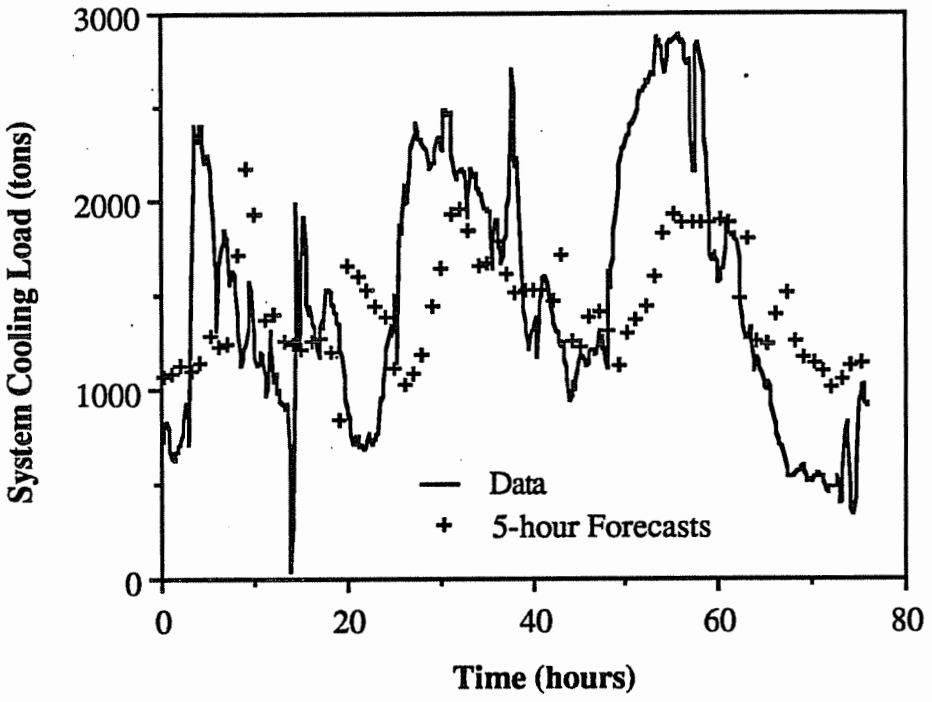

Figure 7.6. Five-Hour Forecasts of March D/FW Cooling Load Data for AR(4) Model

An improved model results if some of the determinism is removed by fitting a trigonometric polynomial to the data. If a combined model is fit to the data then the adequate model has 4 auto-regressive parameters and two periods (24 and 12 hours). In this case, the root-mean square (rms) error of one-step ahead forecasts is 287. This is a significantly improved model over the pure AR(4). The combined model does an extremely good job of forecasting the cooling loads 1 hour ahead. In addition to the improved 1-step predictions, the ability of the model to perform 5-hour forecasts is vastly improved. Figure 7.7 shows comparisons between five-step ahead predictions of the combined model with the March data. The rms of the errors for 5-step predictions of the combined model is 398, as compared with 625 for the pure AR(4).

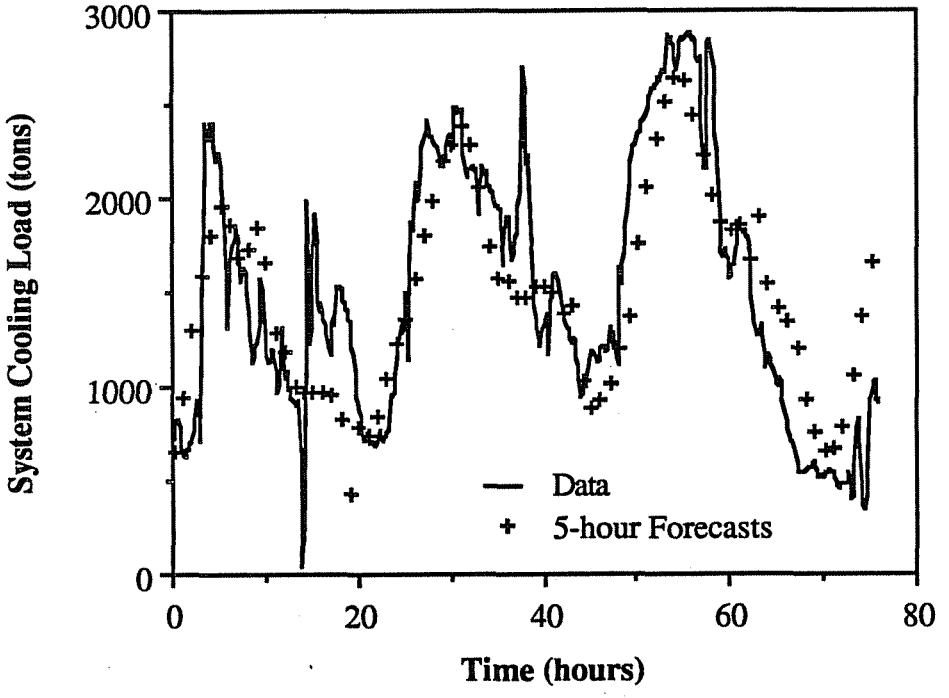

Figure 7.7. Five-Hour Forecasts of March D/FW Cooling Load Data for Combined Deterministic and Stochastic Model

Even better long-term predictions can be realized by using a larger sampling interval for the data. The model determined with a sampling interval of 2.5 hours gives significantly better results for the long-term predictions (rms of 296 versus 398). The 1 hour sampling interval gives a model that utilizes only the most recent information concerning the load. This occurs because the model is fit using the errors of the 1-step ahead prediction and there is a large degree of randomness in the data at 1 hour samples. The larger sampling period more appropriately captures the larger scale variations in the data. The forecasts associated with a 5 hour sampling interval are better still. It might be advantageous to have separate models for short and long-term forecasting that utilize different sampling intervals.

A good test of the model determined with the March data is to compare it with

another data set. A comparison with October data gave good results for one-hour forecasts, but the five-hour predictions were very poor. There is a seasonal effect that alters the characteristics of the deterministic part of the data. The cooling requirement is coupled closely to the ambient temperature. Generally, the peak cooling load occurs at about the same time of the day as the maximum ambient temperature. During October, this peak occurs later in the day than in March. In fitting a combined deterministic and stochastic model to the October data, the adequate linear model was also found to be AR(4) with a deterministic part having two periods. The accuracy of the forecasts was similar to that for the model fit to the March data.

In an attempt to further improve the long-term forecasts of the model, the ambient temperature was used as a deterministic input to the model. At the D/FW airport, the cooling requirement is strongly coupled to the ambient conditions. However, since the ambient temperature and cooling requirement are essentially in phase, there was little improvement in the results with the additional information. In other words, the history of the ambient temperature is almost completely reflected in the cooling load history.

It would be advantageous to use recursive on-line identification for this forecasting model so that the parameters could be adjusted to account for changes that occur on a seasonal basis, such as those discussed for the October and March data.. This can be accomplished in two ways. First of all, the incoming measured data may be weighted more heavily than past data (e.g. exponential weighting) such that the parameter estimates more correctly reflect the current state of the system. Secondly, periodicities that reflect seasonal changes in the climate may be included.

7.3 Summary

Dynamic Programming was applied as a numerical tool for determining optimal control of systems with stratified thermal storage. In the absence of time-varying utility rates, thermal storage provided little or no operating cost savings as compared with no storage for the systems considered. For systems with time-of-day utility rates, a simple strategy for near-optimal control was identified.

The advantage of the Dynamic Programming methodology over the simpler strategy is that it provides a "true" solution to the optimization problem and can adapt to changing circumstances. The algorithm is simple enough so as to be implementable on a microcomputer. Although demand charges were not considered in this study, peak power demands could be reduced by assigning large stage costs for "high" power consumptions.

The near-optimal control strategy involves maximizing the operation of the system in the full discharge mode whenever the utility rates are high and minimizing the operation in the charge mode when the utility rates are low. If the storage capacity is insufficient to meet the load during the high rate period, then the system operates in the direct mode during the hours when the wet bulb is low. During the low rate period, the storage is charged at the full capacity of the chiller during the hours of lowest wet bulb. For the remainder of this period, the system operates in the direct mode. The advantage of this near-optimal control strategy is that it is easily implemented and gives operating costs similar to that for optimal control.

In order to apply either the optimal or near-optimal strategy for controlling storage, it is necessary to forecast the total cooling requirements. Pure time-series and combined deterministic plus time-series models were fit to cooling load data for the D/FW airport. In all cases, the models worked well for making forecasts of one hour.

In order to make longer term predictions, it was necessary to include deterministic components in the model. The results of 5-hour predictions with the combined model were good. The resulting model is simple enough to be fit with linear least-square methods.

Chapter 8
Conclusions and Recommendations

In this study, general methodologies were developed for design and control of central chilled water systems. These methodologies are in form of mathematical models, optimization algorithms, and guidelines for design and control synthesized from results of optimal control applied to chilled water systems. The computer programs developed in this study are listed in a separate document (Braun [1988]). Specific conclusions and recommendations concerning this work follow.

8.1 Mathematical Models

In Chapter 2, a detailed mechanistic model for variable-speed centrifugal chillers was developed. The model requires only design parameters and the operating conditions in order to estimate the power requirement. The model is also capable of estimating the compressor speed at which surge develops or the maximum chiller cooling capacity at a given power input or speed. Results of the model were compared with measurements from the D/FW airport. *The mechanistic model works well in estimating both the power requirement and the speed associated with the onset of surge for variable-speed centrifugal chillers. Additional work is necessary to develop mechanistic models for analyzing the performance of fixed-speed, variable-vane controlled chillers.*

Using results of the mechanistic model, a simpler empirical model for correlating performance data was also identified. *Chiller power consumption correlates as a quadratic function of only two variables: the load and temperature difference between the leaving condenser and chilled water flows. The empirically-based model fits data*

for both variable-speed and fixed-speed with vane control chillers. Models for correlating the limits of chiller operation associated with surge and capacity were also presented.

In Chapters 3 and 4, effectiveness models were developed for cooling towers and cooling coils. These models utilize existing effectiveness relationships for sensible heat exchangers with modified definitions for number of transfer units and the capacitance rate ratio. Simple methods were also developed for estimating the water loss in cooling towers and the performance of cooling coils having both wet and dry portions. *Results of the effectiveness models for cooling towers and cooling coils compare well with the results of more detailed numerical solutions to the basic heat and mass transfer equations and with experimental data. The advantages of this approach are its simplicity, accuracy, and consistency with the methods for analyzing sensible heat exchangers. Future work should involve application of this modeling approach to other wet surface heat exchangers.*

Models were also presented for the power requirements of cooling tower and air handler fans and condenser water and chilled water pumps. It was shown that *quadratic functions work well in correlating the power consumptions of the auxiliary devices in central chilled water facilities.* The use of quadratic functions for the chiller and auxiliary equipment was an important result in the development of an efficient method for determining optimal control.

8.2 Optimal Control Methodologies

Two methodologies were presented for determining optimal control points for chilled water systems without storage. A component-based non-linear optimization algorithm was developed as a simulation tool for investigating optimal system performance. Results of this algorithm implemented in a computer program, led to the

development of a simpler system-based methodology for near-optimal control.

The advantage of the component-based algorithm over the system-based approach is that it provides a "true" solution to the optimization problem, including any nonlinear constraints. Each of the components in the system is represented as a separate subroutine with its own parameters, controls, inputs, and outputs. Models of components may be either mechanistic or empirical in nature, so that *the component-based methodology is useful for evaluating both system design or control characteristics.*

The component-based algorithm takes advantage of the quadratic cost behavior of the components found in chilled water systems in order to solve the optimization problem in an efficient manner. However, in order to utilize this methodology as a tool for on-line optimization, it is necessary to have detailed performance data for each of the individual system components. *Results of detailed optimizations identified simplifications that reduced the number of control variables to five and uncontrolled variables to two.* The system-based near-optimal control methodology utilizes an overall system cost function in terms of these variables. This cost function leads to a set of linear control laws for the continuous control variables in terms the total chilled water load and ambient wet bulb temperature. Separate control laws are required for each feasible combination of discrete controls and the costs associated with each combination are compared to identify the optimum. *Results of the system-based optimization methodology agree well with those of a more detailed non-linear optimization analysis. The system-based procedure is simple enough so as to be implementable either manually or on-line using microcomputers.* For manual control applications, charts could be used to determine optimal control as a function of load and wet bulb.

Additional work is necessary in order to apply either the component-based or system-based methodologiy to on-line optimal control. In particular, methods for determining parameters of the models need to be investigated. The performance characteristics of the system may change over time, so that it could be necessary to update the model parameters. It is also important to identify an appropriate time interval for making control decisions. There may be inefficiencies associated with changing controls too frequently in response to small changes in the uncontrolled variables. The next step is to test these methodologies as part of an energy management system for controlling an actual system.

A methodology was presented for determining the optimal control of stratified thermal storage systems using Dynamic Programming that is simple enough so as to be implementable on a microcomputer. Although demand charges were not considered in this study, peak power demands could be reduced by assigning large stage costs for "high" power consumptions. *Future work should consider the best strategy for including peak demand charges in the optimization algorithm.*

For systems with time-of-day utility rates, a simple strategy for near-optimal control was identified. The advantage of this near-optimal control strategy is that it is easily implemented and gives operating costs similar to that for optimal control.

Both the optimal and near-optimal strategies should be adaptable to systems that incorporate ice storage, however these concepts need to be tested. Systems that incorporate storage in-line with the chilled water distribution system, rather than in parallel should also be considered. It is also necessary to develop strategies for near-optimal control of systems that utilize more than one day of storage.

In order to apply either the optimal or near-optimal strategy for controlling storage, it is necessary to forecast the total cooling requirements. Pure time-series and combined deterministic plus time-series models were fit to cooling load data for the

D/FW airport. *Pure time-series models work well for making forecasts of one hour. In order to make longer term predictions, it was necessary to include deterministic components in the forecasting model.* The results of 5-hour predictions with the combined model were good. *The resulting deterministic and time-series model is simple enough so that its coefficients may be fit with linear least-square methods. More data is necessary to determine whether the model works well under all circumstances. Methods for recursive parameter estimation should also be tested for this forecasting model.*

In determining the optimal control of systems with storage, both the load and ambient wet bulb temperature were assumed to be knowns. *Future work should address the effect of inaccuracies in forecasts on the accuracy of the optimal control solution.*

8.3 Guidelines for Design and Control

Optimization techniques were applied to the control of chilled water systems. *The important uncontrolled variables that effect system performance and optimal control variable settings were identified as the total chilled water load and ambient wet bulb temperature. Additional secondary uncontrolled variables that could be important if varied over a wide range would be the individual zone latent to sensible load ratios and the ratios of individual sensible zone loads to the total sensible loads for all zones.*

Control guidelines that reduce the number of independent control variables and simplify the optimization were also identified. These general results were utilized to develop near-optimal control strategies for chilled water systems with and without storage. The guidelines are also useful to plant engineers for improved control practices and are summarized as follows.

1) Variable-Speed Tower Fans: *Operate all cooling tower cell fans at identical fan speeds.*

2) Multi-Speed Tower Fans: *Increment lowest cooling tower fans first when adding tower capacity. Reverse for removing capacity.*

3) Variable-Speed Pumps: *The sequencing of variable-speed pumps should be directly coupled to the sequencing of chillers, to give peak pump efficiencies for each possible combination of operating chillers. Multiple variable-speed pumps should be controlled to operate at equal fractions of their maximum speed.*

4) Chillers: *Multiple chillers should have identical chilled water set temperatures and the evaporator and condenser water flows for multiple chillers should be divided according to the chillers relative cooling capacities.*

5) Air Handlers: *All parallel air handlers should have identical supply air setpoint temperatures.*

6) Stratified Thermal Storage: *A near-optimal control strategy involves maximizing operation of the system in the full discharge mode whenever the utility rates are high and minimizing operation in the charge mode when the utility rates are low. Otherwise, the system should operate in the direct mode, if necessary, during times of lowest wet bulb temperature. This control strategy should also be tested for systems with ice storage.*

No general simplifications could be found for the optimal sequencing of chillers and fixed-speed pumps. It is necessary to evaluate the overall system performance in order to determine the optimal points for adding or removing chillers. In general, it is not optimal to sequence fixed-speed pumps with chillers.

Additional results and conclusions concerning both control and design under optimal control of chilled water systems are summarized as follows.

1) *There is a strong incentive for the use of optimal or near-optimal control of chilled water systems.* Depending upon the load characteristics, fixed values of chilled water and supply air setpoints and cooling tower approach and range resulted in approximately 7 - 19% greater cooling season operating costs than that for optimal control in Dallas and Miami.

2) *In the determination of optimal control points, the humidity should be allowed to float freely, unless it falls outside the bounds of human comfort.* In effect, the addition of any constraint reduces the number of free control variables by one and results in operation at a higher cost.

3) *There are significant operational cost savings associated with the use of variable-speed equipment for chilled water systems.* Depending upon the load characteristics, the cooling season operating costs were approximately 26 - 43% greater for all fixed-speed equipment as compared with all variable-speed in Dallas and Miami. The most significant difference was attributed to the chiller.

4) *The current practice of orienting multiple chillers in parallel is near-optimal and*

should be continued. The performance of multiple chillers is enhanced by orientation in series rather than parallel. However, the increase in pumping power requirements for series chillers offsets the chiller improvements and the overall performance for the two configurations is similar.

5) *The choice of chiller refrigerant can have a significant effect upon operating costs.* For the D/FW chiller, the peak performance associated with the use of R-500 shows on the order of 5 - 10% improvement over the orginal charge of R-22. This particular chiller was derated from its original capacity due to changes in the load requirements.

6) *In the absence of time-varying utility rates, thermal storage provided little or no operating cost savings as compared with no storage for the systems considered.* Part of the reason for this is due to the assumption of a constant chilled water supply temperature during charging of storage and a constant load return water temperature during discharge. *Future work should be performed to compare the performance of optimally controlled storage systems with the charging and discharging temperatures as "free" variables in the optimization. Analysis of systems with poorer part-load characteristics could also change this conclusion. In addition, systems that incorporate ice storage should be compared with water storage systems both with and without time-of-day electric rates.*

Appendix A

Refrigerant Property Data

Liquid Refrigerant Thermal Conductivity Correlations

The following correlations require temperature, T, in degrees Fahrenheit and give thermal conductivity, k_f, in Btu/hr-ft-F.

R-500: $k_f = 0.05300 - 0.000127\ T$

R-22: $k_f = 0.06298 - 0.000159\ T$

R-12: $k_f = 0.04902 - 0.000117\ T$

Liquid Refrigerant Viscosity Correlation

Refrigerant viscosities, μ_f, are in lbm/ft-hr and temperatures, T, are degrees Fahrenheit.

R-500: $\mu_f = 0.6851 - 3.2943e\text{-}03\ T + 6.4430e\text{-}06\ T^2$

R-22: $\mu_f = 0.6517 - 2.5943e\text{-}03\ T + 5.6101e\text{-}06\ T^2$

R-12: $\mu_f = 0.7630 - 3.8905e\text{-}03\ T + 9.8810e\text{-}06\ T^2$

Refrigerant Sonic Velocity Data at 50 degrees Fahrenheit

Refrigerant	a_o (ft/sec)
R-500	490
R-22	534
R-12	446

Appendix B

Method for Determining the Performance of Partially Wet and Dry Cooling Coils

Water will begin to condense on the surface of a cooling coil at the point where surface temperature equals the dewpoint of the entering air. The process of determining the relative areas associated with the wet and dry portions of the coil is iterative. In terms of the exit water temperature, the dry coil surface area and the flow stream conditions at the point where condensation occurs are found by solving the flow stream energy balance and rate equations for the dry section and setting the surface temperature at the condensation point equal to the dewpoint point temperature, T_{dp}. The resulting equation for the fraction of the total coil surface area that is dry is

$$f_{dry} = -\frac{1}{K}\ln\left[\frac{(T_{dp} - T_{w,o}) + C^{*}(T_{a,i} - T_{dp})}{(1 - K/Ntu_{o})(T_{a,i} - T_{dp})}\right] \tag{B.1}$$

where,

$$K = Ntu_{dry}(1 - C^{*}) \tag{B.2}$$

The effectivenesses for the wet and dry portions of the coil, $\varepsilon_{a,wet}$ and $\varepsilon_{a,dry}$ are

$$\varepsilon_{a,wet} = \frac{1 - \exp(-(1 - f_{dry})Ntu_{wet}(1 - m^{*}))}{1 - m^{*}\exp(-(1 - f_{dry})Ntu_{wet}(1 - m^{*}))} \tag{B.3}$$

$$\varepsilon_{dry,a} = \frac{1 - \exp(-f_{dry} Ntu_{dry}(1 - C^*))}{1 - C^* \exp(-f_{dry} Ntu_{dry}(1 - C^*))} \tag{B.4}$$

The water temperature at the point where condensation begins is

$$T_{w,x} = \frac{T_{w,i} + C^* \varepsilon_{wet,a}(h_{a,i} - h_{s,w,,i})/C_{pm} - C^* \varepsilon_{wet,a} \varepsilon_{dry,a} T_{a,i}}{(1 - C^* \varepsilon_{wet,a} \varepsilon_{dry,a})} \tag{B.5}$$

and a new estimate of the exit water temperature is

$$T_{w,o} = C^* \varepsilon_{dry,a} T_{a,i} + (1 - C^* \varepsilon_{dry,a}) T_{w,x} \tag{B.6}$$

An excellent initial estimate of the outlet temperature is the larger of the temperatures obtained from the completely wet and dry analyses (i.e. $f_{dry} = 0$ and $f_{dry} = 1$). As shown in Figures 4.2 and 4.3, the all wet or dry assumption gives results that are close to those of the partially wet and dry analysis. As a result, the above iterative process converges very quickly, typically within two iterations.

The outlet air state from the coil is determined from

$$T_{a,o} = T_{s,e} + (T_{a,x} - T_{s,e}) \exp(-(1 - f_{dry}) Ntu_o) \tag{B.7}$$

where, the effective surface temperature in the wet coil section is the saturation temperature corresponding to an effective enthalpy condition determined as

$$h_{s,s,e} = h_{a,i} + \frac{h_{a,o} - h_{a,x}}{1 - \exp(-(1 - f_{dry})Ntu_o)} \quad \text{(B.8)}$$

The air temperature and enthalpy at the point at which condensation occurs are

$$T_{a,x} = T_{a,i} - \varepsilon_{dry,a}(T_{a,i} - T_{w,x}) \quad \text{(B.9)}$$

$$h_{a,x} = h_{a,i} - \varepsilon_{dry,a}C_{pm}(T_{a,i} - T_{w,x}) \quad \text{(B.10)}$$

Appendix C

Component Data for Base System of Chapter 6

I. Chiller Power Consumption (see Chapter 2)

$$\frac{P_{ch}}{P_{des}} = a_0 + a_1X + a_2X^2 + a_3Y + a_4Y^2 + a_5XY$$

where,

$$X = \frac{\dot{Q}_e}{\dot{Q}_{des}}$$

$$Y = \frac{(T_{cwr} - T_{chws})}{\Delta T_{des}}$$

Parameter	Variable-Speed	Fixed-Speed	Lau	Hackner
a_0	0.07336	0.0516	0.1107	0.2642
a_1	-0.3259	1.2199	0.3198	0.0207
a_2	0.5744	-0.2517	0.4662	0.2643
a_3	-0.03888	-0.6448	-0.0956	-0.4460
a_4	0.3321	0.8963	0.2152	0.3555
a_5	0.3684	-0.3119	-0.0656	0.5176
$\dot{Q}_{des}$	5421.	5421.	1250.	550.
ΔT_{des}	46.	46.	50.	50.
P_{des}	3580.	3627.	961.	453.

II. Cooling Tower Cells (see Chapter 3)

$$Ntu = c\left[\frac{\dot{m}_w}{\dot{m}_a}\right]^{1+n}$$

where,

$c = 2.0$

$n = -0.63$

Design Air Flow: 635,000 cfm

Design Fan Power: 100 kW

Sump Make-Up Water Temperature: 50 F

III. Cooling Coil Data (see Chapter 4)

$$Ntu_i = k_1\left[\frac{\dot{m}_w}{\dot{m}_{w,des}}\right]^{k_2}$$

$$Ntu_o = k_3\left[\frac{\dot{m}_a}{\dot{m}_{a,des}}\right]^{k_4}$$

where,

$k_1 = 2.25$ $\quad$ $k_2 = -0.20$

$k_3 = 1.70$ $\quad$ $k_4 = -0.38$

Total Design Air Flow: 1,800,000 cfm

Total Design Fan Power: 1000 kW

IV. **Pump Analysis** (see Chapters 3 and 4)

Pressure Drops

Component	Design Flow (gpm)	Design ΔP (psi)
Chiller Condenser	10,000	10
Chiller Evaporator	10,000	25
Cooling Tower Nozzle	5,000	5
Condenser Water Loop Static		30
Chilled Water Loop Static		20

Pump Pressure Rise

$$\Delta P_p = \Delta P_{p,max}\left[1 - \left(\frac{\dot{m}_{cw}}{\dot{m}_{p,max}}\right)^2\right]$$

$$\Delta P_{p,max} = \gamma_p^2 \Delta P_{p,max,des}$$

$$\dot{m}_{p,max} = \gamma_p \dot{m}_{p,max,des}$$

where,

$\Delta P_{p,max,des} = 100$ psi

$\dot{m}_{p,max,des} = 10{,}000{,}000$ lbm/hr

Pump Efficiency

$$\eta_p = a_0 + a_1\left[\frac{\dot{m}_{cw}}{\gamma_p \dot{m}_{p,max,des}}\right] + a_2\left[\frac{\dot{m}_{cw}}{\gamma_p \dot{m}_{p,max,des}}\right]^2$$

where,

$a_0 = 0.0$

$a_1 = 2.93$

$a_2 = -2.64$

References

1. Arnold, J.A., et al., "Supervisory Control and System Optimization of Chiller - Cooling Tower Combinations Via Simulation Using Primary Equipment Models - Part II Simulation and Optimization," Proceedings of the Workshop on HVAC Controls and Modeling and Simulation, Georgia Institute of Technology, February 2-3, 1984.

2. ASHRAE Handbook of Fundamentals, American Society of Heating, Refrigerating, and Air Conditioning Engineers, Atlanta, pp. 3.1-3.16, 1981.

3. ASHRAE Equipment Guide, American Society of Heating, Refrigerating, and Air Conditioning Engineers, Atlanta, Chapter 3, 1983.

4. ASHRAE Technical Data Bulletin, "Thermal Storage," A collection of papers presented during the ASHRAE Winter Meeting, ASHRAE, Inc., Atlanta, Georgia, January 1985.

5. Bellman, R., Dynamic Programming, Princeton University Press, Princeton, N.J., 1957.

6. Berman, L.D., Evaporative Cooling of Circulating Water, 2nd edition, translated from Russian by R.Hardbottle and edited by Henryck Sawistowski, Pergamon Press, New York, 1961.

7. Braun, J.E., Mitchell, J.W., Klein, S.A., and Beckman, W.A., "Models for Variable-Speed Centrifugal Chillers," ASHRAE Transactions, Vol. 93, Part 1, 1987.

8. Braun, J.E., Mitchell, J.W., Klein, S.A., and Beckman, W.A., "Performance and Control Characteristics of Large Central Cooling System," ASHRAE Transactions, Vol. 93, Part 1, 1987.

9. Braun, J.E., "Programs for Modelling and Optimizing the Performance of Central Chilled Water Systems," Solar Energy Laboratory, University of Wisconsin-Madison, 1988.

10. Bullock, C.E. "Dynamic Simulation Models for Commercial Air Conditioning and Heat Pump Systems," Proceedings of the Workshop on HVAC Controls Modeling and Simulation, Georgia Institute of Technology, February 2-3, 1984

11. Carey, W.F. and Williamson, G.F., "Gas Cooling and Humidification: Design of Packed Towers from Small-Scale Tests," Proceedings of the Institution of Mechanical Engineers, Vol. 163, pp. 41-53, 1950.

12. Davis, F.T. and Corripio, A.B., "Dynamic Simulation of Variable-Speed Centrifugal Compressors, " Instrumentation in the Chemical and Petroleum Industries, Vol. 10, ISA, Pittsburgh, Pa., Feb. 1974.

13. Downing, R.C.,"Refrigerant Equations," Dupont Company"

14. Elmahdy, A.H. and Mitalas, G.P., "A Simple Model for Cooling and Dehumidifying Coils for Use in Calculating the Energy Requirements of Buildings," ASHRAE Transactions, Vol. 83, Part 2, p. 103, 1977.

15. Elmahdy, A.H. and Biggs, R.C., "Finned Tube Heat Exchanger Correlation of Dry Surface Heat Transfer Data," ASHRAE Transactions, Vol. 85, Part 2, pp. 262-273, 1979.

16. Farris, D.R. and McDonald, T.E., "Adaptive Optimal Control - An Algorithm for Direct Digital Control," ASHRAE Transactions, Part 1, 1980.

17. Ferguson, The Centrifugal Compressor Stage, Butterworth and Company, London, 1963.

18. Gill, P.E., Murray W., and Wright, M.G, Practical Optimization, Academic Press, London, 1981.

19. Gunewardana, D.R., Tomizuka, M., Auslander, D.M., "Application of Optimal Preview Control to Power Plant Cooling Systems," ASME Journal of Dynamic Systems, Measurement and Control, Vol. 101, June 1979.

20. Hackner, R.J., Mitchell, J.W., and Beckman, W.A., "HVAC System and Energy Use in Existing Buildings - Part I", ASHRAE Transactions, Paper KC-84-09, 1984.

21. Hackner, R.J., Mitchell, J.W., and Beckman, W.A., "HVAC System Dynamics and Energy Use in Buildings - Part II," ASHRAE Transactions, Vol.91, Part 1, 1985.

22. Hackner, R.J., Mitchell, J.W., and Beckman, W.A., "System Dynamics and Energy Use," ASHRAE Journal, June, 1985.

23. Hittle, D.C., "BLAST - Building Loads Analysis and System Thermodynamics Program, Version 3.0: User Manual, " Technical Report E-171, U.S. Army Construction Engineering Research Laboratory, 1981.

24. Jaber, H. and Webb, R.L, "Design of Cooling Towers by the Effectiveness-NTU Method," ASME Winter Annual Meeting, Boston, Massachusetts, December, 1987.

25. Jacobson, D.H. and Mayne, D.O., Differential Dynamic Programming, Elsevier, New York, 1970.

26. Jakob, M., Heat Transfer, Vol. II, John Wiley & Sons, New-York, pp. 342-345, 1957.

27. Johnson, G.A. "Optimization Techniques for a Centrifugal Chiller Plant Using a Programmable Controller," ASHRAE Transactions, Vol. 91, Part 2, 1985.

28. Klein, S.A., et al., TRNSYS" - A Transient System Simulation Program," University of Wisconsin - Madison, Engineering Experiment Station Report 38-12, Version 12.1, 1984.

29. Larson, R.E., State Increment Dynamic Programming, American Elsevier, 1967.

30. Lau, A.S., Beckman, W.A., and Mitchell, J.W., "Development of Computer Control Routines for a Large Chilled Water Plant", ASHRAE Transactions, Vol. 91, Part 1, 1985.

31. Lichtenstein, J., "Performance and Selection of Mechanical-Draft Cooling Towers," ASME Transactions, Vol. 65, No. 7, pp. 779-787, 1943.

32. Ljung, L. and Soderstrom, T., Theory and Practice of Recursive Identification, MIT Press, Cambridge, MA.,1983.

33. Maclaine-cross, I.L., Banks, P.J., "A General Theory of Wet Surface Heat Exchangers and its Application to Regenerative Cooling," ASME Journal of Heat Transfer, Vol. 103, No. 3, pp. 579-585, 1981.

34. Marcev, C.L., "Steady-State Modeling and Simulation as Applied to Energy Optimization of a Large Office Building Integrated HVAC System," M.S. Thesis, University of Tennessee, 1980.

35. Merkel, F., "Verdunstungskuhlung," VDI Forschungsarbeiten, No. 275, Berlin, 1925.

36. Mickley, H.S., "Design of Forced Draft Air Conditioning Equipment," Chemical Engineering Progress, Vol. 45, No. 12, pp. 739-745, 1949.

37. Morin, T.L., "Computational Advances in Dynamic Programming," p. 53, Dynamic Programming and Its Applications, Edited by Martin L. Puterman, Academic Press, 1979.

38. Myers, J.E. and Katz, "Boiling Coefficients Outside Horizontal Plain and Finned Tubes, " Refrigeration Engineering, Vol. 60, No. 1, p. 56, January, 1952.

39. Nizet, J.L, Lecomte, J., and Litt, F.X., "Optimal Control Applied to Air Conditioning in Buildings," ASHRAE Transactions, 1984.

40. Nizet, J.L, "Development of Cooling Tower Models," Internal Report, Laboratoire de Physique du Batiment, University of Liege, Belgium, 1985.

41. Nottage, H.B., "Merkel's Cooling Diagram as a Performance Correlation for Air-Water Evaporative Cooling Systems, " ASHRAE Transactions, Vol. 47, pp. 429-448, 1941.

42. Nugent, D.R., Klein, S.A., and Beckman, W.A., "Investigation of Control Alternatives for a Steam Turbine Driven Chiller, ASHRAE Winter Annual Meeting, Dallas, 1988

43. Pandit, S.M. and Wu, S.M., Time Series and System Analysis with Applications, John Wiley, 1983.

44. Pontryagin, L.S., Boltyanskii, V.G., Gamkrelidze, R.V., and Mishchenko, E.F., The Mathematical Theory of Optimal Process, Wiley - Interscience, New York, 1962.

45. Simpson, W.M. and Sherwood, T.K., "Performance of Small Mechanical Draft Cooling Towers," Refrigerating Engineering, Vol. 52, No. 6, pp. 535-543, 574-576, 1946.

46. Singh, M.G. and Titli, A., Systems: Decomposition, Optimization, and Control, Permagon Press, 1978.

47. Stoecker, W.F. (editor), Proposed Procedures for Simulating the Performance of Components and Systems for Energy Calculations, Second Edition, New York, ASHRAE, 1971.

48. Sud, I., "Control Strategies for Minimum Energy Usage," ASHRAE Transactions, Vol. 90, Part 2, 1984.

49. Sutherland, J.W., "Analysis of Mechanical Draught Counterflow Air/Water Cooling Towers", Journal of Heat Transfer, Vol. 105, pp. 576-583, 1983.

50. Threlkeld J.L., Thermal Environmental Engineering, Prentice-Hall, New York, Second Edition, 1970.

51. "TRACE Documentation Manual," TRANE Company, LaCrosse, WI 54601.

52. Treichler, W.W., "Variable Speed Pumps for Water Chillers, Water Coils, and Other Heat Transfer Equipment," ASHRAE Transactions, Vol. 91, Part 1, 1985.

53. Webb, R.L, "A Unified Theoretical Treatment for Thermal Analysis of Cooling Towers, Evaporative Condensers, and Fluid Coolers," ASHRAE Transactions, Vol. 90, Part 2, 1984.

54. Wiesner, F.J. and Caswell, H.E., "How Refrigerant Properties Affect Impeller Dimensions, " ASHRAE Journal, October, 1959.

55. Wiesner, F.J., "Practical Stage Correlations for Centrifugal Compressors", ASME Transactions, Gas Turbine Power and Hydraulic Conference, Houston, Texas, March 6-9, 1960, Paper No. 60-HYD-17.

56. Whillier A., "A Fresh Look at the Calculation of Performance of Cooling Towers," ASHRAE Transactions, Vol. 82, Part 1, pp. 269-282, 1976.

57. White, F.M., Fluid Mechanics, McGraw-Hill, Second Edition, New York, 1986.

58. York, D.A. and Tucker, E.F., Editors, "DOE-2 Reference Manual (Version 2.1)," Los Alamos Scientific Laboratory, LA-7689-M, Los Alamos, 1980.